An operational perspective on holographic entanglement

ROTA, MASSIMILIANO

An operational perspective on holographic entanglement

Massimiliano Rota

A Thesis presented for the degree of
Doctor of Philosophy

Department of Mathematical Sciences
University of Durham
England
March 2016

An operational perspective on holographic entanglement

Massimiliano Rota

Submitted for the degree of Doctor of Philosophy
March 2016

Abstract

The work presented in this thesis is a contribution towards the understanding of holographic entanglement from an operational perspective. Following the interpretation which is most natural for quantum information theory, entanglement is viewed as a resource that can be produced, stored, transferred and used for practical purposes.

The first chapter introduces the main concepts which are necessary throughout the discussion. Quantum entanglement, as opposed to merely classical correlation, is presented in detail within the framework of quantum mechanics. This is followed by a brief overview on the current state of knowledge about entanglement in quantum field theory and more specifically in gauge/gravity duality.

The second chapter investigates a particular measure of entanglement, known as negativity, in the context of holographic field theories. This is further explored in the following (third) chapter, where an interesting dependence of the entanglement between a region and its complement on the topology of their interface is presented.

The forth chapter investigates qubits systems and compares equivalence classes of entanglement structures to known properties of holographic states.

The fifth chapter focuses on the behaviour of the tripartite information for highly entangled states, both in a bipartite and multipartite sense, in relation to the sign definiteness imposed by holography.

A final chapter comments on future directions of investigation within this program.

Declaration

The work in this thesis is based on research carried out at the Department of Mathematical Sciences at Durham University. The results are based on the following collaborative works:

- M. Rangamani and M. Rota, *Comments on Entanglement Negativity in Holographic Field Theories, JHEP* **1410** (2014) 60, [arXiv:1406.6989]
- E. Perlmutter, M. Rangamani and M. Rota, *Central Charges and the Sign of Entanglement in 4D Conformal Field Theories, Phys.Rev.Lett.* **115** (2015) 17, [arXiv:1506.01679]
- M. Rangamani and M. Rota, *Entanglement structures in qubit systems, J.Phys. A* **48** (2015) 38, [arXiv:1505.03696]
- M. Rota, *Tripartite information of highly entangled states*, to appear in *JHEP*, [arXiv:1512.03751]

No part of this thesis has been submitted for a degree in this or any other institution.

Acknowledgements

It is a pleasure to express my gratitude to the people who contributed in a special way to this work and into making my experience in Durham so wonderful.

First of all my supervisor, Mukund Rangamani, for his continuous support and encouragement, and for always giving me the opportunity to explore all aspects of physics which I find more fascinating. To him I will always be grateful.

Veronika Hubeny, for countless wonderful discussions on many fundamental and fascinating aspects of physics, and for creating with Mukund such a nice research environment.

Felix and Henry, for all the time spent together discussing physics and from which I learned so much.

My friends Cesare, Alice and Ntina, for making my time in Durham special even when I was not doing physics.

And finally my parents, for their continuous support that helped me leaving a country to which I never belonged.

Contents

Chapter 1

Introduction

In 1975 Hawking proposed that information might be lost as a consequence of black holes evaporation. While black holes are one of the most important windows onto quantum phenomena in gravity, unitary evolution of closed systems, and hence conservation of information, is the cornerstone of quantum mechanics. The tension between these two paradigms of gravitational and quantum theory, dubbed the *black hole information paradox*, has been at the center of many discussions for the last forty years but a satisfactory resolution still seems out of reach and will probably require a full theory of quantum gravity. Despite these difficulties, the paradox is one of the first indications that *quantum information* is a physically meaningful concept and might be a fundamental element of a quantum theory of gravity.

While the theory of classical information has a long history which goes back to the seminal paper by Shannon in 1948, its quantum version has eluded physicists for many decades. Besides practical reasons, such as the difficulty of protecting quantum systems from decoherence, this is probably a consequence of the counterintuitive character of quantum behaviour as opposed to the classical. Indeed, for long time the fundamental ingredient of the future theory of quantum information, namely *quantum entanglement*, was considered to be merely a curiosity.

After the seminal work in the 80's and 90's by a relatively small group of people, *quantum information theory* is now a well developed and quickly growing subject. Similarly to its classical counterpart, the new theory describes how quantum systems can be manipulated and constitutes the theoretical foundation of countless applications. It is this *operational perspective* that will be central in the discussion presented in this work.

Besides practical applications, the development of quantum information theory is also sharpening our understanding of quantum behaviour, providing new powerful tools of investigation. It is striking how after almost a century quantum mechanics is still able to surprise us with unexpected predictions. Indeed, part of the research in quantum information theory is intimately related to investigations on the foundations of quantum theory. While it is conceivable that a fully satisfactory theory of quantum gravity will require some modifications of quantum mechanics, for the purposes of this work the theory of quantum information might be considered as the theory of manipulations of systems

governed by the laws of conventional quantum mechanics.

To make progress towards a deeper understanding of the role played by quantum information in gravity we need to extend the theory to the relativistic framework of field theory. From an operational perspective this is a highly non trivial problem because the language of field theory is much more unnatural than the one of quantum mechanics for the description of manipulations of quantum systems. Nevertheless we now have new tools to start tackling the problem. On the one hand there are in field theory computable measures of quantum entanglement for which we can look for an operational interpretation starting from their counterparts in quantum mechanics. On the other hand investigations of entanglement structures in quantum mechanics might be a guidance for further progress in field theory.

If one could develop an operational understanding of quantum entanglement in field theory, one can then make contact with quantum gravity using the gauge/gravity duality, or AdS/CFT correspondence. The duality is a concrete realization of the holographic principle, asserting that quantum gravity in a region of spacetime can be fully described by the information contained on its boundary. In 2006 Ryu and Takayanagi showed that entanglement entropy of a boundary region, perhaps the most important of all entanglement measures, is associated holographically to a geometric object in the gravity dual. Its value is given by the famous Bekenstein-Hawking formula associating entropies to areas in gravity. The discovery opened a new area of investigations where quantum information principles are used for investigations in quantum gravity. The work presented in this thesis is a modest step towards the understanding of this correspondence from the operational perspective, the one which is more natural in quantum information theory.

1.1 The concept of quantum entanglement

The origin of the notion of quantum entanglement goes back to Schrödinger and his reply to the famous argument by Einstein, Podolsky and Rosen advocating the incompleteness of quantum theory. Several attempts to "complete" quantum mechanics made used of *local hidden variables*, an important example being Bohm formulation. It was only in 1964 that Bell proved a no-go theorem against this approach [1]. He showed that any attempt to reproduce correlations of quantum theory with local variables would inevitably conflict with special relativity. This subtle interplay between causality and locality is the essence of Bell's theorem and can be used to define quantum entanglement.

1.1.1 Spooky action at a distance

Causality and locality can be nicely defined in an abstract fashion using only probability theory. Consider two experimentalists, Alice and Bob, that are space-like separated and hence cannot communicate. Suppose they share a physical system composed of two subsystems A and B that have been prepared in advance and may in general contain some sort of correlations. A pictorial representation of the set-up is shown if Fig. 1. The nature of

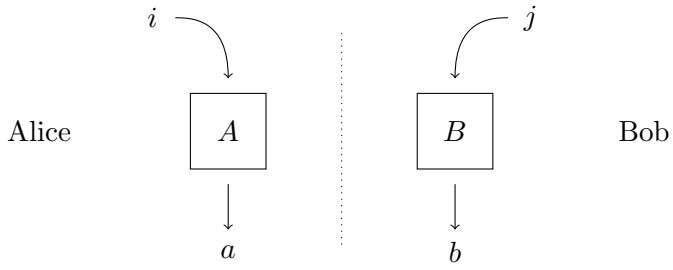

Figure 1: A pictorial representation of PR boxes. The boxes A and B represent a physical system made of two space-like separated subsystems, the random variables i and j label the possible choices of experiments and the variables a and b the possible outcomes. The vertical line reminds of the fact that we are assuming A and B to be space-like separated.

these correlations is what we want to study. The two observers have the freedom to chose randomly the experiment they want to perform to probe the subsystems (the observable to be measured for example). This is encoded in the random variables i and j. For a particular choice of experiments the subsystems will respond producing the outcomes a and b respectively. The correlations are encoded in the joint probability distribution $\mathbb{P}_{ab|ij}$ of getting the results (a, b) for the choice (i, j). For consistency with probability theory we must have

$$\begin{aligned} \sum_{a,b} \mathbb{P}_{ab|ij} &= 1 \qquad \forall i, j \\ \mathbb{P}_{ab|ij} &\geq 0 \qquad \forall a, b, i, j \end{aligned} \tag{1.1.1}$$

At this stage a generic realization of the joint probability distribution might allow communication between the observers because there might be an *observable* dependence of the outcome a on the choice of the experiment j (and similarly of b on i). To prevent this, consistently with the assumption of space-like separation, one has to impose the following *no-signaling* condition on the marginal probabilities

$$\begin{aligned} \mathbb{P}_{a|ij} \equiv \sum_b \mathbb{P}_{ab|ij} = \sum_b \mathbb{P}_{ab|ij'} \equiv \mathbb{P}_{a|ij'} \qquad \forall a, i, j, j' \\ \mathbb{P}_{b|ij} \equiv \sum_a \mathbb{P}_{ab|ij} = \sum_a \mathbb{P}_{ab|i'j} \equiv \mathbb{P}_{b|i'j} \qquad \forall b, j, i, i' \end{aligned} \tag{1.1.2}$$

In other words, the marginal probabilities of a and b are independent on j and i respectively. We can then write

$$\mathbb{P}_{a|ij} \equiv \mathbb{P}_{a|i} \qquad \mathbb{P}_{b|ij} \equiv \mathbb{P}_{b|j} \tag{1.1.3}$$

Note that the no-signaling condition does not imply for example

$$\mathbb{P}_{ab|ij} = \mathbb{P}_{ab|ij'} \tag{1.1.4}$$

because the two observers can learn about joint probabilities only when they are in causal contact.

If the correlations between subsystems are a consequence of a "hidden variable", i.e. some random variable shared by the observers, the joint probability distribution can be written as

$$\mathbb{P}_{ab|ij} = \int d\lambda\, p(\lambda)\chi_{a|i}(\lambda)\chi_{b|j}(\lambda) \tag{1.1.5}$$

where the functions χ are "response functions" of the subsystems A and B, λ is the random variable that determines the response and $\mathcal{P}$ is its probability distribution. The assumption of *locality* of correlation is encoded in the requirement that the response functions do not depend on the choices j and i respectively. By excluding this dependence we are restricting the possible values of $\mathbb{P}_{ab|ij}$. One can then call *entangled* all states which contain correlations that violate this locality constraint. In specific cases, one can follow this procedure to derive inequalities that are violated by entangled states, these are the Bell inequalities.

1.1.2 A constructive definition of entanglement

The previous formulation is not optimal for practical purposes. Bell inequalities are in general difficult to derive and the definition does not make direct contact to our ability of manipulating the system. With the development of quantum information theory, it has become clear that entanglement is the key resource for the implementation of all interesting protocols. It is then important to have a definition of entanglement based on a preparation procedure.

Imagine a situation similar to the one presented in the previous section, where now the two agents Alice and Bob are not causally separated any more and instead can communicate classical information. By this we mean that they can for example send messages describing measurement outcomes but they are still not allowed to send quantum systems. Under these assumptions the class of operations that they are able to perform on their subsystems is the set of all local quantum operations, such as unitary evolution and measurements, where the operations they decide to apply can depend on shared classical information. These operations are called LOCC, which stands for *local operations and classical communication*.

Suppose now that Alice and Bob have two subsystems which initially are in a product, and hence uncorrelated, state. We consider the most general scenario where these states are both mixed. The initial state is then $\rho_{AB}^{(i)} = \rho_A^{(i)} \otimes \rho_B^{(i)}$. Clearly, since the choice of operations that Alice can perform can depend on the outcome of Bob's operations (and vice versa), they can implement a protocol that produces a new state $\rho_{AB}^{(f)}$ which contains some kind of correlation between A and B. What is the most general form of a state that Alice and Bob can build in this way?

Let us reformulate the set-up slightly differently. Since quantum measurements are stochastic, the effect of sharing the outcomes using classical communication is equivalent to the case where Alice and Bob have access to a shared random variable λ, similarly as in our previous discussion for Bell inequalities. According to the value of λ they then extract

states from the ensembles $\{\rho_A^i\}$ and $\{\rho_B^i\}$ according to a probability distribution $p(\lambda)$. In this way they can build any state with the following form

$$\sum_i p_i \rho_A^i \otimes \rho_B^i \,, \qquad \sum_i p_i = 1 \,, \qquad p_i \geq 0 \tag{1.1.6}$$

States that can be written in this way are called *separable states*. Since the correlations contained in separable states can be build by a procedure that makes use of only LOCC, it is natural to assume that these are *local* correlations. We then define *non-local* correlations as the one that cannot be realized by LOCC operations. For these reason, in quantum information theory, it is customary to define *entangled states* as the one that are not separable.

1.1.3 Non-locality and the physical principle of quantum mechanics

The two definitions given above are not fully equivalent. For pure states they agree, since the only pure states which are separable are the product states, while any state which cannot be written as a product violates some Bell inequality. On the other hand the situation for mixed states is much less clear. Indeed, there are states that are explicitly non-separable but nevertheless do not violate any Bell inequality. We will further discuss the discrepancy between the two definitions of entanglement in chapter 2.

Even if the two definitions do not completely match, it is quite clear that non-locality is one of the key elements which distinguish quantum behaviour from the classical and it is interesting to ask whether this is the essential physical principle of quantum theory. Indeed quantum mechanics is defined by a set of postulates which are justified "a posteriori", by their ability to make predictions that reproduce results of experiments with remarkable accuracy. But the physical principles behind the theory that could justify the postulates "a priori" are still rather obscure.

In 1994 Popescu and Rohrlich asked if the non-signaling condition together with the assumption of violation of locality could be enough to define quantum mechanics [2]. Interestingly, the answer turned out to be negative. It is important to note that the definition of entanglement based on probability theory is completely independent from any detail of the language of quantum mechanics. We can imagine the two subsystems A and B to be two "black boxes", called PR-boxes, containing systems governed by some physics which in principle could be more general than quantum mechanics. The power of the formalism is the fact that it can be used to investigate the nature of correlations in a theory independent way, using only probability theory. In the simplest possible set-up where the random variables $i, j, a, b \in \{0, 1\}$, one can define a correlator $\langle B \rangle$, often called the Bell observable, which satisfies $\langle B \rangle \leq 2$. This is a Bell inequality known as the CHSH inequality [3] and of course can be violated by quantum correlations. Popescu and Rohrlich found that by allowing non-locality, with the only constraints of consistency of probability and no-signalings the bound is $\langle B \rangle \leq 4$. On the other hand, it was proved by Tsirelson [4] that quantum mechanics allows for a strength of correlations only up to

$\langle B\rangle \leq 2\sqrt{2}$. What is the physical principles that produces this bound and does not allow for correlations with $2\sqrt{2} < \langle B\rangle \leq 4$? The question is still open, see [5] for a nice review.

1.2 Quantum information theory

Quantum information theory encompasses a broad range of subjects in the area of quantum mechanics and its applications. Sometimes the term is used more specifically to refer to the generalization of Shannon's classical theory of communication to the realm of quantum systems. Throughout this work instead we will use it in a broader sense, including other areas of investigations and applications of quantum mechanics such as the theory of quantum computation, protocols like teleportation, or the research on the foundations of quantum theory.

It is perhaps this desire of better understanding quantum phenomena that leaded to the development of the new theory although its origins are difficult to track in a clear way. Rather, the field emerged in the 80's and 90's from investigations regarding entanglement and from the desire of acquiring practical control over quantum systems.

Quantum information theory is now a very wide field which continues to grow very quickly and a detailed presentation is beyond the scope of this work. In the next section we will limit ourselves to the presentation of some important elements of the theory and briefly comment on each of them. What really is remarkable is the fact that in the last few years nearly all of them have at some level entered the discussion about quantum gravity and holography.

1.2.1 Quantum wonders

The no-cloning theorem this is one of the first results that started the field of quantum information theory. The theorem asserts that it is not possible to build a machine which, given an unknown quantum state $|\psi\rangle$ together with an additional system in some reference state $|0\rangle$, produces as outputs two copies of $|\psi\rangle$. The impossibility of cloning quantum information has played a role in several recent discussion regarding the black hole information paradox and the firewall argument [6].

Quantum computation: a quantum version of the Universal Turing Machine was first proposed by Deutsch in 1985. A set of simple unitary operations acting on single qubits or pairs of qubits, called quantum gates, was shown to be universal, in the sense that any unitary evolution can be realized using an appropriate circuit of these quantum gates. The interest in quantum computers largely increased after the proof by Shor of the possibility of factorizing numbers in polynomial time, showing the power of quantum computers over their classical version. In recent years other schemes for quantum computation have been developed, including one based on measurements known as *one way quantum computation* [7]. In this case entanglement is the resource contained in the initial state which is consumed to run the computation. The ability of black holes to process information very

efficiently, in particular the conjecture that they are fast scramblers, suggests an analogy between black holes and quantum computers [8].

Teleportation: this is perhaps the most striking application of quantum information theory. Using entanglement, it allows to transfer a quantum state from one agent to another using only measurements and classical communication. Suppose Alice and Bob share a Bell pair AB, one particle each. Furthermore, Alice has a qubit C in a state $|\psi\rangle_C$ and she wants to transfer the state to Bob. She just needs to do a Bell measurements on the two qubits AC and communicate the result to Bob. The measurement creates a new Bell pair on AC and Bob can use the received classical information to perform a local unitary transformation on B that produces $|\psi\rangle_B$. Quantum teleportation can also be used to build an alternative scheme for quantum computation [9]. In quantum gravity, a modified version of teleportation where Bob can produce $|\psi\rangle_B$ without receiving any information from Alice, known as post-selected teleportation, has been used to propose a solution to the black hole information paradox, the black hole final state proposal [10].

Quantum noiseless coding theorem: this is the first of various theorems proved in the context of quantum communication along the lines of its classical counterpart. It was proved by Schumacher in 1995 and is the direct generalization of Shannon's theorem to the quantum world, where the role of Shannon entropy is now played by the von Neumann entropy. Consider a message composed of "letters" where each letter is a pure quantum state drawn from an ensemble $\{|\psi_1\rangle, ..., |\psi_n\rangle\}$ with probabilities $\{p_1, ..., p_n\}$. The theorem says that there exists a code that compresses the message to $S(\rho)$ qubits per letter, where $\rho = \sum_{i=1}^{n} p_i \, |\psi_i\rangle\langle\psi_i|$ and $S(\rho)$ is the von Neumann entropy.

Quantum error correction: the ability to correct errors is crucial for all practical applications of quantum information theory, both in quantum communication and quantum computation. Suppose that we want to send a state $|\psi\rangle$ of some physical system associated to a Hilbert space $\mathcal{H}$. To protect the message we can encode the same state on some larger system with Hilbert space $\tilde{\mathcal{H}}$. To do this, a subspace of this new enlarged Hilbert space $\mathcal{H}_{\text{code}} \subset \tilde{\mathcal{H}}$ is sufficient, this is called the "code subspace". The details of how this should be done depend on the kind of noise one want to protect the state from. Essentially, the mechanism works because the information contained in the original message is encoded in a redundant manner in the enlarged system. Again, entanglement plays a crucial role, tailor made entanglement structures should be used to define the code subspace and guarantee the ability of the receiver to correct the error. In the context of AdS/CFT, recent work suggested that a similar mechanism is the way the boundary reproduces the bulk [11].

Entanglement distillation: is a procedure that can be used to extract Bell pairs from a quantum state using LOCC. Distillability of entanglement is used to define *distillable*

entanglement, an important measure of entanglement which will be introduced in the next section.

Quantum state merging: conditional entropy is an important quantity in classical information theory and its quantum counterpart is the conditional von Neumann entropy $S(A|B) = S(AB) - S(A)$. Interestingly, this quantity can be negative, this happens for example any time AB is in a pure state and there are correlations between A and B. Quantum state merging is a protocol that gives an interpretation to this quantity, even when negative. Consider a situation where, using entanglement and classical communication, a sender wants to send a state to a receiver who already has some information about the full state. The conditional entropy is a measure of the minimal amount of entanglement which is necessary to implement this protocol. When this quantity is negative, the sender can transfer the state without entanglement, while some amount of entanglement is instead produced. In holography, a version of this protocol has been proposed to give an operational interpretation to the length of certain curves in the bulk [12].

1.2.2 Measuring entanglement

Given a generic state of a (for simplicity) bipartite system, one can in principle use the definition of entanglement based on separability to determine if the state is entangled or not. Nevertheless the problem is known to be computationally hard. Tools like Bell inequalities, called in general *entanglement witnesses*, can be used to determine whether a state contains some entanglement, but they are not always conclusive and do not provide a full characterization of the entanglement in the state. The discussion in the previous section should have made clear that quantum correlations are now viewed as a *resource* that should be produced, stored, transformed and used in desired applications. It is then crucial to develop measures which have a clear operational interpretation and are able to quantify the amount of entanglement that pertains to the state.

The first measure to be introduced, and certainly one of the most important, is *entanglement entropy*. For a given pure state $|\psi\rangle_{AB} \in \mathcal{H}_A \otimes \mathcal{H}_B$ of a bipartite system, the entropy of entanglement between A and B is given by the von Neumann entropy of the reduced density matrix ρ_A (or ρ_B)

$$S_A = -\mathrm{Tr}_A \rho_A \log \rho_A \,, \qquad \rho_A = \mathrm{Tr}_B \, |\psi\rangle\langle\psi| \tag{1.2.7}$$

As a consequence of purity, the result is independent on which one of the subsystem we choose, i.e. $S_A = S_B$. This is not true any more if the original global state was mixed. In this case the von Neumann entropy is not a good measure of entanglement.

In general the von Neumann entropy satisfies a set of inequalities which are of particular importance not only in quantum information theory but also for later discussions in field theory and holography:

- subadditivity: $S_{AB} \leq S_A + S_B \quad \forall A, B$
- strong subadditivity: $S_{ABC} + S_B \leq S_{AB} + S_{BC} \quad \forall A, B, C$
- Araki-Lieb: $|S_A - S_B| \leq S_{AB} \quad \forall A, B$

Even for pure states, the von Neumann entropy is just a single number and is not able to completely characterize the full entanglement structure of a state, to this end we need additional measures. Furthermore, one would like to have measures of entanglement with a nice operational interpretation which can be used also for mixed states. An axiomatic theory of entanglement measures is not fully developed yet, nevertheless there are several properties that are usually required to be satisfied by good candidates for measures of entanglement:

- An entanglement measure $E(\rho)$ is a mapping: $\rho \to E(\rho) \in \mathbb{R}^+$
- $E(\rho) = 0$ for separable states
- On average, $E(\rho)$ does not increase under LOCC, it is an *entanglement monotone*
- For pure state, i.e. $\rho = |\psi\rangle\langle\psi|$, the measure reduces to entanglement entropy
- Convexity: $E\left(\sum_i p_i \rho_i\right) \leq \sum_i p_i E\left(\rho_i\right)$ Intuitively, the motivation behind this requirement is the fact that in going from a selection of identifiable states ρ_i to a mixture $\rho = \sum p_i \rho_i$ some information is lost
- Additivity: $E\left(\rho^{\otimes n}\right) = nE(\rho)$ is the weaker form of additivity. A much stronger requirement, which is not satisfied by most measures is instead $E(\rho \otimes \sigma) = E(\rho) + E(\sigma)$
- Continuity

Over the years several measures have been proposed satisfying all or part of these properties, see [13] for a review. Here we briefly mention two of them which, at least conceptually, are perhaps the most satisfactory.

Entanglement cost $E_C(\rho)$: is the minimal number of maximally entangled states, i.e. Bell pairs, which are required to create copies of a state ρ using only LOCC operations. More precisely, for a given state ρ, this measure quantifies the maximal possible rate at which one can convert blocks of Bell pairs into output states that approximate many copies of ρ, such that the approximation becomes vanishingly small in the limit where the size of the block is large. The maximization is over all possible protocols that can be used to implement the procedure, for this reason this measure is an extremely difficult quantity to evaluate.

Distillable entanglement $E_D(\rho)$: intuitively, this is the opposite of entanglement cost. It is the maximal rate at which one can convert copies of a state ρ into copies of approximately maximally entangled pairs. Again, as for entanglement cost, the maximization is over all possible protocols and makes this measure very hard to compute.

For pure states these two measure match and are equal to entanglement entropy, which also serves for their calculation. Quite interestingly, this is not always true for mixed states where in general one has $E_C(\rho) \geq E_D(\rho)$. This irreversibility in manipulations of entanglement suggests that one could hope to develop a "thermodynamics" of entanglement [14]. States for which the inequality is strict are called *bound entangled*, stressing that the entanglement of the state is in some form that cannot be distilled. An important example of a measure that is sensible to this kind of entanglement is the *negativity*. This quantity is important for practical purposes because at least in quantum mechanics can be easily computed. We will define it rigorously and discuss its properties extensively in the following chapters, which will focus on the role that negativity plays in field theory and holography.

1.3 Entanglement in Quantum Field Theory

In quantum field theory entanglement is much less understood than in quantum mechanics, even more so from an operational perspective. One could argue that quantum field theory is just the continuous limit of quantum mechanics and that the same definitions we presented above should apply. Nevertheless there are several complications. To begin with, the notions of causality and locality introduced with the PR-boxes formalism are not fully equivalent to the concept of microcausality which is instead natural in field theory. Further technical issues arise as a consequence of the infinite dimensionality of Hilbert spaces and the fact that, for gauge theories, the Hilbert space does not factorize for a given bipartition. A definition of entanglement based on LOCC seems unnatural for field theories, where operations such as measurements are much less understood than in quantum mechanics. In this regard one could appeal to the algebraic formulation of the theory, but this is notoriously difficult to deal with for practical purposes. Finally there is the problem of defining information theoretical quantities in a relativistic covariant fashion. *Relativistic* quantum information theory is a new area of research which is still at its infancy.

1.3.1 Towards a notion of entanglement for field theory

Although much work still has to be done, we briefly review here some known facts which will potentially play a crucial role in defining entanglement along the same lines as in quantum mechanics.

Violation of Bell inequalities: in the algebraic formulation, it was proved in 1987 by Summers and Werner [15] that the violation of Bell inequalities is a generic fact in the vacuum of an arbitrary field theory.

Reeh-Schlieder theorem: the theorem is derived in the axiomatic framework of quantum field theory. It asserts that in the vacuum of a field theory, the space of states generated by operators acting on an arbitrary subregion is dense in the Hilbert space of the theory. This means that by acting locally with an appropriate operator, although in principle it can be very complicated, we can produce a state which is arbitrarily closed to any possible desired state. Naively, one is tempted to interpret this result as suggesting that the vacuum of an arbitrary field theory contains a large amount of entanglement which can be used for practical applications. Quite differently from the result concerning Bell inequalities, this theorem seems to be more in line with an operational interpretation of field theory entanglement.

Tsirelson problem: in the previous section we discussed how the formalism of PR-boxes can be used to investigate, using only probability theory, the interplay between non-locality and causality that characterises quantum correlations. Using the formalism of quantum mechanics, the set $\mathcal{Q}$ of correlations that can be produced corresponds to joint probability distributions that can be written as

$$\mathbb{P}_{ab|ij} = \langle \psi | \, M_{a|i} \otimes M_{b|j} \, | \psi \rangle \tag{1.3.8}$$

where $|\psi\rangle$ is the state of the system AB in a Hilbert space that factorizes $\mathcal{H}_A \otimes \mathcal{H}_B$. Note that in general the state of AB can be mixed, but we can always enlarge the system to purify the state and write the probability distribution in this form. For quantum field theory on the other hand, probability distributions are given by expressions like

$$\mathbb{P}_{ab|ij} = \langle \psi | \, M_{a|i} M_{b|j} \, | \psi \rangle \tag{1.3.9}$$

where we instead of requiring factorization of the Hilbert space, we impose the micro-causality condition between local operators $\left[M_{a|i}, M_{b|j}\right] = 0$. We call the set obtained in this way $\mathcal{Q}'$. Since $\left[M_{a|i} \otimes \mathbb{1}_B, \mathbb{1}_A \otimes M_{b|j}\right] = 0$ it immediately follows $\mathcal{Q} \subseteq \mathcal{Q}'$. It is an open question [16] whether the inclusion is strict and $\mathcal{Q} \neq \mathcal{Q}'$.

1.3.2 Entanglement measures in field theory

At present, an axiomatic approach to entanglement measures in field theory along the lines of the quantum mechanical case still has to be developed. Most of our understanding of entanglement comes from the calculation in field theory of some of the measures defined for quantum mechanics, but an operational interpretation of these quantities is far from clear. Furthermore, already in quantum mechanics most measure are very difficult to compute and the situation gets even more complicated in field theory.

In practice, the measures that can be computed in field theory are generalization of the von Neumann entropy known as Renyi entropies, which are defined as follows. Consider a field theory state at some instant in time. Pick a subregion of interest A and build the reduced density matrix ρ_A by integrating out the degrees of freedom of its complement A^c. The Renyi entropies of ρ_A are defined as

$$S_q(\rho_A) = \frac{1}{1-q}\mathrm{Tr}(\rho_A^q) \tag{1.3.10}$$

While it is natural to expect that the full set of Renyi entropies, usually called the *entanglement spectrum*, carries complete information about the pattern of correlations of a state, unfortunately they do not have an operational interpretation. This is one of the reasons that motivated us to look at other quantities for the investigations presented in the following chapters.

From Renyi entropies one can derive the von Neumann entropy by differentiation with respect to q

$$S(\rho_A) = -\left.\frac{\partial}{\partial q}\mathrm{Tr}_A\rho_A^q\right|_{q=1} = \left.\frac{\partial}{\partial q}\log\mathrm{Tr}_A\rho_A^q\right|_{q=1} \tag{1.3.11}$$

This is the technique which can be used to derive entanglement entropy in field theory, where the direct computation of the logarithm of a density matrix is not possible. If the original state of the field theory from which ρ_A was derived is a pure state, and if the Hilbert space factorizes $\mathcal{H}_A \otimes \mathcal{H}_{A^c}$, it is natural to interpret this quantity as the field theory generalization of quantum mechanical entanglement entropy.

To compute Renyi entropies in field theory we can use the "replica trick" [17] to evaluate $\mathrm{Tr}_A\rho_A^q$. We start with a path integral representation of the reduced density matrix ρ_A. For the ground state of a field $\Phi(x)$ the wave functional is given by path integration in Euclidean time on the interval $t_E \in (-\infty, 0)$

$$\Psi(\phi(x)) = \int_{t_E=-\infty}^{\Phi(t_E=0)=\phi} \mathcal{D}\Phi\, e^{-S(\Phi)} \tag{1.3.12}$$

where $\phi(x)$ is the filed configuration of $\Phi(x)$ at $t_E = 0$. To build the total density matrix we need the complex conjugate $\overline{\Psi}(\phi'(x))$, which is given by integration on $t_E \in (0, +\infty)$. The density matrix is then given by a Euclidean integral on $t_E \in \mathbb{R}$ with a cut along $t_E = 0$

$$\rho(\phi, \phi') = \Psi(\phi(x))\overline{\Psi}(\phi'(x)) = \int_{\substack{\Phi(t_E=0^-)=\phi \\ \Phi(t_E=0^+)=\phi'}} \mathcal{D}\Phi\, e^{-S(\Phi)} \tag{1.3.13}$$

To derive the reduced density matrix ρ_A we need to trace over the degrees of freedom in A^c. We impose then the condition $\phi(x) = \phi'(x)$ for $x \in A^c$ and integrate over x. This is equivalent to "gluing" $\Psi(\phi(x))$ and $\overline{\Psi}(\phi'(x))$ on A^c leaving boundary conditions to be specified only in A

$$\rho_A(\phi, \phi') = \int_{\substack{\Phi(t_E=0^-, x\in A)=\phi \\ \Phi(t_E=0^+, x\in A)=\phi'}} \mathcal{D}\Phi\, e^{-S(\Phi)} \tag{1.3.14}$$

Now to compute ρ_A^q we take multiple copies of ρ_A and glue each sheet to the following one by matching boundary conditions along the cuts which correspond to the copies of region A: $\phi_i(x) = \phi'_{i+1}(x)$ with $i = 1, 2, ..., q$. Finally, we get $\mathrm{Tr}_A \rho_A^q$ by gluing the q-th copy to the first one. The result is a path integral on an q-sheeted Riemann surface $\mathcal{R}_q$

$$\mathrm{Tr}_A \rho_A^q = \int_{(t_E,x)\in\mathcal{R}_q} D\Phi\, e^{-S(\Phi)} \tag{1.3.15}$$

Following this procedure one can derive the analogous result for a field theory in a thermal state at temperature $T = 1/\beta$. The path integral representation of the density matrix is obtained by integrating for an interval in Euclidean time of length β. The reduced density matrix obtained by gluing along A^c becomes a cylinder with a cut along A and the Riemann surface $\mathcal{R}_q$ is obtained as before by gluing multiple copies of the cylinder along the cuts.

For an arbitrary region A, which in particular could be disconnected, in an arbitrary quantum field theory of dimension d, the calculation of these path integrals is intractable. Nevertheless for some specific cases, (1.3.15) can be evaluated. This happens for example when the field theory is a two dimensional conformal field theory. In this case the Riemann surface $\mathcal{R}_q$ can be mapped to a sphere with the insertion of operators at the endpoint of the intervals corresponding to the region A. These operators, called *twist operators*, are primary operators of dimension $\frac{c}{12}(q-\frac{1}{q})$ and encode the gluing conditions that defined $\mathcal{R}_q$. The partition function is then given by a $2q$-point correlation function of twist operators. For $q > 1$ the result is not universal and depends on the details of the theory. On the other hand, when A is a single interval, the result is universal. For the ground state one gets

$$S_A = \frac{c}{3} \log \frac{l}{\epsilon} + \text{cons} \tag{1.3.16}$$

and for the thermal state

$$S_A = \frac{c}{3} \log \left(\frac{\beta}{\pi\epsilon} \sinh \frac{\pi l}{\beta} \right) + \text{cons} \tag{1.3.17}$$

where ϵ is a UV cut-off and the constant term is not universal.

For more complicated choices of A or in higher dimensions few results are known, although this is a very active area of research. Nevertheless, for the simplest situation where A is a ball region, entanglement entropy can be computed and it is known to satisfy an *area law* . This means that the entropy is not proportional to the volume of the ball but rather to the area of the spherical surface which constitutes its boundary

$$S_A \sim \frac{\mathcal{A}(\partial A)}{\epsilon^{d-2}} + \text{subleading terms} \tag{1.3.18}$$

where ϵ is a UV cut-off in the field theory and $d > 2$. This was first proved in free field theory in [18] and later shown to be true in several situations also with numerical techniques. Indeed, in the context of condensed matter theory, several tools have been introduced specifically to approximate this particular entanglement structure that characterizes ground states of local Hamiltonians. Tensors networks are an important example which is currently of very much interest also for holography.

1.4 Holographic entanglement

The famous result due to Bekenstein and Hawking associates an entropy to a black hole given by

$$S_{BH} = \frac{\mathcal{A}}{4G_N} \tag{1.4.19}$$

where $\mathcal{A}$ is the area of the event horizon. This suggests that gravity might be *holographic* and that all information about a region of spacetime is somehow encoded on its boundary. A concrete realization of this *holographic principle*, and certainly the most important so far, is the AdS/CFT correspondence, or gauge/gravity duality, proposed by Maldacena in 1997 [19].

1.4.1 Gauge/gravity duality

In essence the duality asserts that string theory on an asymptotically Anti de Sitter background is *dual*, and hence equivalent, to a certain field theory which lives on the boundary of that spacetime. The most important example of the correspondence relates type IIB superstring theory on $AdS_5 \times S^5$ to $\mathcal{N} = 4$ super Yang-Mills theory in $3 + 1$ dimensions with gauge group $SU(N)$. On the string theory side, both Anti de Sitter space and the sphere have radius of curvature L, the free parameters are the string coupling g_s and the ratio L^2/α', where $\alpha' = l_s^2$ and l_s is the length of the string. On the other hand on the field theory side the free parameters are the rank of the gauge group N and the coupling constant g_{YM}^2. The correspondence is established by the following identifications

$$g_{YM}^2 = 2\pi g_s\,, \qquad\qquad 2g_{YM}^2 N = \frac{L^4}{\alpha'^2} \tag{1.4.20}$$

For the purposes of the discussion presented in this work, we will need a particular regime of the parameters where the AdS side is not dominated by stringy effects but rather reduces to classical gravity. We then make the assumption $g_s \ll 1$ while keeping $L/\sqrt{\alpha'}$ fixed, such that the strings are weakly coupled and tree level diagrams dominate in perturbation theory. On the field theory side it follows from (1.4.20) that $g_{YM} \ll 1$ while $g_{YM}^2 N$ remains finite. This is equivalent to taking the 't Hooft limit $N \to \infty$ for fixed $\lambda = g_{YM}^2 N$. Finally, if we take the limit $\lambda \to \infty$ in the field theory, this is equivalent to $\sqrt{\alpha'}/L \to 0$ for the strings. In this regime the string is very small compared to the radius of curvature of AdS and this side of the duality reduces to type IIB supergravity on $AdS_5 \times S^5$. This particular example can be generalized to motivate a duality AdS_{d+1}/CFT_d.

Once the correspondence is established, it is important to clarify the dictionary that maps between objects on the two sides. An important feature of the correspondence is the fact that the symmetry groups on the two sides match. This allows to map operators O on the field theory side to supergravity fields ϕ in the AdS background. More specifically, the boundary value ϕ_0 of the supergravity fields are interpreted as a source for the operators O. This allows to formulate the correspondence as an equivalence between partition functions

on the two sides. In its strongest form, the duality equates the partition function of the field theory to that of string theory on the AdS background

$$\mathcal{Z}_{\mathrm{QFT}}[\phi_0] = \left\langle \exp \int d^d x \phi_0 O \right\rangle_{\mathrm{QFT}} = \mathcal{Z}_{\mathrm{string}} \tag{1.4.21}$$

where $\mathcal{Z}_{\mathrm{string}}$ is not known explicitly. On the other hand in the regime we are interested in, a saddle point approximation to the string action is given by the on-shell action of supergravity. The correspondence is then

$$\mathcal{Z}_{\mathrm{QFT}}[\phi_0] = \left\langle \exp \int d^d x \phi_0 O \right\rangle_{\mathrm{QFT}} = e^{\mathcal{S}_{\mathrm{sugra}}}[\phi \to \phi_0] \tag{1.4.22}$$

The supergravity action is evaluated on the solution of the equations of motion of supergravity with boundary condition

$$\lim_{z \to 0} \phi(z, x) z^{\Delta - d} = \phi_0(x) \tag{1.4.23}$$

where Δ is the scaling dimension of the operator O and z is the radial coordinate in the bulk of AdS. Once this relation is established, one can then compute correlation functions as usual by taking functional derivatives.

The great advantage that derives from the correspondence is the fact that it can be used as a tool to investigate one side working with the other. In the regime we are focusing onto, the field theory is strongly couple and perturbation theory is useless. But on the other side the string dual reduces to classical gravity which can then be used as a tool to investigate strongly coupled field theories. While this is certainly the property that makes the AdS/CFT correspondence useful in countless applications, we are interested in a slightly different aspect of the duality. Understanding how the correspondence works and what are its physical foundations, would probably represent an important step towards the development of a theory of quantum gravity.

1.4.2 Holographic entanglement entropy

In the regime where the bulk dual is just classical gravity, one can ask if the correspondence is able to tell us anything about information theoretic quantities in the boundary field theory. Remarkably, in 2006 Ryu and Takayanagi proposed that when a classical holographic dual is available for a given state of a field theory, the von Neumann entropy of a boundary subregion is given by a nice geometric quantity [20].

More precisely, for a static situation, consider a time-slice of the asymptotically AdS geometry. On the boundary pick a subregion of interest A, with boundary ∂A, for which we want to compute the von Neumann entropy. The holographic prescription tells us to look for the bulk surface Σ_{min} with boundary ∂A that minimizes the area. The von Neumann entropy is then given by

$$S_A = \frac{\mathcal{A}\left(\Sigma_{\mathrm{min}}\right)}{4 G_N} \tag{1.4.24}$$

where G_N is the Newton constant in the bulk. The formula is of crucial importance for practical application, as it gives a tool to easily compute the von Neumann entropy in many situations where it would be inaccessible with other techniques such as the replica trick. The analogy to the Bekenstein-Hawking formula is striking and once more suggests that there is some deep connection between gravity and information theory.

When the field theory is in a pure state, we know that $S_A = S_{A^c}$. This is straightforward to see in the holographic picture, where the bulk minimal surface anchored to ∂A is the same for A and A^c. On the other hand, when the state of the field theory is mixed, we known that the entropies o a subregion and its complement are different. A typical example is the thermal state of the field theory that corresponds holographically to the geometry of an eternal black hole in AdS. In this case the prescription for the computation of holographic entanglement entropy should be modified by introducing an additional requirement. The bulk minimal surface should not only be anchored to ∂A, it should also be *homologous* to A.

With such a prescription at hand, one should then check that it satisfies all the properties of the von Neumann entropy. This in particular means that all the inequalities presented in (1.2.2) should be satisfied. Strong subadditivity was checked in [21] while the Araki-Lieb inequality is guaranteed to be satisfied by the homology constraint. Remarkably, for this static situation, the Ryu-Takayanagi prescription has now been proved [22].

The results obtained from this holographic prescription are divergent, this is the consequence of the fact that the boundary of AdS is at infinite proper distance from any point in the bulk. The correct regularization procedure consists in truncating the geometry at some finite large distance, this corresponds to the UV cut-off on the field theory side. Taking the limit where the truncation of the geometry is at infinity is dual in field theory to the limit where ϵ goes to zero.

Unfortunately, the Ryu-Takayanagi prescription we just reviewed applies only to stationary scenarios. One would like instead a prescription that can be used in any dynamical situation. Such generalizations was found by Hubeny-Rangamani-Takayanagi in [23]. For a field theory state on some Cauchy slice one can define the von Neumann entropy as before, but now the bulk geometry has Lorentzian signature. In this case one cannot minimize the area of bulk surfaces as the area is not bounded from below any more. The new prescription then requires to find all *extremal* surfaces homologous to A with boundary ∂A and among them the one that minimizes the area. The entropy is then again given by (1.4.24).

1.4.3 Holographic entanglement structures

One of the interesting consequences of the holographic entanglement entropy prescription is that under some conditions the Araki-Lieb inequality is saturated, this phenomenon is called *entanglement plateaux*. For a field theory in a thermal state, when the region of interest A is large enough, the minimal surface splits into two terms, one being the minimal surface which computes the entropy of A^c and the other the black hole horizon.

For arbitrary states the Araki-Lieb inequality is known to be very difficult to saturate, suggesting that the entanglement structure of the field theory in this holographic setting could be quite special. We will explore this behaviour for qubits systems in chapter 4.

Another interesting consequence of the Ryu-Takayanagi prescription is a further constraint independent on (1.2.2). For any three subregions A, B, C holographic states satisfy the following inequality

$$S_A + S_B + S_C - S_{AB} - S_{AC} - S_{BC} + S_{ABC} \leq 0 \tag{1.4.25}$$

The quantity on the left hand side is called *tripartite information*. This inequality will be investigated for qubits systems in chapter 4 and for some special highly entangled states in 5.

The results reviewed above suggest that there is a deep connection between bulk geometric quantities and quantum information on the boundary. More generally, it has been argued by various recent works that the bulk geometry somehow "emerges" from the pattern of entanglement of the boundary theory. This entanglement structure, and in particular its operational interpretation, are the main subjects of this work.

A promising approach to investigations of entanglement structures in holography are tensor network constructions, see for a general review [24]. An arbitrary quantum state of N qu-d-its (the higher dimensional generalization of a qubit) can be written as

$$|\psi\rangle = \sum_{i_1,i_2,...,i_N} \mathcal{T}_{i_1,i_2,...,i_N} \, |i_1, i_2, ..., i_N\rangle \tag{1.4.26}$$

with $i_1, i_2, ..., i_N \in \{0, 1, ..., d-1\}$. The state is specified by the coefficient of the tensor $\mathcal{T}$. Since the dimension of the Hilbert space of such a system grows exponentially with N ($\dim\mathcal{H} = d^N$), both analytical and numerical investigations become infeasible even for relatively small N. Depending on the situations one can then focus attention on particular structures of $\mathcal{T}$. An appropriate choice of the tensors used to build the network leads to states which satisfy an area law for entanglement, making them good ansatz to approximate ground states of local Hamiltonian. An important example in the context of holography is the MERA (multi-scale entanglement renormalization ansatz) [25], which was first related to holography in [26]. Other tensor networks have also been used to suggest a form of the exact holographic mapping between Hilbert spaces of boundary and bulk theories [27], and to analyse the connection between holography and quantum error correction [28]. Tensor networks will not enter directly into the discussion presented in the main body of this work, but they constitute the natural prosecution of our investigations. We will comment more on this in the final outlook.

The connection between entanglement and geometry is so deep that it has even be suggested that it could be upgraded to a full equivalence in quantum gravity. The proposal goes under the name ER=EPR [29], where ER stands for Eistein-Rosen bridge, referring to geometric connectedness, and EPR for Einstein-Podolski-Rosed, referring to entanglement. This conjecture as originally formulated is a general statement about quantum gravity which in principle could be independent from holography. Nevertheless it is

quite natural to imagine an holographic version, where entanglement refers to quantum correlations in the boundary theory and geometric connectedness to the bulk. If this is true to some extent, it would be interesting to understand the operational interpretation of the equivalence. Is there an holographic dual to protocols performed by agents acting on the boundary? Understanding this potentially striking and fascinating phenomenon is perhaps the final goal of the kind of investigations presented in this work.

Chapter 2

Entanglement Negativity in Field Theory

This chapter is a reproduction of the paper *Comments on Entanglement Negativity in Holographic Field Theories* [30], written in collaboration with Mukund Rangamani.

This work initiated the investigation of a measure of quantum entanglement called *negativity* in the context of holographic field theories. Negativity is a measure of bipartite quantum entanglement that can be used even for global mixed states, where other measures based on the von Neumann entropy, such as the mutual information, are not able to distinguish classical from quantum correlations.

In quantum mechanics negativity can be easily computed and has an operational interpretation. It is an upper bound to the amount of quantum entanglement that can be distilled from a system. In the context of field theory, negativity was first explored in [31], which for the case of global pure states established an important relation to Renyi entropies.

Here we look at holography and after a thorough introduction to negativity and its properties, we compute the entanglement negativity for the thermofield double state, the state dual to the eternal black hole geometry in AdS. The answer is a function of the free energy of the field theory at different temperatures which matches entanglement entropy, and hence the entropy of the black hole, in the limit of infinite temperature.

We then use this result to compute the negativity for spherical regions in the vacuum of different field theories, both free and strongly coupled. Interestingly, a comparison of these results shows that the negativity seems to be smaller at strong coupling. Naively it is tempting to interpret this result as suggesting that when the fields are strongly coupled fewer Bell pairs can be distilled from the vacuum. Unfortunately, a rigorous interpretation along this lines will require a much deeper understanding of the operational perspective on entanglement in field theory.

For pure states entanglement entropy coincides with the amount of entanglement that can be distilled from the system, while negativity, which is just an upper bound, is a larger quantity. In four dimensions the leading contribution to both entropy and negativity is

proportional to the area of the entangling surface, but this term is unphysical as it depends on the regularization scheme. The logarithmic terms instead are scheme independent and their coefficients carry important physical information. We conjecture that the ratio between the coefficients of the universal terms for the negativity and entanglement entropy is always greater than one, in accordance with the operational interpretation of these quantities. The conjecture is supported by some explicit examples, but will be falsified by a counterexample in the next chapter. We will see that under some conditions the ratio depends non trivially on the topology of the entangling surface and for complicated topologies can be less than one.

Finally, we comment on a possible connection between negativity and the entanglement plateaux phenomenon of [32]. This behaviour will be further explored in the chapter 4 in the case of simple qubits systems.

2.1 Introduction

Quantum mechanics, as is well appreciated, is characterized by an important feature, entanglement. While the colloquial usage of the word "entanglement" often simply refers to presence of correlations which could simply be of classical nature, nature of quantum entanglement transcends this interpretation. A natural question is to segregate and quantify in a given quantum state the genuinely quantum parts of entanglement from those that are inherited from underlying classical correlations.

One way to proceed would be to use the intuition garnered from Einstein-Podolsky-Rosen (EPR) like entangled states, which are non-product (pure) states in the quantum Hilbert space. One of the characteristic hallmarks of these states as elucidated by Bell [1] is that they fail to satisfy the Bell inequality (and hence its generalization, the CHSH inequalities). We now understand quite well that this means that the entanglement inherent in the EPR state is a genuine quantum aspect and relatedly that one cannot invoke some local hidden variable (LHV) to describe the quantum state. A-priori one might have thought that the Bell/CHSH inequalities provide a complete characterization of the nature of entanglement.

While for pure states this is true, the state of affairs is much less clear in case of mixed states. Consider a bipartite system in a state ρ with two Hilbert spaces which we will refer to as the left and right Hilbert space, $\mathcal{H}_L$ and $\mathcal{H}_R$ respectively. Such a state is called *separable* if it can be written as

$$\rho = \sum_i p_i \, \rho_i^R \otimes \rho_i^L \,, \qquad \sum_i p_i = 1 \,, \qquad p_i \geq 0 \,, \tag{2.1.1}$$

otherwise it is called *entangled*. Physically this definition attempts to encode the fact that separable states are classically correlated as they can be produced using only local operations and classical communication (LOCC).[1] In particular, it introduces a distinction

[1] LOCC for two parties consists of steps in each of which any party is allowed to perform local mea-

between the correlations that are classical and those that ought to be considered quantum.

In analogy with pure states above, one would then be inclined to think that even in the case of mixed states any entangled state violates some Bell inequality. Surprisingly this is not true, as demonstrated by Werner in [33], where mixed entangled states that can nevertheless be described by a LHV model were constructed. In some sense, despite manifesting some quantum correlation, these states ought to be viewed as *local* as they are not in tension with the notion of local realism.[2] Furthermore, if we have access to several copies of the state then it is sometimes possible using only LOCC to *distill* a new state that violates some Bell inequality [35] (see [36] for details on distillation). One might then be led to the intuition that this process should be achievable starting from any mixed state; therefore the only states that always satisfy all Bell inequalities are the separable ones. Unfortunately, even this intuition fails; to put it mildly the boundary between classicality and quantumness is rather fuzzy with no clear demarcation. The main lesson we wish to emphasize is one ought to distinguish different notions of entanglement in the quantum realm.

Because of the intricate nature of entanglement for mixed states, several measures of entanglement have been proposed. The concept of distillation for example can be used to define the *distillable entanglement* as a measure of how much pure entanglement it is possible to extract from some state using only LOCC. On the other hand the *entanglement of formation* quantifies the amount of pure entanglement required to create a given state.[3] In case of pure states these measures are equal and agree with entanglement entropy (for a comprehensive review on entanglement measures see [13]). Unfortunately the drawback is that these measures cannot be computed because they are given by variational expressions over possible LOCC protocols. A more pragmatic approach is to therefore consider a quantity that is computable [37] – this leads us to the consideration of *entanglement negativity* which will form the focus of the present investigation. Heuristically, the concept uses the spectral data of the density matrix[4] (sometimes called entanglement spectrum) to ascertain the amount of entanglement inherent in the mixed state (cf., §2.2 for a precise definition) .

While the above discussion has been firmly rooted in the realm of quantum mechanics, one expects that many of these issues generalize to relativistic quantum field theories, see e.g., [38]. Understanding the nature of entanglement in different quantum states in this context is not only interesting in its own right, but also from the potential connections with holographic dualities. Indeed, the geometrization of the notions of entanglement entropy in the gauge/gravity context for holographic field theories as originally proposed

surements and communicate the outcome to the other using classical channels.

[2] For a discussion on the properties of Werner states in the context of teleportation see e.g., [34].

[3] These measures must be interpreted in an asymptotic sense. They give extremal rates achievable when one has many copies of the state ρ.

[4] We actually need the spectral data of an auxiliary matrix constructed from the density matrix; we will be more precise below.

in [20,39] (and made geometrically covariant in [23]) makes one wonder if there are further lessons one can learn by understanding the distinct notions of entanglement in the context holographic field theories.

Moreover, the connections between geometry and entanglement as we now are starting to understand are perhaps much more intimate. The original arguments espoused in [26] and [40,41] suggest a close association between entanglement inherent in a quantum state and the realization of the holographic dual in terms of classical geometry. The relation between entanglement and the emergence of a macroscopic spacetime, is further bolstered by the arguments of [29] who suggest an intimate connection between EPR like states and Einstein-Rosen bridges, succinctly summarized by the catchphrases "ER =EPR" or "entanglement builds bridges".[5]

While these fascinating developments hint at an underlying structure wherein entanglement of quantum states plays an important role in emergence of macroscopic geometry and gravitational physics from the microscopic quantum dynamics, it is fair to ask whether the different notions of entanglement as described above have any useful intuition to impart in explicating the general structure. Does the spacetime geometry care if the entanglement is EPR like, or if it undistillable, or if the quantum entanglement is contaminated by classical correlations? These are, we believe, interesting questions whose answers may potentially shed some light into the geometrization of quantum entanglement.

In this chapter, we undertake a modest step in this direction by studying the properties of entanglement negativity, which as previously mentioned is a computable measure of entanglement, in relativistic field theories. We begin in §2.2 by reviewing the necessary definitions in quantum mechanics and use these to guide our intuition for negativity in simple examples. We first show quite generally that the entanglement negativity of a thermofield double state (the pure entangled state in a tensor product Hilbert space) has a very simple expression in terms of the difference of free energies.

While this result is a corollary of a more general result known already in [37] relating the entanglement negativity of pure states in a bipartite system to a particular Renyi entropy (at index $\frac{1}{2}$) of the reduced density matrix for one of the components, it casts the general result in simple terms, which in turn allows us to extract some lessons. We argue for instance in §2.3 that it allows us to recover the negativity of the vacuum state of a CFTs for a spherical partitioning of the spatial geometry. In particular, employing the conformal mapping developed in [48], we give results for the entanglement negativity for spherical regions for d-dimensional CFTs. In this context it bears mentioning that the results for entanglement negativity have been obtained in 2-dimensional CFTs by employing the replica trick in [31, 49]. These results are of course more powerful and express the computation of the entanglement negativity in terms of twist operator correlation functions for cyclic orbifolds. In §2.4 we make some general comments on extracting the negativity

[5] See also [42] for suggestions relating growth of entanglement with that of spacetime volume created thus using analogies with tensor networks and [43–47] for attempts to recover gravitational dynamics from quantum information.

in holographic field theories using the generalized gravitational entropy prescription of [22] and comment on some general lessons one can learn from these analysis. We conclude with a discussion of open questions in §4.6.

2.2 Entanglement negativity

While our ultimate aim is to explore quantum information theoretic ideas in the holographic realm, we first however need to explain the basic concepts. We therefore begin our discussion with a review of the salient issues relevant for discussing entanglement negativity in quantum mechanics, and postpone generalizations to relativistic quantum field theories to a later stage.

As discussed in §4.1, given a density matrix describing a mixed state of some bipartite system it is natural to ask whether there is any way we can reveal if it is separable or entangled. More generally one could hope to find a criterion to distinguish different kinds of entanglement in general, which could prove useful in various contexts as discussed hitherto.

A powerful tool in this direction is the so called *positive partial transpose* criterion (PPT). Consider the set-up described in §4.1 where we have a bipartite system[6] in a tensor product Hilbert space $\mathcal{H}_L \otimes \mathcal{H}_R$. We pick a basis in the space of each subsystem $|\mathfrak{r}_a\rangle$ and $|\mathfrak{l}_\alpha\rangle$ with $a \in \{1, 2, \cdots, \dim(\mathcal{H}_R)\}$ and $\alpha \in \{1, 2, \cdots, \dim(\mathcal{H}_L)\}$, making clear left-right distinction in our notation. A general density matrix ρ (or indeed any operator $\mathcal{O}$) in the tensor product $\mathcal{H}_L \otimes \mathcal{H}_R$ has matrix elements in our chosen basis

$$\rho_{a\alpha,b\beta} = \langle \mathfrak{r}_a \mathfrak{l}_\alpha | \rho | \mathfrak{r}_b \mathfrak{l}_\beta \rangle . \tag{2.2.2}$$

On occasion we will need to also talk about the reduced density matrix of one of the components $\mathcal{H}_{R,L}$. We define then $\rho^R = \mathrm{Tr}_L(\rho)$ as the reduced density matrix inherited for the right subsystem from ρ (similarly ρ^L). Given such a density matrix, one defines the *partial transpose* with respect to the one of the systems, which w.l.o.g. we take to be the left system.[7] Denoting this partial transposed density matrix as ρ^Γ we have its matrix elements in the aforementioned basis to be

$$\rho^\Gamma_{a\alpha,b\beta} = \rho_{a\beta,b\alpha} = \langle \mathfrak{r}_a \mathfrak{l}_\beta | \rho | \mathfrak{r}_b \mathfrak{l}_\alpha \rangle . \tag{2.2.3}$$

If ρ^Γ has non-negative eigenvalues then ρ is said to have positive partial transpose (PPT). With these definitions one has the following criterion due to Peres [52]

$$\rho \textit{ is separable} \implies \rho \textit{ is PPT}$$

[6] We focus exclusively on bipartite entanglement. Attempts to understand multipartite entanglement in the holographic context can be found in [50] (see also [51]).

[7] With this understanding we denote the partial transpose of ρ by ρ^Γ, economizing notation by dispensing with indicating that the left subsystem was transposed.

The converse is true only for two-qubit (and qubit-trit) systems but not for higher dimensional Hilbert spaces [53].

As discussed earlier all distillable states are in direct conflict with local realism, so one could think that only separable states are undistillable. Here the PPT criterion comes strongly into play showing that this intuition is wrong. In fact it was proved in [54] that

$$\rho \textit{ is PPT} \implies \rho \textit{ is undistillable}$$

For this reason these states are called *bound entangled* in contrast to *free entanglement* that can be distilled. In other words if a state is bound entangled it is not possible to extract pure entanglement from it using only LOCC. The authors of [54] proposed an interesting analogy with thermodynamics. To prepare a bound entangled state some amount of entanglement is necessary, but the process is irreversible, as after the state is produced it is not possible to distill the initial entanglement back.

It is then reasonable to ask whether a PPT state, which is undistillable, is local in the sense of Werner. Indeed Peres conjectured in [55] that this is the case, i.e., if a state is PPT it cannot violate *any* Bell inequality. The question remained open for fifteen years even if strong evidence has been found in its support (cf., results in [56,57] and references therein). Very recently the conjecture has finally been disproved in [58] where a small violation of a Bell inequality has been found for a particular PPT state. This shows that local Werner states cannot be exactly identified with undistillable states.

As we see above, while the PPT criterion per se is not conclusive in identifying local entanglement, it can be used to define a measure of the amount of distillable entanglement contained in a state. This measure, called *negativity*, was introduced first in [37] and will form the focus of our investigation.

Given a density matrix ρ one defines the *negativity* as measure of entanglement based on the amount of violation of the PPT criterion[8] [37]

$$\text{Negativity:} \qquad \mathscr{N}(\rho) = \frac{||\rho^\Gamma||_1 - 1}{2}\,, \tag{2.2.4}$$

$$\text{Logarithmic Negativity:} \qquad \mathscr{E}(\rho) = \log ||\rho^\Gamma||_1\,, \tag{2.2.5}$$

where $||\mathcal{O}||_1$ denotes the trace-norm of an operator

$$||\mathcal{O}||_1 = \mathrm{Tr}\left(\sqrt{\mathcal{O}^\dagger \mathcal{O}}\right). \tag{2.2.6}$$

Recall that operationally the trace norm computes the sum of the absolute values of the eignevalues of an operator $||\mathcal{O}||_1 = \sum_i |\lambda_{\mathcal{O},i}|$, i.e., $||\mathcal{O}||_1 = \mathrm{Tr}|\mathcal{O}|$. As a result one is effectively computing a "signed trace" with non-trivial weighting for the negative eigenvalues of the partial transposed matrix ρ^Γ.

[8] A comment about the notation: the negativities depend not only on the state ρ but also the bipartitioning. We refrain from explicitly indicating the latter to keep the notation clean.

For completeness we also recall the notions of entanglement entropy and entanglement Renyi entropies:

$$S(\rho) = -\mathrm{Tr}\,(\rho \log \rho) = \lim_{q\to 1} S^{(q)}(\rho)\,,$$
$$S^{(q)}(\rho) = \frac{1}{1-q}\,\log \mathrm{Tr}\,(\rho^q)\,, \qquad\qquad q \in \mathbb{Z}_+ \tag{2.2.7}$$

From the definition of the trace norm it then follows that the negativity provides a measure of the number of negative eigenvalues of the density matrix ρ^Γ. Indeed, passing to a Schmidt basis, with eigenvalues of ρ^Γ being $\{\lambda_i^{(+)}, \lambda_j^{(-)}, 0_k\}$, with the non-zero eigenvalues separated by their parity, we see that

$$\mathrm{Tr}(\rho^\Gamma) = \sum_i \lambda_i^{(+)} + \sum_j \lambda_j^{(-)} \equiv 1 = \mathrm{Tr}(\rho)\,. \tag{2.2.8}$$

Here and in the following we will assume that the density matrix to be normalized as indicated. Note that while the eigenvalues of ρ^Γ are different from those of ρ generically, the trace is invariant under partial transposition. On the other hand

$$\mathscr{N}(\rho) = \frac{1}{2}\left(\sum_i |\lambda_i^{(+)}| + \sum_j |\lambda_j^{(-)}| - 1\right) = \sum_j |\lambda_j^{(-)}|\,, \tag{2.2.9}$$

is the sum of the absolute values of the negative eigenvalues of ρ^Γ, explaining the terminology. At the risk of being pedantic, let us note that the negativity is a property of the original density matrix ρ (the partial transpose ρ^Γ is just a computational aid).

Properties of negativities have been discussed in the literature on quantum information, cf., [37,59–62]. By construction both the negativity and the logarithmic negativity fail to detect bound entangled states and for this reason they do not quantify the total amount of entanglement inherent in a mixed state of the system. Furthermore it is important to note that even in case of pure states these quantities do not in general agree with entanglement entropy. Specifically, the logarithmic negativity gives in general a larger measure of entanglement, as we will see explicitly below, while the negativity reduces to one half of the *entanglement robustness*[9]. Agreement with entanglement entropy on pure states is a property commonly required in the construction of an axiomatic entanglement measure[10], but the case of negativities is different. This fact distinguishes negativities from most entanglement measures, such as entanglement of formation and distillation, which instead reduce to entanglement entropy for pure states. Nevertheless negativities can be used to quantify entanglement provided that they do not increase under any LOCC, i.e., they are *entanglement monotones*. This is indeed the case, as proved in [60][11].

[9] The robustness of entanglement can be understood as a measure of the amount of noise required to disrupt the entanglement of the system. See [63] for more details.

[10] For more details on the axioms that have to be satisfied by entanglement measures see [13] .

[11] It was actually shown that negativities are entanglement monotones under a larger class of operations called PPT-operations. This is the class of all operations that map the set of PPT states to itself. For further properties of negativities relatively to PPT-operations see [59].

The previous properties are shared by both negativities, but each of them has peculiar properties of interest by itself. The logarithmic negativity for example has been shown to give an upper bound to the distillable entanglement of ρ and to satisfy an additivity relation. For a separable state of a bipartite system of two parties A and B one indeed has

$$\mathscr{E}(\rho_A \otimes \rho_B) = \mathscr{E}(\rho_A) + \mathscr{E}(\rho_B)\,. \tag{2.2.10}$$

On the other hand the negativity can be related to the maximal fidelity that can be achieved in a teleportation protocol that uses ρ as a resource.

It is interesting to note that the negativity satisfies an interesting disentangling theorem. Consider a tripartite system ABC in a pure state $|\Psi_{ABC}\rangle$ and denote the negativity between A and BC as $\mathscr{N}_{A|BC}$ and the negativity between A and B as $\mathscr{N}_{A|B}$. It was recently proved in [61] that if and only if $\mathscr{N}_{A|BC} = \mathscr{N}_{A|B}$ then there exists a partitioning of B into B_1 and B_2 such that the state of the whole system factorizes

$$|\Psi_{ABC}\rangle = |\Psi_{AB_1}\rangle \otimes |\Psi_{B_2C}\rangle \tag{2.2.11}$$

It is an immediate consequence that under the hypothesis of the theorem the negativity between A and C (denoted as $\mathscr{N}_{A|C}$) is zero, equivalently the reduced density matrix obtained from $|\Psi_{ABC}\rangle$ by tracing out B factorizes: $\rho_{AC} = \rho_A \otimes \rho_C$. Furthermore, in this particular case, one has the saturation of a monogamy inequality for the square of the negativity previously proved by [62] for systems of three qubits

$$\mathscr{N}^2_{A|BC} \geq \mathscr{N}^2_{A|B} + \mathscr{N}^2_{A|C} \tag{2.2.12}$$

The authors of [61] conjectured that this inequality should be true in general giving numerical results in its support. Finally it interesting to mention that contrary to what one could expect, the previous inequality does not hold for the negativity itself.

To build some intuition for the negativity, we would like to understand its properties in simple situations. It should be no surprise to the reader that negativity can be non-vanishing even in pure states. After all the simple Bell state for a 2-qubit system we can have an EPR state $\frac{1}{\sqrt{2}}(|\uparrow\uparrow\rangle + |\downarrow\downarrow\rangle)$ which is pure, but entangled. It is easy to verify that for this state the negativity is $\frac{1}{2}$. Perhaps more usefully, the logarithmic negativity is $\log 2$ which is also the von Neumann entropy for the reduced density matrix for one of the qubits. It is easy to see that this result is not restricted to two-qubit systems. One has the following general result:

Logarithmic entaglement negativity of a maximally entangled state ψ_{max} in a bipartite system equals the Entanglement entropy of the reduced density matrix $\rho^{L,R}_{max}$ for one of the subsystems.

$$\mathscr{E}(\psi_{\max}) = S(\rho^{R,L}_{\max})\,. \tag{2.2.13}$$

While this statement illustrates the basic feature of this particular measure of entanglement it is useful to look at a simple generalization that will allow us to build some intuition for the negativity.[12]

[12] We find it convenient to notationally distinguish pure and mixed states and therefore denote a pure

2.2.1 Negativity in thermofield state

Let us consider the thermofield double state $|\Psi\rangle_\beta$ in with $\mathcal{H}_{L,R}$ being two copies of the same physical system. Working in an energy eigenbasis with spectrum $\{E_i\}$ we have[13]

$$|\Psi\rangle_\beta = \frac{1}{\sqrt{Z(\beta)}} \sum_{a=1}^{N} e^{-\frac{\beta}{2}E_a} |\mathfrak{r}_a \mathfrak{l}_a\rangle \tag{2.2.14}$$

The state in the tensor product is of course pure, but entangled. We want to take a measure of this entanglement, using the logarithmic negativity $\mathscr{E}(\psi_\beta)$ with

$$\psi_\beta = |\Psi\rangle_\beta \langle \Psi|_\beta = \frac{1}{Z(\beta)} \sum_{a,b=1}^{N} e^{-\frac{\beta}{2}(E_a+E_b)} |\mathfrak{r}_a \mathfrak{l}_a\rangle \langle \mathfrak{r}_b \mathfrak{l}_b| \tag{2.2.15}$$

It is then trivial to see that

$$\psi^\Gamma{}_\beta = \frac{1}{Z(\beta)} \sum_{a,b=1}^{N} e^{-\frac{\beta}{2}(E_a+E_b)} |\mathfrak{r}_a \mathfrak{l}_b\rangle \langle \mathfrak{r}_b \mathfrak{l}_a| \tag{2.2.16}$$

and

$$\psi^{\Gamma\dagger}{}_\beta \psi^\Gamma{}_\beta = \frac{1}{Z(\beta)^2} \sum_{a,b=1}^{N} e^{-\beta(E_a+E_b)} |\mathfrak{r}_b \mathfrak{l}_a\rangle \langle \mathfrak{r}_b \mathfrak{l}_a| \tag{2.2.17}$$

whence it follows that

$$\mathscr{E}(\psi_\beta) = \log \frac{Z(\frac{\beta}{2})^2}{Z(\beta)} = \beta\,(F(\beta) - F(\beta/2)) \tag{2.2.18}$$

with the final result written in terms of the free energy $F(\beta) = -\frac{1}{\beta}\log Z(\beta)$.

The logarithmic negativity of the thermofield state ψ_β is proportional to the difference of free energies of the system at temperature T and $2T$ respectively.[14] This is main observation which we will exploit in the sequel to obtain some insight into the nature of entanglement in quantum field theories. On the other hand the reduced density matrix $\rho_\beta^{R,L}$ for the right or left systems has a von Neumann entropy $S(\rho_\mathcal{A})$ which is obtained directly from $Z(\beta)$ itself. In the limit $\beta \to 0$ we recover the previous assertion (2.2.13) for maximally entangled states.

2.2.2 Renyi Negativities

For the thermofield state there is a simple relation between the negativity of the total density matrix and that of the reduced matrix of one component. This in fact generalizes

state density matrix as $\psi = |\Psi\rangle\langle\Psi|$.

[13] We have for simplicity assumed that we are dealing with a finite system where $\dim(\mathcal{H}_L) = \dim(\mathcal{H}_R) = N$.

[14] The simplicity of the final result in terms of the free energy difference is the reason for preferring the logarithmic negativity over the negativity itself. We henceforth will focus on $\mathscr{E}$ and refer to it as the negativity in the rest of our discussion for convenience.

to pure states of the bipartite system quite simply. To get further intuition for the negativity, it is worthwhile to follow the line of thought that led to the replica analysis for entanglement entropy. Just as we consider the moments of the density matrix in order to compute its von Neumann entropy, we now examine the moments of the partial transpose ρ^Γ.

Consider following [31] the notion of Renyi negativity for a density matrix ρ:

$$\exp\left(\mathscr{E}^{(q)}(\rho)\right) = \mathrm{Tr}\,(\rho^\Gamma)^q = \begin{cases} \sum_i \left(\lambda_i^{(+)}\right)^{q_e} + \sum_j \left(\lambda_j^{(-)}\right)^{q_e}, & q_e \in 2\,\mathbb{Z}_+ \\ \sum_i \left(\lambda_i^{(+)}\right)^{q_o} - \sum_j \left(\lambda_j^{(-)}\right)^{q_o}, & q_o \in 2\,\mathbb{Z}_+ + 1 \end{cases} \tag{2.2.19}$$

As is clear from the above definition the parity of the integer q plays a crucial role. Should we wish to employ the replica construction and recover the logarithmic negativity from these Renyi entropies then we will need to exclusively use the even sequence. The logarithmic negativity is obtained by an analytic continuation of even Renyi negativities to $q_e \to 1$, i.e.,

$$\mathscr{E}(\rho) = \lim_{q_e \to 1} \mathscr{E}^{(q_e)}\,, \qquad q_e \in 2\mathbb{Z}_+ \tag{2.2.20}$$

Using the definition (2.2.19) we can immediately generalize our considerations for the thermal state to any pure state $\psi = |\,\Psi\rangle\langle\,\Psi\,|$ of a bipartite system. We have [49]

$$\begin{aligned} \mathscr{E}^{(q_e)}(\psi) &= 2\,(1 - \frac{q_e}{2})\; S^{(q_e/2)}(\rho^{R,L})\,, \\ \mathscr{E}^{(q_o)}(\psi) &= (1 - q_0)\; S^{(q_o)}(\rho^{R,L})\,. \end{aligned} \tag{2.2.21}$$

In particular note that

$$\mathscr{E}(\psi) = S^{(1/2)}(\rho^{R,L})\,, \tag{2.2.22}$$

as the generalization of our previous assertions (2.2.13) and (2.2.18). We note that the Renyi negativities have been used to extract the negativities in two dimensional conformal field theories (CFTs) in [31, 49]. The technical tool involved is to appropriately map the computation as in the case of entanglement entropy to that of computing twist operator correlation functions. We will have occasion to comment on some of their results in due course.

2.3 Negativity of a CFT vacuum

Having defined the basic quantity of interest let us now turn to its computation in relativistic field theories. To our knowledge the only study of negativity in such as context are the aforementioned works [31,49] who examine its behaviour in $2d$ CFTs. Our interest is in understanding properties of negativity more generally. In what follows we explain how one can exploit (2.2.18) to find explicit results for a certain choice of bipartitioning of the vacuum state of a CFT. Subsequently we describe how to tackle the problem more generally.

Consider a relativistic QFT in d-dimensions on some background geometry $\mathcal{B}$. As remarked earlier in §4.1 we want to ask how to quantify the entanglement of the vacuum

state in this theory. For the present we are going to use the concept of logarithmic negativity introduced in §2.2 to serve as the measure of interest.

A natural way to proceed is to consider a spatial Cauchy slice Σ and consider some region $\mathcal{A} \subset \Sigma$. One can ask how degrees of freedom in $\mathcal{A}$ are entangled with those in $\mathcal{A}^c = \Sigma \backslash \mathcal{A}$. By now we have a good idea about the entanglement entropy associated with the reduced density matrix $\rho_{\mathcal{A}} = \mathrm{Tr}_{\mathcal{A}^c}(|\,0\rangle\langle\,0\,|)$ either by direct field theory computation in $d = 2$ using the replica trick or using holography in all d.

To be be specific let us examine two situations which are particularly simple, where the field theory calculation boils down effectively to a spectral computation. Consider a conformally invariant field theory which we will place on one of two background geometries for the present:

(i). $\mathcal{B}_d = \mathbb{R}^{d-1,1}$ (Mink): $|\,0_p\,\rangle$ is the Minkowski or Poincaré vacuum and $\mathcal{A}$ is a ball shaped region centered w.l.o.g. at the origin

$$\mathcal{A} \subset \mathbb{R}^{d-1}: \quad r \leq R\,, \qquad ds^2_{\mathcal{B}} = -dt^2 + dr^2 + r^2\, d\Omega^2_{d-2}\,. \tag{2.3.23}$$

(ii). $\mathcal{B}_d = \mathbf{S}^{d-1} \times \mathbb{R}$ (ESU). $|\,0_g\,\rangle$ is the global or vacuum and $\mathcal{A}$ is a polar-cap region about the north pole of $\mathbf{S}^{d-1}$

$$\mathcal{A} \subset \mathbf{S}^{d-1}: \quad \theta \leq \theta_{\mathcal{A}}\,, \qquad ds^2_{\mathcal{B}} = -dt^2 + R^2\left(d\theta^2 + \sin^2\theta\, d\Omega^2_{d-2}\right). \tag{2.3.24}$$

The reasons for using R to denote the size of the ball as well as the curvature radius of the sphere in the two distinct cases will become clear momentarily. For these two cases we will exploit a well known fact about the reduced density matrix $\rho_{\mathcal{A}}$ to make some inferences about the negativity.

Let us begin by recalling some salient features elucidated in [48]. For our two regions the domain of dependence D is conformally equivalent to the hyperbolic cylinder $\mathbb{H}_d = H_{d-1} \times \mathbb{R}$, with the curvature radius of the hyperbolic space H_{d-1} being R. Since the entanglement structure is a property of an entire causal domain, not just a spatial region, we can as well think of $\mathscr{E}(\rho_{\mathcal{A}})$ as a function defined on D.[15]

With this understanding the conformal mapping of [48] implies that the reduced density matrix $\rho_{\mathcal{A}}$ is unitarily equivalent to the thermal density matrix for the CFT on the hyperbolic cylinder[16] $\mathbb{H}_d$

$$\rho_{\mathcal{A}} = \mathcal{U}\,\rho_\beta\,\mathcal{U}^\dagger\,, \qquad \beta = 2\,\pi\,R\,. \tag{2.3.25}$$

We note that the temperature is set by R and in particular it is independent of $\theta_{\mathcal{A}}$ for the theory on ESU. This is intuitive on dimensional grounds, though we should note that the angular dependence is implicit in $\rho_{\mathcal{A}}$. For e.g., in computing entanglement entropy a

[15] In the language of [64] we should think of the negativity also as a wedge observable. Thus it is also subject to the constraints of causality as described therein for entanglement entropy.

[16] We refer the reader to [48] for explicit expressions of the unitary map.

$\theta_{\mathcal{A}}$ dependence will arise by relating the UV cut-off on ESU with the IR cut-off for the CFT on the hyperbolic cylinder. It is perhaps more instructive to note that the modular Hamiltonian defined via $\rho_{\mathcal{A}} = e^{-H_{\mathcal{A}}}$ has an explicit dependence on the angular extent of the polar-cap (see e.g., [65]).

We interpret this result as follows. The vacuum state of the tensor product $\mathcal{H}_{\mathcal{A}} \otimes \mathcal{H}_{\mathcal{A}^c}$ for the aforementioned choice of regions is expressible in terms of the thermal state on the hyperbolic cylinder. Schematically, we can write

$$\psi_0\big|_{\text{Mink, ESU}} = \psi_\beta\big|_{\mathbb{H}}\,, \tag{2.3.26}$$

From this observation using (2.2.18) we infer that (for either $|0_p\rangle$ or $|0_g\rangle$)

$$\mathscr{E}(\psi_0) = 2\,\pi\,R\,(F_{\mathbb{H}}(2\pi R) - F_{\mathbb{H}}(\pi R))\,, \tag{2.3.27}$$

where $F_{\mathbb{H}}$ is the free energy of the CFT on the hyperbolic cylinder.

So the problem of computing negativity in the vacuum state of a CFT can thus be mapped to computing the spectrum on the hyperbolic space. As long as we have this spectral data we can then immediately infer the negativity of the vacuum. It will turn out that the negativity has an inherent UV divergence and necessitates a UV regulator for its computation.

To ascertain the divergence structure we note that a UV regulator on $\mathcal{B}_d$ maps to an IR regulator on $\mathbb{H}_d$ by virtue of the conformal mapping. We have from the analysis of [48] the relations

$$L_{\mathbb{H}} = \log\left(\frac{2R}{\epsilon_{\text{Mink}}}\right)\,, \qquad L_{\mathbb{H}} = \log\left(\frac{2\,R}{\epsilon_{\text{ESU}}}\,\sin\theta_{\mathcal{A}}\right)\,, \tag{2.3.28}$$

in the two cases of interest. Here $L_{\mathbb{H}}$ is the IR regulator of the length scale in the hyperbolic cylinder and $\epsilon_{\mathcal{B}}$ is the UV cut-off in the background indicated. This mapping between the cut-offs can be used to express the volume of the hyperbolic cylinder in terms of field theory data on $\mathcal{B}_d$. Denoting by $\text{Vol}(H_{d-1})$ the spatial volume of a unit radius of curvature hyperbolic space,using the explicit expression mapping the cut-offs (2.3.28), one obtains the desired expression for $\mathcal{B}_d = \text{Mink}_d$,

$$\begin{aligned}\text{Vol}(H_{d-1}) &= \omega_{d-2}\int_1^{\frac{R}{\epsilon}} dx\,(x^2-1)^{\frac{d-3}{2}}\,, \qquad \omega_{d-2} = \frac{2\,\pi^{\frac{d-1}{2}}}{\Gamma\left(\frac{d-1}{2}\right)} \\ &\simeq \frac{\omega_{d-2}}{d-2}\left[\left(\frac{R}{\epsilon}\right)^{d-2} - \frac{(d-2)(d-3)}{2\,(d-4)}\left(\frac{R}{\epsilon}\right)^{d-4} + \cdots + V_{\text{univ}}\right]\end{aligned} \tag{2.3.29}$$

where

$$V_{\text{univ}} = \frac{\sqrt{\pi}}{2}\,\frac{\Gamma(\frac{d-1}{2})}{\Gamma(\frac{d}{2})}\begin{cases} (-1)^{\frac{d}{2}-1}\,\dfrac{2}{\pi}\,\log\left(\dfrac{2\,R}{\epsilon}\right)\,, & d \in 2\mathbb{Z}_+ \\ (-1)^{\frac{d-1}{2}}\,, & d \in 2\mathbb{Z}_+ + 1 \end{cases} \tag{2.3.30}$$

Similar expressions can be derived for $\mathcal{B}_d = \text{ESU}_d$; all we would need to do is replace the upper limit of the integral in (2.3.29) by the appropriate cut-off expression given in (2.3.28). Armed with this information we now present some expressions for the negativity using various results already present in the literature.

CFTs in 2 dimensions: In $d = 2$ we have a simplifying feature that H_1 is flat. Indeed using the result $F(T) = -\frac{\pi}{12}(c_L + c_R)\, T^2\, L$ for a thermal CFT at temperature T in spatial volume L we find

$$\mathscr{E}(\psi_0) = \frac{c}{2}\log X\,, \qquad X = \begin{cases} \frac{2R}{\epsilon}\,, & \mathcal{B} = \text{Mink} \\ \frac{2R}{\epsilon}\sin\theta_{\mathcal{A}}\,, & \mathcal{B} = \text{ESU} \end{cases} \tag{2.3.31}$$

One may alternatively have derived this answer by using (2.2.22) and the familiar result $S^{(q)} = \frac{c}{6}\left(1 + \frac{1}{q}\right)\log X$ for CFT_2.

Free CFTs in various dimensions: The second example where we can explicitly compute the negativity is to use the results for the free energy $F_{\mathbb{H}}$ of free fields in various dimensions. Results for free scalars in all dimensions were derived initially in [66] and analogous results for various theories in $d = 3$ were obtained in [67]. From here we can immediately read off the answer for the Renyi entropy at $q = \frac{1}{2}$ and thence the negativity using (2.2.22).

For a free field of mass m in $\mathbb{R}^{2,1}$ one has the free energy on $\mathbb{H}$ at temperature β explicitly in closed form [67] in terms of the function

$$\mathcal{I}_{\eta,q}(m) = \int_0^\infty d\lambda\, \lambda\, \tanh^\eta(\pi\lambda)\, \log\left(1 - \eta\, e^{-2\pi q\sqrt{\lambda^2+m^2}}\right). \tag{2.3.32}$$

Here $\eta = \pm 1$ encode the statistics ($\eta = +1$ for bosons and $\eta = -1$ for fermions respectively). One then finds that the negativity for free massless fields are given as

$$\begin{aligned} \mathscr{E}(\psi_p^\eta) &= \frac{\text{Vol}(H_2)}{\pi}\left(\mathcal{I}_{\eta,1}(0) - 2\,\mathcal{I}_{\eta,\frac{1}{2}}(0)\right) \\ &= \frac{\text{Vol}(H_2)}{\pi}\int_0^\infty d\lambda\, \lambda\, \tanh^\eta(\pi\lambda)\, \log\left(\frac{1 - \eta\, e^{-2\pi\lambda}}{\left(1 - \eta\, e^{-\pi\lambda}\right)^2}\right). \end{aligned} \tag{2.3.33}$$

Note that the integral is convergent and all the divergences are encoded in the pre-factor $\text{Vol}(H_2)$, which we have already expressed in terms of the relevant variables in Eq. (2.3.29). The expression for $\mathscr{E}(\psi_g)$ would be similar with an appropriate replacement of the volume of the hyperbolic space.

Let us also record the expression for the entanglement entropy for the reduced density matrix $\rho_{\mathcal{A}}$ for comparison. One has from [67]

$$S(\rho_{\mathcal{A}}^\eta) = \frac{\text{Vol}(H_2)}{2\pi}\left[\mathcal{I}_{\eta,1}(0) - \frac{(7-\eta)\,\zeta(3)}{8\,\pi^2}\right]. \tag{2.3.34}$$

We see from (2.3.33) and (2.3.34) that the divergent terms in the negativity are (structurally) the same as in the entanglement entropy; the numerical coefficient however is rather different. Let us define the ratio

$$\mathcal{X}_d = \left|\frac{\mathtt{C}_{\text{univ}}\left[\mathscr{E}(\psi_{\mathtt{p}})\right]}{\mathtt{C}_{\text{univ}}\left[S(\rho_{\mathcal{A}})\right]}\right| \tag{2.3.35}$$

where $\mathtt{C}_{\rm univ}[x]$ denotes the coefficient of the universal term $V_{\rm univ}$ occurring in the expression x. We claim that this quantity gives a precise measure of the negativity for $|0\rangle$ in terms of the entanglement entropy of the reduced density matrix $\rho_{\mathcal{A}}$.

For a free massless scalar in $d = 3$ we find $\mathcal{X}_3^{\rm free} \approx 2.716$, while for a massless fermion $\mathcal{X}_3^{\rm free} \approx 1.888$. We note that $\mathcal{X}_3(m)$ defined formally for massive fields is a monotonically increasing function of m. We will return to this ratio below once we also obtain analogous results from holography for strongly coupled CFTs.

Results for Renyi entropies for spherical entangling regions are also known for free $SU(N)$ $\mathcal{N} = 4$ Super-Yang Mills theory in $d = 4$ [68]. From these results we find

$$\begin{aligned} \mathscr{E}(\psi_p) &\simeq N^2 \left[\frac{R^2}{\epsilon^2} - \frac{41}{24}\log\left(\frac{R}{\epsilon}\right)\right] \\ S(\rho_{\mathcal{A}}) &\simeq N^2 \left[\frac{1}{2}\frac{R^2}{\epsilon^2} - \log\left(\frac{R}{\epsilon}\right)\right] \end{aligned} \tag{2.3.36}$$

This is a peculiar example where the structure of divergent terms in the negativity for the ground state differs from that in the entanglement entropy of the reduced density matrix induced in the spherical region $\mathcal{A}$.[17] From the expressions above we find that $\mathcal{X}_4 = \frac{41}{24} \simeq 1.708$ for free $\mathcal{N} = 4$ SYM.

Holographic CFTs in diverse dimensions: Our final example is the class of holographic field theories in various dimensions. While the computation of the spectrum of an interacting CFT on $\mathbb{H}$ is in general unfeasible, holography provides us with a simple answer when the CFTs in question have (a) large central charge and (b) a sufficient gap in the spectrum. The reason is that the computation of the free energy at temperature β amounts to finding an asymptotically locally AdS_{d+1} geometry whose boundary is $\mathbb{H}_d$, with the Euclidean time direction having a period β. The relevant geometry is well known, it is the so called hyperbolic black hole in AdS_{d+1} [69]. The bulk metric is given as

$$ds^2 = -\frac{\ell_{\rm AdS}^2}{R^2} f(r)\, dt^2 + \frac{dr^2}{f(r)} + r^2\, d\Sigma^2_{H_{d-1}}\,, \qquad f(r) = \frac{r^2}{\ell_{\rm AdS}^2} - \left(\frac{r_+}{r}\right)^{d-2}\left(\frac{r_+^2}{\ell_{\rm AdS}^2} - 1\right) - 1 \tag{2.3.37}$$

whose conformal boundary is indeed $\mathbb{H}$ with the desired spatial curvature R. r_+ is the location of the horizon and we have explicitly kept the AdS length scale $\ell_{\rm AdS}$. We note that the combination of this length scale and the $(d+1)-$dimensional Newton's constant $G_N^{(d+1)}$ gives the effective central charge $c_{\rm eff}$ of the dual CFT: $c_{\rm eff} = \frac{\ell_{\rm AdS}^{d-1}}{16\,\pi\, G_N^{(d+1)}}$.

This geometry has in fact been used before to compute the Renyi entropies for holographic field theories in [70] and we can in fact use their results to infer the behaviour of

[17] We find this rather peculiar in light of the conformal mapping described above. Given the free scalar/fermion and holographic results one might have been tempted to consider the ratio of the negativity to the entanglement entropy en masse, without isolating the universal part (assuming both computations be regulated in a similar fashion). We thank Horacio Casini and Tadashi Takayanagi for useful discussions on this point.

the negativity directly. We first note that the black hole thermodynamic data are given in terms of the geometric parameters as

$$T = \frac{d\, r_+^2 - (d-2)\, \ell_{\rm AdS}^2}{4\,\pi\, R\, \ell_{\rm AdS}\, r_+}\,, \qquad S = \frac{1}{4\, G_N^{d+1}}\, r_+^{d-1}\, {\rm Vol}(H_{d-1})\,. \tag{2.3.38}$$

Given that we know the free energy and the entropy, we can invoke standard thermodynamic relation $S(T) = -\frac{\partial F}{\partial T}$ to obtain the final result [70]

$$\mathscr{E}(\psi_p) = \pi\, c_{\rm eff}\, {\rm Vol}(H_{d-1})\, \mathcal{X}_d^{\rm hol} = S(\rho_{\mathcal{A}})\, \mathcal{X}_d^{\rm hol}\,, \tag{2.3.39}$$

where the dimension dependent coefficient $\mathcal{X}_d^{\rm hol}$ for holographic CFTs is a simple function of the spacetime dimension

$$\mathcal{X}_d^{\rm hol} = \left(\frac{1}{2}\, x_d^{d-2}\, (1+x_d^2) - 1\right)\,, \qquad x_d = \frac{2}{d}\left(1 + \sqrt{1 - \frac{d}{2} + \frac{d^2}{4}}\right)\,. \tag{2.3.40}$$

This function interpolates rather mildly between $\mathcal{X}_2^{\rm hol} = \frac{3}{2}$ and $\lim_{d\to\infty} \mathcal{X}_d^{\rm hol} = (e-1) \approx 1.718$, hinting that up to an overall multiplicative renormalization much of the information is already contained in the entanglement entropy.

It is also curious to note that in $d = 3$ one can compare the free field answers to the strong coupling results obtained above.[18] For a free scalar field we find $\mathcal{X}_3^{\rm hol} \approx 0.601\, \mathcal{X}_3^{\rm free}$, while for a free Dirac field the proportionality is larger $\mathcal{X}_3^{\rm hol} \approx 0.864\, \mathcal{X}_3^{\rm free}$.

It would be interesting to understand this ratio which suggests a decrease in (distillable?) entanglement in the strong coupling regime from first principles. The ratio of our measure at weak and strong couplings $\frac{\mathcal{X}^{\rm hol}}{\mathcal{X}^{\rm free}}$ can decrease either by the total entanglement being reduced at strong coupling or more simply by just the negativity decreasing. In the latter case one would only find a decrease in the amount of distillable entanglement at strong coupling. Ascertaining which of these scenarios is realized might provide new clues in the relation between geometry and entanglement.

A similar comparison for $\mathcal{N} = 4$ SYM gives a much more intriguing result $\mathcal{X}_4^{\rm hol} \approx 0.98\, \mathcal{X}_4^{\rm free}$, where we switched to using the ratio of the coefficient of the universal logarithmic terms (2.3.35) owing to the non-trivial behaviour of the free theory answer (2.3.36). In this case it is rather curious that the free field result undergoes a very mild reduction as we crank up the coupling. Similar comparisons for the Renyi entropies of $\mathcal{N} = 4$ SYM at different q are described in some detail in [71].

2.4 Holographic negativity: general expectations

Having understood the basic features of entanglement negativity in the vacuum state of a CFT for bipartitioning by spherical regions, we now turn to more general situations. Most

[18] Since we are considering ratios of the negativity to the entanglement, the precise normalization of central charge $c_{\rm eff}$ is immaterial, unlike the case when we compare the entanglement entropy at weak and strong coupling.

of the discussion below will be of a qualitative nature, devoted to explaining some of the general features.

2.4.1 Arbitrary bipartitions of pure states

Let us start with pure states $|\Psi\rangle$. Once again we can focus on bipartitioning a Cauchy slice of the background geometry for the field theory as $\Sigma = \mathcal{A} \cup \mathcal{A}^c$. We can then relate the negativity $\mathscr{E}(\psi)$ to the Renyi entropy $S^{(1/2)}(\rho_{\mathcal{A}})$ (for the bipartition $\mathcal{H}_{\mathcal{A}} \cup \mathcal{H}_{\mathcal{A}^c}$). Hence as long as we are in a position to compute the Renyi entropies for non-integral values, we would be able to ascertain the negativity.

To obtain the Renyi entropy at index half, we follow the the holographic computation of [22].[19] For an arbitrary region $\mathcal{A}$ we therefore consider replicating the background geometry $\mathcal{B}$ to $\mathcal{B}_q$ on which we place our field theory. $\mathcal{B}_q$ would as usual be characterized by having branch points inside $\mathcal{A}$ (and its images under the replica construction). Having obtained the answers for integral q which involves finding bulk saddle points with boundary $\mathcal{B}_q$ we then analytically continue to $q = \frac{1}{2}$. A-priori it is not clear that this last step can be carried out for all choices of $\mathcal{A}$.

One can infer the following about the negativity in pure states of a CFT from the basic definition even in the absence of an explicit computation:

- The negativity in a pure state is divergent with the leading divergent term scaling like the area of the entangling surface $\partial\mathcal{A}$.
- The structure of the sub-leading divergent terms is identical to that encountered in the computation of the entanglement entropy for the reduced density matrix $\rho_{\mathcal{A}}$ in holographic field theories. This follows from the fact that the divergent terms encountered in the evaluation of the on-shell action in gravity during the computation of the Renyi entropies is independent of q.
- Perhaps more importantly the value of the negativity $\mathscr{E}(\psi)$ is in general larger than the entanglement entropy $S(\rho_{\mathcal{A}})$. The difference we conjecture should be in a geometric factor. To wit, the ratio $\mathcal{X}_{\mathcal{A}}$ defined analogously to (2.3.35) should depend just on the geometry of the entangling surface $\partial\mathcal{A}$.

2.4.2 Mixed state negativity

In principle in the holographic discussion we do not need to restrict attention to pure states. In fact, given that the negativity is naturally intended to test mixed states, one ought to be considering density matrices ρ and attempt to compute their negativity. This as far as we know has been only achieved in $d = 2$ CFTs in [49]. While we have no concrete

[19] At this stage we have to restrict states $|\Psi\rangle$ to have a moment of time reflection symmetry and at this preferred instant of time. A general prescription for computing holographic Renyi entropies (even for integer q) in time-dependent states is not available at present.

computation to report in this context, it is worth recording various cases of interest for future exploration.

The general situation which one can consider can be motivated in the following manner. Given a state in some quantum field theory, we focus on some region $\mathcal{A}$ lying on a particular Cauchy slice. By integrating out the degrees of freedom in $\mathcal{A}^c = \Sigma \backslash \mathcal{A}$ we obtain the reduced density matrix $\rho_{\mathcal{A}}$ as usual. Now we further bipartition $\mathcal{A}$ itself, i.e., divide $\mathcal{A} = \mathcal{A}_L \cup \mathcal{A}_R$. With this decomposition at hand we define the negativity $\mathscr{E}(\rho_{\mathcal{A}})$ as before by partial transposing the part of the density matrix associated with $\mathcal{A}_L$. As concrete examples consider:

(a). Take $\mathcal{A}$ to be the spherical region of size R in $\mathbb{R}^{d-1}$ considered in §2.3 in our previous construction and pick any two mutually adjoining regions for $\mathcal{A}_L$ and $\mathcal{A}_R$ respectively.

(b). $\mathcal{A}$ itself could be the composed of two disconnected regions which we can associate with the bipartitioning of interest.

(c). $\mathcal{A} \subset \Sigma_R$ in the thermofield double state $|\Psi\rangle_\beta \in \mathcal{H}_L \otimes \mathcal{H}_R$. One can attempt to quantify the negativity of ρ_β^R for the bipartition defined by $\Sigma_R = \mathcal{A} \cup \mathcal{A}^c$.

For these situations it no longer suffices to compute a particular Renyi entropy for some reduced density matrix. Instead one computes the Renyi negativities for the density matrix $\rho_{\mathcal{A}}$, and analytically continues the even sequence of these down to $q_e \to 1$ as explained earlier. The state of the art is the computations of [49] in $d = 2$ CFTs for certain specific configurations. For instance, for $\mathcal{A} \subset \mathbb{R}$ being a segment of length ℓ bipartitioned into two segments of length $\ell\,\alpha$ and $\ell\,(1-\alpha)$ respectively the negativity was found to be $\mathscr{E}(\rho_{\mathcal{A}}) = \frac{c}{4} \log\left[\alpha\,(1-\alpha)\,\frac{\ell}{\epsilon}\right]$. The computation was made possible by explicit computation of twist operator correlation functions in $d = 2$. We refer the reader to [49] for a discussion of other configurations and corresponding results for finite systems, disjoint regions, etc..

It should be possible to carry out in some specific holographic situations a direct computation of the relevant quantities. We postpone this to the future, concentrating at present on the general lessons to be learnt from holography.

Bipartitioning of $\mathcal{A}$ and phase transitions?: Let us start with cases (a) and (b) described above where $\mathcal{A}$ is partitioned into $\mathcal{A}_L \cup \mathcal{A}_R$ (case (c) is elaborated upon in §4.6). In such cases one commonly considers the mutual information $I(\mathcal{A}_R, \mathcal{A}_L)$. This is defined in terms of the entanglement entropy for the reduced density matrices induced on the two components:

$$I(\mathcal{A}_L, \mathcal{A}_R) = S(\rho_{\mathcal{A}_L}) + S(\rho_{\mathcal{A}_R}) - S(\rho_{\mathcal{A}})\,. \tag{2.4.41}$$

If $\partial\mathcal{A}_L \cap \partial\mathcal{A}_R \neq \emptyset$ as in case (a), then both the mutual information and the negativity diverge as the area of this common boundary owing to the UV degrees of freedom in its vicinity.

There is an interesting phenomenon that occurs for holographic theories[20] in case (b) where $\mathcal{A}$ is composed of two disjoint regions. The mutual information vanishes to leading order in c_{eff} when the regions are widely separated [39]. In the holographic construction this occurs because one has to pick the globally minimal area surface (subject to boundary conditions and the topological homology constraint), which allows for phase transitions.

Moreover, this behaviour is well understood in $d = 2$ in large $c_{\text{eff}} = c$ CFTs in terms of a phase transition in Renyi entropies for widely separated intervals [72,73]. To understand this let us describe the region by its end-points as $\mathcal{A} = [u_1, v_1] \cup [u_2, v_2] \subset \mathbb{R}$. The computation of the Renyi entropy $S^{(q)}$ involves computing the four-point correlation function of $\mathbb{Z}_q$ twist operators $\mathcal{T}_q$

$$S^{(q)}: \quad \langle\, \mathcal{T}_q(u_1)\, \bar{\mathcal{T}}_q(v_1)\, \mathcal{T}_q(u_2)\, \bar{\mathcal{T}}_q(v_2)\, \rangle \tag{2.4.42}$$

which depends only on the cross-ratio $x = \frac{(v_1-u_1)\,(v_2-u_2)}{(u_2-u_1)\,(v_2-v_1)} \in [0,1]$ (up to some universal scale invariant factor). At large central charge c this correlation function undergoes a phase transition at $x = \frac{1}{2}$. This is seen by decomposing the above using the OPE expansion and evaluating the contributions of the conformal block in a saddle point approximation (valid for large c). For small x the result is dominated by the s-channel factorization but for $x > \frac{1}{2}$ the t-channel factorization takes over. In the bulk the transition is between a single connected surface and two disconnected surfaces computing $S(\mathcal{A})$.

One might anticipate that a similar behaviour will pertain in the negativity as well since to compute the negativity one instead evaluates [49]

$$\mathscr{E}: \qquad \langle\, \mathcal{T}_{q_e}(u_1)\, \bar{\mathcal{T}}_{q_e}(v_1)\, \bar{\mathcal{T}}_{q_e}(u_2)\, \mathcal{T}_{q_e}(v_2)\, \rangle \tag{2.4.43}$$

Up to a switch of the insertions $u_2 \leftrightarrow v_2$ the computation is very similar to the one required for Renyi (2.4.42). The correlator (2.4.43) has a non-trivial dependence on the cross-ratio x, in addition to some universal contribution arising from scale invariance. This seems to suggest that there ought be a similar phase transition in the negativity at $x = \frac{1}{2}$ for large central charge theories.

The argument however appears to be a bit more subtle than suggested above.[21] To see the issue first consider the four-point functions relevant for the Renyi computation (2.4.42). By a suitable conformal transformation we map this to

$$\langle\, \mathcal{T}_q(0)\, \bar{\mathcal{T}}_q(x)\, \mathcal{T}_q(1)\, \bar{\mathcal{T}}_q(\infty)\, \rangle \equiv \mathtt{F}_q(x) \tag{2.4.44}$$

and we recall that $\mathcal{T}_q$ is a twist or anti-twist operator with dimensions

$$h_q = \bar{h}_q = \frac{c}{24}\left(q - \frac{1}{q}\right). \tag{2.4.45}$$

[20] A necessary condition in field theory terms is that the field theories have large central charge $c \gg 1$ (so as to admit a planar limit) and a low density of states for energies below a gap set by c.

[21] We thank Tom Hartman and Alex Maloney for discussions on this issue.

It is sufficient to understand the behaviour of this function, since one can by utilizing the swap $u_2 \leftrightarrow v_2$ map the four-point function required for the negativity (2.4.43) to above. Tracking through the conformal transformations one finds [49]

$$\frac{\langle\, \mathcal{T}_q(u_1)\, \bar{\mathcal{T}}_q(v_1)\, \bar{\mathcal{T}}_q(u_2)\, \mathcal{T}_q(v_2)\,\rangle}{\langle\, \mathcal{T}_q(u_1)\, \bar{\mathcal{T}}_q(v_1)\, \mathcal{T}_q(u_2)\, \bar{\mathcal{T}}_q(v_2)\,\rangle} = (1-x)^{8\,h_q}\, \frac{\mathtt{F}_q\left(\frac{x}{x-1}\right)}{\mathtt{F}_q(x)} \tag{2.4.46}$$

We thus have a direct link between the two computations and all we need is the behaviour of the function $\mathtt{F}_q(x)$. One has control on this function for $x \in [0,1]$ from the analysis of [73] in the large c limit (cf., footnote 20), which can be used to argue that the Renyi entropies undergo a phase transition. To make an argument for the negativity however requires that we also control the function outside this domain. It is tempting to conjecture that the phase transition does indeed happen and moreover one encounters a similar behaviour in higher dimensions. We leave a more detailed analysis for the future.

2.5 Discussion

In this chapter we have focussed on properties of entanglement negativity, defined as a measure of distillable entanglement in a given state of a quantum system. The rationale for its definition lies in understanding the entanglement structure of mixed states. To gain some intuition for this quantity we explored its properties in simple states such as the vacuum of a CFT in various dimensions. While we laid out some general expectations for the behaviour of negativity in holographic field theories more generally, we did not offer any concrete computations in supporting evidence. We hope to remedy this in the near future. It is nevertheless useful to take stock and examine some of the questions posed by the analysis we have undertaken.

First of all, it is interesting to ask if there is some intrinsic meaning to the geometric pre-factor $\mathcal{X}_{\mathcal{A}}$. Since $\mathscr{E}$ provides only an upper bound on the distillable entanglement, what physical interpretation, if any, should be ascribed to its being greater than the entanglement entropy? Can one think of $\mathcal{X}_{\mathcal{A}}\, c_{\text{eff}}$ as a measure of the effective number of Bell pairs that can be distilled out of a pure state in a CFT?

We have also seen earlier that this function renormalizes and for spherically symmetric regions $\mathcal{X}_{\mathcal{A}}$ it was smaller (in magnitude) at strong coupling. Does this reduced amount in distillable entanglement have a fundamental significance in how spacetime geometry is related to the presence of entanglement? It would be instructive to know whether one can formalize some statement along these lines in a quantitative fashion. At a more prosaic level it would be interesting to understand this function both as a function of the state ψ as well as the geometry of the region $\mathcal{A}$.

Secondly, all of our discussion has been restricted to density matrices at a moment of time symmetry (or in special cases static density matrices). This allowed us in the general context to make use of the generalized gravitational entropy construction of [22] to compute the Renyi entropies and negativities for integer values of the index q. These are clearly special situations and one would like to be able to make statement for time-evolving

states. As in the case of entanglement entropy extending the construction to dynamical situations could perhaps teach us some new lessons about spacetime and entanglement.

As a final comment, we turn to the situation where $\mathcal{A}$ is a single connected region, but one has a mixed state on the entire Cauchy slice Σ (denoted ρ_Σ) (case (c) in §2.4.2). As remarked earlier one of the main reasons to focus on negativity is to understand the precise nature of entanglement in mixed states. In the holographic context one encounters an interesting feature for the entanglement entropy of reduced density matrices $\rho_\mathcal{A}$ induced from a parent thermal state. When $\mathcal{A}$ is a sufficiently large region of the Cauchy slice one finds an interesting phenomena dubbed entanglement plateaux [32]: $S(\rho_\mathcal{A}) = S(\rho_{\mathcal{A}^c}) + S_{\rho_\Sigma}$, i.e., Araki-Lieb inequality [74] is saturated. This behaviour has been argued to be robust in holographic field theories for finite systems at large c_{eff}.

One can interpret this to mean that the entanglement inherent in $\rho_\mathcal{A}$ has two distinct contributions: (i) the quantum entanglement between the region and its complement encapsulated in $S(\rho_{\mathcal{A}^c})$ and (ii) correlations built into the thermal density matrix S_{ρ_Σ}. This distinction seems to suggest that in this regime there is a clear demarcation in the degrees of freedom inside $\mathcal{A}$ in terms of their entanglement properties [75] (see also [76] for related considerations). Indeed this interpretation is natural from the perspective of the disentangling theorem for tripartite systems described in §2.2. The thermofield double state which purifies the density matrix ρ_Σ factorizes as in (2.2.11) with $B = \mathcal{H}_\mathcal{A}$. It would be fascinating to see this arise directly by computing the negativities in the holographic context.

Chapter 3

Topology and the sign of entanglement in field theory

This chapter is a reproduction of the paper *Central Charges and the Sign of Entanglement in 4D Conformal Field Theories* [77], written in collaboration with Eric Perlmutter and Mukund Rangamani.

In the previous chapter we introduced the ratio between the coefficients of the universal terms of respectively, the logarithmic nagativity and entanglement entropy, for spherical regions in the vacuum of a field theory. Motivated by quantum information arguments we conjectured that for any field theory this quantity should be larger than one. Further evidence was derived in [78] [79] that considered, in perturbation theory, deformation of the entangling surface.

For arbitrary regions, the general structure of the universal term of Renyi entropies in four dimensional CFTs was derived in [68]. It is the sum of three integrals of geometric data, specifically the intrinsic curvature, extrinsic curvature and Weyl tensor, each of which is multiplied by a function of the anomalies of the theory. Various properties of these functions were derived in [78] [79], which also provided evidence for further constrains.

Drawing on their analysis, this work shows that in the quite unusual case where the anomalies satisfy the condition $a > c$, and if the genus of the entangling surface is large enough, the ratio defined above can be smaller than one.

Note: the results presented in this chapter rely on some assumptions about the coefficients of the formula derived in [68]. It has recently be argued in [80] that the relation $f_b(q) = f_c(q)$ might not be correct.

3.1 Introduction

States of a quantum mechanical system are distinguished by the presence of entanglement. Oftentimes one characterizes this by bipartitioning the system and computing the entanglement entropy, S. In continuum quantum systems, the natural subdivision is geometric:

we partition the state across a fiducial *entangling surface*. While (for pure states) S is the best measure of the total amount of quantum entanglement between a region and its complement, other measures provide additional information about the pattern of entanglement for the same bipartition. A natural question is: given a fixed state of the system, how does entanglement depend on the geometry and topology of the entangling surface?

While S is plagued with UV divergences in a continuum QFT, its universal piece contains non-trivial physical information, including central charges and RG monotones [48, 81–83]. In many respects, these universal terms are the natural counterparts of quantum-mechanical entropies, which are positive. Another interesting measure is the logarithmic negativity $\mathscr{E}$ [37, 59, 60], which gives an upper bound on distillable entanglement in quantum mechanics, and is thus strictly greater than the entanglement entropy.

These intuitive analogies with quantum mechanics suggest that, in QFT, the universal, cutoff-independent terms of S and of $\mathscr{E} - S$ are also positive-definite. Indeed, this appears to be true for spherical entangling surfaces in vacuum states of CFTs in flat spacetime [30, 48, 82, 83]. As we will prove, however, these signs depend non-trivially on the topology of the entangling surface and, in particular, can be negative.

We focus on connected entangling surfaces in 4d CFTs, which are Riemann surfaces. While for simple topologies the universal terms are positive-definite, we show that one can always pick complex enough entangling surfaces to violate this bound. Curiously, the violation hinges on the difference of the central charges a and c. Specifying to entanglement entropy, the universal part of S becomes negative for a suitable choice of surface if and only if $a > c$; the effect is linear in the product of $a - c$ and the genus of the surface, exhibiting a novel interplay between central charges and topological sensitivity of entanglement.

3.2 Entanglement measures

Consider a (relativistic) QFT on a d-dimensional spacetime $\mathcal{B}$; the state ρ ($=|\,\psi\rangle\langle\,\psi\,|$ if pure) is defined on a spatial Cauchy slice Σ at fixed time. The biparitioning is provided by geometrically dividing $\Sigma = \mathcal{A} \cup \mathcal{A}^c$ across a smooth spacetime codimension-2 entangling surface $\partial\mathcal{A}$. Defining the reduced density matrix $\rho_{\mathcal{A}} = \mathrm{Tr}_{\mathcal{A}^c}(\rho)$, the entanglement and Rényi entropies are:

$$\begin{aligned} S(\rho_{\mathcal{A}}) &= -\mathrm{Tr}\,(\rho_{\mathcal{A}}\,\log\rho_{\mathcal{A}}) = \lim_{q\to 1} S^{(q)}(\rho_{\mathcal{A}})\,, \\ S^{(q)}(\rho_{\mathcal{A}}) &= \frac{1}{1-q}\,\log\mathrm{Tr}\,({\rho_{\mathcal{A}}}^q)\,. \end{aligned} \tag{3.2.1}$$

Another quantity of interest to us will be the negativity which is defined in terms of an auxiliary partial transposed density matrix ρ^Γ. Picking a basis, $|\,\mathfrak{r}_i\rangle$ for $\mathcal{A}$ and $|\,\mathfrak{l}_n\rangle$ for $\mathcal{A}^c$, one defines the map $\rho \to \rho^\Gamma$ as:

$$\langle\,\mathfrak{r}_i\,\mathfrak{l}_n\,|\,\rho^\Gamma\,|\,\mathfrak{r}_j\mathfrak{l}_m\rangle = \langle\,\mathfrak{r}_i\,\mathfrak{l}_m\,|\,\rho\,|\,\mathfrak{r}_j\mathfrak{l}_n\rangle\,. \tag{3.2.2}$$

Thence, the *logarithmic negativity* is given in terms of the trace norm, $\|\mathcal{O}\|$, viz.,

$$\mathscr{E}(\rho) = \log\|\rho^\Gamma\| = \log\left[\mathrm{Tr}\left(\sqrt{(\rho^\Gamma)^\dagger\,\rho^\Gamma}\right)\right] \tag{3.2.3}$$

It is important to note that the negativity provides an upper bound on entanglement inherent in the state and as such satisfies $\mathscr{E} \geq S_{\mathcal{A}}$. For mixed states the negativity is notoriously hard to compute (see [31, 49, 84, 85] for results in 2d CFTs). For pure states one can relate it to the Rényi entropy [31], viz., $\mathscr{E}(\rho = |\,\psi\rangle\langle\,\psi\,|) = S^{(\frac{1}{2})}(\rho_{\mathcal{A}})$. This was exploited in [30] to explore negativity for ball-shaped regions with $\partial\mathcal{A} = \mathbf{S}^{d-2}$ in a CFT vacuum.

Local dynamics of a QFT implies that the measures, collectively denoted as $\mathsf{E} = \{S, S^{(q)}, \mathscr{E}\}$ are UV divergent. Given a UV cut-off ϵ one finds [39]

$$\mathsf{E} = \sum_{k=0}^{d-4} \frac{\mathsf{E}_k}{\epsilon^{d-2-2k}} - \begin{cases} C_{\rm univ}[\mathsf{E}]\, \log \frac{\ell_{\mathcal{A}}}{\epsilon} + C_0\,, & d = \text{even} \\ (-1)^{d-1}\, C_{\rm univ}[\mathsf{E}]\,, & d = \text{odd} \end{cases} \tag{3.2.4}$$

The leading UV-divergence obeys an area law, $\mathsf{E}_0 \propto \text{Area}(\partial\mathcal{A})$, followed by scheme-dependent (but state independent) subleading pieces E_k. $C_{\rm univ}[\mathsf{E}]$ depends on the state and captures important universal physical information; for $\partial\mathcal{A} = \mathbf{S}^{d-2}$ in the vacuum, for instance, $C_{\rm univ}[S(\rho_{\mathcal{A}})]$ is a measure of degrees of freedom.

3.3 Entangling geometries

Our specific interest will be in $d = 4$, where $\partial\mathcal{A}$ can be taken to be a Riemann surface of arbitrary topology; we will explore how topology imprints itself on the entanglement. Two particular issues will be of concern to us:

- Is $C_{\rm univ}[S(\rho_{\mathcal{A}})] \equiv S_{\rm u}$ sign-definite?
- Consider the ratio
$$\mathcal{X} = \frac{C_{\rm univ}[\mathscr{E}(\rho)]}{C_{\rm univ}[S(\rho_{\mathcal{A}})]} \tag{3.3.5}$$
defined originally in [30]. Is $\mathcal{X} - 1 \equiv \widehat{\mathcal{X}}$ positive definite?

Recently, variants of this question have been addressed by several authors: [86] and [87] examined the shape dependence of entanglement entropy for entangling surfaces of spherical topology in d dimensions. The latter conjectured that $\partial\mathcal{A} = \mathbf{S}^{d-2}$ minimizes the universal term in that topological class. In [88], the authors searched for surfaces that maximize entanglement entropy keeping the area of $\partial\mathcal{A}$ fixed. They related the construction to a well-known geometric problem called the Willmore conjecture [89]. Their conclusion was that in $d = 4$, the maximizer over *all* topological classes is $\partial\mathcal{A} = \mathbf{S}^2$. We will make use of their techniques to show that this is, in fact, not true for general CFTs, and appears to rely on the tacit assumption that $a = c$.

3.3.1 Universal Rényi entropy of 4d CFTs

To make progress we will make use of a result for $C_{\rm univ}[S^{(q)}] \equiv S_{\rm u}(q)$ in 4d CFTs [68] (nb $S_{\rm u} = S_{\rm u}(1)$):

$$S_{\rm u}(q) = \frac{f_a(q)}{2\pi}\, \mathcal{R}_{\partial\mathcal{A}} + \frac{f_b(q)}{2\pi}\, \mathcal{K}_{\partial\mathcal{A}} - \frac{f_c(q)}{2\pi}\, \mathcal{C}_{\partial\mathcal{A}} \tag{3.3.6}$$

The geometric quantities depend on intrinsic and extrinsic geometry of $\partial\mathcal{A} \subset \mathcal{B}$. For an embedded 2-surface X,

$$\begin{aligned}\mathcal{R}_X &= \int_X d^2x\,\sqrt{\gamma}\,{}^{\gamma}R\,,\\ \mathcal{K}_X &= \int_X d^2x\,\sqrt{\gamma}\left[K^{\alpha}_{ij}\,K^{\alpha ij} - \frac{1}{2}\,(K^{\alpha\,i}_{i})^2\right]\\ \mathcal{C}_X &= 2\int_X d^2x\,\sqrt{\gamma}\,C_{\mu\nu\rho\sigma}t^\mu s^\nu t^\rho s^\sigma\end{aligned} \tag{3.3.7}$$

Here γ_{ij} is the intrinsic metric on X, $g_{\mu\nu}$ that of the full spacetime $\mathcal{B}$, K^{α}_{ij} is the extrinsic curvature of X with $\alpha = \{t, s\}$ indexing the two normal directions (one timelike t^μ and the other spacelike s^μ) and $\mathcal{C}_X$ is the pullback of the Weyl tensor $C_{\mu\nu\rho\sigma}$ onto X.

We see here a clean separation between the geometric data and the intrinsic field theory features captured by the coefficient functions $f_{a,b,c}(q)$. In the $q \to 1$ entanglement limit [81],

$$f_a(1) = a\,, \qquad f_b(1) = f_c(1) = c\,. \tag{3.3.8}$$

For generic q, these functions are known not to obey a universal form.

We now have some ammunition to tackle the questions we raised. For simplicity we will take $\mathcal{B} = \mathbb{R}^{3,1}$ (or equivalently $\mathcal{B} = \mathbf{S}^3 \times \mathbb{R}$ as appropriate for radial quantization). These backgrounds being conformally flat, one finds no contribution from $f_c(q)$, for $\mathcal{C}_{\partial\mathcal{A}} = 0$. If we further restrict attention to regions $\mathcal{A}$ which lie on constant time slices, $K^t_{\mu\nu} = 0$. We can then focus on the purely spatial geometry of 2-surfaces $\partial\mathcal{A}$ embedded in either $\mathbb{R}^3$ or $\mathbf{S}^3$. This allows us to use some useful results in Riemannian geometry to make precise statements.

With this understanding let us focus attention on $S_{\rm u}(q)$ and $\widehat{\mathcal{X}}$, and ask if they obey any sign-definiteness properties.

3.3.2 Of central charges and Rényi coefficients

Let us start by noting some basic results that hold for unitary CFTs. The central charges a, c are positive definite and their ratio is bounded as [90]

$$\frac{1}{3} \leq \frac{a}{c} \leq \frac{31}{18}\,. \tag{3.3.9}$$

The bounds are tighter in superconformal field theories. Recently it has been argued that the Rényi coefficient functions are not independent and satisfy

$$f_b(q) = f_c(q) = \frac{q}{q-1}\left[a - f_a(q) - (q-1)\,f_a'(q)\right] \tag{3.3.10}$$

The first of these equalities has not been shown in full generality but holds in both free and holographic CFTs [91]. We will however assume this in what follows. The second has been proved directly in Rényi index perturbation theory [78]. One can further prove

$$f_a(q) > 0\,,\;\; f_a'(q) < 0 \quad\Longrightarrow\quad f_c(q) > 0\,,\quad \forall\; q \tag{3.3.11}$$

where we used (3.3.10) in obtaining the implication. The inequalities on $f_a(q)$ follow from the fact that $S(\rho_{\mathcal{A}})$ obeys general inequalities for any $\mathcal{A}$ [92], and that $S(\rho_{\mathcal{A}}) \propto f_a(q)$ for $\partial\mathcal{A} = \mathbf{S}^2$.

3.3.3 Geometry of entangling surfaces

To make progress we need to examine the geometry of the Riemann surface $\partial\mathcal{A}$. The intrinsic curvature contribution in (3.3.6) is topological; for compact X the Gauss-Bonnet theorem relates it to the Euler number

$$\mathcal{R}_X = 8\pi(1-g)\,. \tag{3.3.12}$$

The extrinsic contribution can be noted to be positive definite (using $K^t_{ij} = 0$, $K^s_{ij} = K_{ij}$)

$$\mathcal{K}_X = \int_X d^2x\,\sqrt{\gamma}\,\left(K_{ij} - \frac{1}{2}\,\gamma_{ij}\,\gamma^{kl}\,K_{kl}\right)^2 \tag{3.3.13}$$

This by itself is not sufficient, but we can invoke some geometry, see [88]. Introduce the Willmore energy functional [89][1]

$$\mathcal{W}_{X\subset\mathbf{S}^3} = \frac{1}{4}\int_X d^2x\,\sqrt{\gamma}\left(1 + \frac{1}{4}\,(\gamma^{ij}\,K_{ij})^2\right). \tag{3.3.14}$$

This functional was introduced by Willmore, who explored surfaces which minimize their mean curvature. It obeys $\mathcal{W}_X \geq 4\pi$ for all X, and is minimized by the equatorial $\mathbf{S}^2 \subset \mathbf{S}^3$. Willmore conjectured that at $g = 1$, the Willmore functional obeys $\mathcal{W}_X \geq 2\pi^2$. This result was proven recently [93]; the unique minimizer is the Clifford torus, whose stereographic projection onto $\mathbb{R}^3$ yields a torus with $\tau = i/\sqrt{2}$. This conjecture was generalized to higher genus, where there exist so-called Lawson surfaces [94] L_g for $g \geq 2$ satisfying

$$4\pi \leq \mathcal{W}_{L_g} \leq 8\pi\ , \tag{3.3.15}$$

which are conjectured to be the unique minimizers of $\mathcal{W}_X$ [95]. The precise value of $\mathcal{W}_{L_g}$ is unknown, but at every genus it has been proven that there is a surface that obeys (3.3.15), irrespective of being the minimizer [95, 96]. These results will suffice for our purposes.[2] See [99] for further details.

To make use of the bounds on the Willmore functional, we exploit the Gauss-Codazzi equations, which are geometric identities which relate intrinsic and extrinsic curvatures. The relation we need is simple (cf., [88]):

$$\mathcal{W}_X = \frac{1}{2}\,(\mathcal{R}_X + \mathcal{K}_X) \tag{3.3.16}$$

For compact X we are immediately in business, since we can use the topological constraint on the Euler number and the geometric constraint (3.3.15) of Lawson surfaces to examine

[1] For surfaces embedded in $\mathbb{R}^3$ we can drop the contribution from the area of the surface.

[2] Lawson surfaces tend to be bulgy with small handles, especially as g increases. We encourage the reader to peruse the numerically-constructed surfaces in Table 1 of [97] or Figure 1 of [98].

bounds on $S_{\rm u}$ and $\widehat{\mathcal{X}}$. In particular, plugging (3.3.16) into (3.3.6), we dial up the genus, driving $\mathcal{R}_{\partial\mathcal{A}}$ negative, while restricting to Lawson surfaces $\partial\mathcal{A} = L_g$ which have $\mathcal{W}_{L_g}$ bounded from above.

3.4 Entanglement bounds

Let us begin by studying the bounds on the universal part of entanglement entropy. It is useful to treat the genus $g = 0$ cases first and then consider $g \geq 1$. For a spherical entangling surface, it is known from [48] that the Rényi entropies are related to thermal entropies on the hyperbolic cylinder $\mathbb{H}^3 \times \mathbb{R}$. The geometry is such that the extrinsic curvature term $\mathcal{K}_{\partial\mathcal{A}}$ vanishes and so $S_{\rm u}(q) = 4f_a(q)$, which we have shown is positive definite, cf., (3.3.11). It then follows as described in [30] that $\widehat{\mathcal{X}} = \frac{1}{a} f_a(\frac{1}{2}) - 1$ is also positive definite. Assuming the sphere is the minimizer of $\widehat{\mathcal{X}}$ at $g = 0$, this establishes positivity for all $g = 0$ entangling surfaces. Alternatively, positivity follows from (3.4.19) if one assumes that $\alpha_W > 0$ for all CFTs. As we will discuss, this is true in all known examples.

Let us turn to entangling surfaces with non-trivial topology. Simplifying (3.3.6) using (3.3.16),

$$\begin{aligned} S_{\rm u} &= \frac{c}{2\pi}\left(2\,\mathcal{W}_{\partial\mathcal{A}} + \left(\frac{a}{c} - 1\right)\,\mathcal{R}_{\partial\mathcal{A}}\right) \\ &= \frac{c}{2\pi}\left(\frac{2a}{c}\,\mathcal{W}_{\partial\mathcal{A}} + \left(1 - \frac{a}{c}\right)\,\mathcal{K}_{\partial\mathcal{A}}\right). \end{aligned} \tag{3.4.17}$$

These equations make it clear that there is a curious interplay between the sign of the central charge difference $c - a$, the topology and geometry of $\partial\mathcal{A}$, and the sign of $S_{\rm u}$. While there is no constraint from toroidal topology (as $c > 0, \mathcal{W} > 0$), we can infer that for $g \geq 2$:

- $a \leq c \implies S_{\rm u} > 0$, $\forall\ \partial\mathcal{A}$ owing to the lower bound on the Willmore functional and positivity of $\mathcal{K}$.
- $a > c \implies S_{\rm u} \gtrless 0$. The indefinite sign owes its origin to the fact that there are Lawson surfaces which have genus-independent bounded $\mathcal{W}$ (3.3.15), but $\mathcal{R}$ that can be made arbitrarily negative by ramping up the genus. The sign flip of $S_{\rm u}$ across such surfaces occurs at a critical genus

$$g_c = 1 + \frac{\mathcal{W}_{L_{g_c}}}{4\pi}\frac{c}{a-c}\,. \tag{3.4.18}$$

  We note in passing that it is strongly believed that $\mathcal{W}_{L_g}$ monotonically increases with g [100].

In [88] it has been conjectured that $\partial\mathcal{A} = \mathbf{S}^2$ minimizes $S_{\rm u}$ (assuming $a = c$). We now see that when $a > c$, there is no minimizer: $S_{\rm u}$ is unbounded from below.

Note that not all higher genus surfaces will render $S_{\rm u} < 0$. However, this is guaranteed to occur above some critical genus for all surfaces whose Willmore energy grows slower

than linearly in g. There are likely other families of surfaces besides the Lawson surfaces, as well as isolated surfaces that exist for particular values of g, that satisfy this criterion. For example, one can smoothly deform Lawson surfaces with fixed topology.[3]

Strictly speaking, the results above pertain to bounded regions $\mathcal{A}$ so that $\partial\mathcal{A}$ is compact. For non-compact entangling surfaces we are not aware of any obvious upper bound on $\mathcal{W}$.

Let us now turn to the negativity and consider the quantity $\widehat{\mathcal{X}}$ which was conjectured in [30] to be positive definite. Using the definition in terms of the Willmore functional and the expressions (3.3.10) we can write:

$$\begin{aligned} \widehat{\mathcal{X}} &= \frac{\alpha_R\,\mathcal{R}_{\partial\mathcal{A}} + 2\,\alpha_W \mathcal{W}_{\partial\mathcal{A}}}{2c\;\mathcal{W}_{\partial\mathcal{A}} + (a-c)\,\mathcal{R}_{\partial\mathcal{A}}} \\ \alpha_R &= \frac{1}{2}\,f_a'(\frac{1}{2}) + c\,, \qquad \alpha_W = f_c(\frac{1}{2}) - c \end{aligned} \tag{3.4.19}$$

We can infer that the sign of $\widehat{\mathcal{X}}$ depends on the coefficients α_R and α_W in a non-trivial fashion.

- For a toroidal entangling surface, $\widehat{\mathcal{X}} \propto \alpha_W$ and so positivity requires $f_c(\frac{1}{2}) > c$. This is seen to be true in all known examples.
- At higher genus, if $a \leq c$ we require that $\alpha_R \leq 0$ to ensure $\widehat{\mathcal{X}} \geq 0$.
- On the other hand if $a > c$, we can easily end up with negative values of $\widehat{\mathcal{X}}$: even if $\alpha_R \leq 0$ there is some genus g for which $\widehat{\mathcal{X}} \leq 0$. This is because whilst the numerator is ensured to be positive, the denominator can be made arbitrarily negative by picking an appropriate Lawson surface. The situation cannot be remedied by changing the sign of α_R in any obvious manner.

3.5 Examples

We have derived above some general conditions for the positivity of $S_{\rm u}$ and $\widehat{\mathcal{X}}$ in terms of the central charges. In Table 3.1 we provide explicit results for a class of free and holographic CFTs [68, 70, 78].

Several comments are in order. First, all known examples obey the inequalities $\alpha_W > 0$ and $\alpha_R < 0$. We believe that these are likely to be true for all CFTs.

Second, $\widehat{\mathcal{X}}$ is shape-independent for the free scalar. It follows from [78] that $\widehat{\mathcal{X}}$ is shape-independent only for theories whose $f_a(q)$ equals that of a free scalar; besides the scalar itself, there are no known examples of such theories.

[3] See [98] for such a construction at $g = 2$, especially Figures 2 and 5 therein.

Theory	$\frac{a}{c}$	$f_a(q)$	$f_c(q)$	α_R	α_W	$S_{\rm u}$	$\widehat{\mathcal{X}}$
Scalar	$\frac{1}{3}$	$\frac{(1+q)(1+q^2)}{4\,q^3}\,a$	$3\,f_a(q)$	$-\frac{11}{2}\,a$	$\frac{33}{4}\,a$	$\frac{(3\,\mathcal{W}-\mathcal{R})}{\pi}a$	$\frac{11}{4}$
Fermion	$\frac{11}{18}$	$\frac{(1+q)(7+37q^2)}{88\,q^3}\,a$	$\frac{3(1+q)(7+17q^2)}{88\,q^3}\,a$	$-\frac{7}{4}\,a$	$\frac{261}{88}\,a$	$\frac{(36\,\mathcal{W}-7\,\mathcal{R})}{22\pi}a$	$\frac{77\,\mathcal{R}-261\,\mathcal{W}}{28\,\mathcal{R}-144\,\mathcal{W}}$
Vector	$\frac{31}{18}$	$\frac{1+q+31q^2+91q^3}{124\,q^3}\,a$	$\frac{3(1+q)(1+11q^2)}{124\,q^3}a$	$-\frac{11}{62}\,a$	$\frac{63}{124}\,a$	$\frac{(13\,\mathcal{R}+36\,\mathcal{W})}{62\pi}a$	$\frac{-11\mathcal{R}+63\,\mathcal{W}}{26\,\mathcal{R}+72\,\mathcal{W}}$
Free $\mathcal{N}=4$	1	$\frac{1+q+7q^2+15q^3}{24q^3}a$	$\frac{(1+q)(1+3q^2)}{8q^3}a$	$-\frac{11}{12}a$	$\frac{13}{8}\,a$	$\frac{\mathcal{W}}{\pi}a$	$\frac{-11\mathcal{R}+39\mathcal{W}}{24\mathcal{W}}$
Einstein	1	$\frac{q}{2(q-1)}(2-x_q^2-x_q^4)a$	$\frac{3q}{2(q-1)}(x_q^2-x_q^4)a$	$-\frac{3}{4}a$	$\frac{1+6\sqrt{3}}{8}a$	$\frac{\mathcal{W}}{\pi}a$	$\frac{-3\mathcal{R}+(1+6\sqrt{3})\mathcal{W}}{8\mathcal{W}}$

Table 3.1: Results for the universal terms in Rényi entropy and their implications for $S_{\rm u}$ and $\widehat{\mathcal{X}}$ in a class of CFTs. We have chosen to write the answers in terms of the a central charge. In the last line, we have defined $x_q \equiv \frac{1}{4q}(1+\sqrt{1+8q^2})$.

Finally, the free vector field is the only theory in this table with $a > c$, and indeed, we see that both $S_{\rm u}$ and $\widehat{\mathcal{X}}$ become negative for sufficiently negative $\mathcal{R}$ and upper-bounded $\mathcal{W}$, as happens for Lawson surfaces. Assuming monotonicity of $\mathcal{W}_{L_g}$ as a function of g, the critical genus is $g_c = 4$. In arriving at this conclusion, we are assuming that the modular Hamiltonian that defines $f_a(q)$ includes the effects of the edge modes described in [101] and [102]. This is necessary for $S_{\rm u}$ to be determined by the a central charge for spherical entangling regions. Curiously, ignoring these modes leads to $S_{\rm u}$ being determined by $\hat{a} = \frac{16}{31}\,a$ [103] which satisfies $\hat{a} < c$. Exploring the dependence of $S_{\rm u}$ on the entangling surface should reveal whether it is controlled by $\hat{a}$ as opposed to the physical central charge a; our diagnostic would simply involve a sign check for a $g = 5$ Lawson entangling surface.

3.6 Discussion

We have found that in CFTs with $a > c$, the universal term in entanglement entropy, $S_{\rm u}$, necessarily becomes negative for certain higher genus entangling surfaces. The negativity ratio $\widehat{\mathcal{X}}$ also generically becomes negative for $a > c$; if $\alpha_R \leq 0$ for all CFTs, this can only happen for $a > c$. It would be nice to establish whether $\alpha_R \leq 0$ and $\alpha_W > 0$ identically, as suggested by all examples.

Aside from the free vector, theories with $a > c$ include the IR fixed point of the $SU(2)$ model of [104], as well as the non-Lagrangian Gaiotto-type T_N theories [105]. The latter are IR limits of worldvolume theories of N $M5$-branes wrapping genus-$\hat{g}$ Riemann surfaces. A characteristic example is the A_{N-1} theory preserving $\mathcal{N}=2$ SUSY, which has $24(a-c) = (N-1)(\hat{g}-1)$ for $\hat{g} > 1$. Central charges for a larger family of related $\mathcal{N}=1$ theories with $a > c$ are given in [106]. At large N [107], where $a, c \propto N^3$, there is an interesting relation between N and the entangling surface topology: namely, the critical genus g_c in (3.4.18) scales like N^2. The growth of g_c with large N will be true of any holographic theory with a sensible derivative expansion in the bulk [108].

It is worth noting that $a - c$ controls and relates to many phenomena in CFT and holography. These include the mixed current-gravitational anomaly [109] in SCFTs; superconformal indices and their high temperature asymptotics [110–112]; violations of the KSS bound on η/s in holographic CFTs [113, 114]; and the size of the single-trace higher spin gap in large N SCFTs [115].

Finally, it is a remarkable and still mysterious fact that nearly all "traditional" CFTs have $a \leq c$ rather than $a > c$. Our result may be regarded as suggesting a naturalness of such asymmetry, along the lines of [110]. It would be very interesting to make this more concrete.

Chapter 4

Qubits systems and holographic entanglement structures

This chapter is a reproduction of the paper *Entanglement structures in qubit systems* [116], written in collaboration with Mukund Rangamani.

In the previous two chapters the discussion pertained mainly measures of entanglement, and in particular logarithmic negativity, in quantum field theory. The main reason to consider such a quantity, instead of other measures like Renyi entropies, is the fact that negativities have an operational interpretation in terms of entanglement manipulations and are sensible to different kinds of entanglement. Unfortunately, at present it is not known how to calculate the logarithmic negativity for a single subregion in a mixed state of a field theory or between two subregions. Furthermore, no measure of multipartite quantum entanglement have even been defined for field theories.

The lack of tools to explore patterns of entanglement directly in field theory forces us to look at simpler systems, where other entanglement measures can be computed and have an operational interpretation. In this chapter we look at quantum mechanics and in particular we focus our attention on systems made of few qubits. We compute negativities between subsystems and explore the ratio between negativity and entropy that was at the centre of the discussion in the previous two chapters. In field theory it was more natural to use the logarithmic version of the negativity, here instead we will prefer the negativity. This is motivated by the fact that for Hilbert spaces of finite dimensions, and for pure states, there is a nice operational interpretation of this quantity called *robustness of entanglement*. Intuitively, this is a measure of the amount of noise that has to be injected into the system to completely erase its quantum entanglement. We explore how the ratio depends on the pattern of entanglement of the entire state.

Furthermore, when the size of the system is small, all the possible states can be classified into equivalence classes of entanglement structures defined by certain operations. Given a state one can use different measures of entanglement to determine the corresponding class and further explore the entanglement structure. In this way we learn what pattern of entanglement produces properties which are known to characterize holographic

states, such as the saturation of the Araki-Lieb inequality or the sign definiteness of tripartite information. Although simple systems of few qubits are very different from field theories, these investigations represent a starting point towards a deeper understanding of entanglement structures in field theory with particular focus on the operational perspective and its meaning for holography.

4.1 Introduction

One of the key features distinguishing quantum mechanics is the presence of entanglement which is a natural consequence of the superposition principle. Usually this is characterized simply by the inability to separate a composite system into its constituent parts without losing some information about the whole. The lack of knowledge of how the individual parts comprise the entire system is encoded by entanglement.

While the presence or absence of entanglement elicits a binary response, one often would like to know more and in particular be able to quantify the precise nature of entanglement in a quantum system. In simple bipartite systems, e.g., two qubits, this is easily done using the von Neumann entropy of the reduced density matrix for one of the components. This quantity which is referred to as the entanglement entropy provides a complete characterization of the entanglement inherent in the state.[1] However, this ceases to be the case in more general scenarios: density matrices of bipartite systems or equivalently pure states of multipartite systems.

To quantify the amount of entanglement in more general cases various measures of entanglement have been proposed in the quantum information literature. Some of these which we shall review in the sequel are easy to compute, while others have restricted applicability. Nevertheless, given that the structure of entanglement in multi-component systems can get rather intricate (if only due to the rapid growth of potential permutations involved), it is interesting to contrast the different observables against each other.

While this is an interesting exercise in its own right in quantum mechanics, part of our motivation in attempting to understand such detailed structure of entanglement stems from potential insights it can offer in the context of holography. One of the amazing facts about the holographic AdS/CFT correspondence is the observation that the entanglement in a class of strongly coupled planar field theories is geometrized in terms of a gravitational background in higher dimensions. This statement is manifest in the holographic entanglement entropy proposals of Ryu and Takayanagi [20, 39] and its covariant generalization [23]. A more intricate and intriguing picture arises when we ask whether the structure of entanglement in the field theory is itself responsible for the emergence of geometry as was first suggested a few years ago in [26, 40, 41]. These ideas have been central to the recent thesis that "entanglement builds geometry" codified succinctly in the

[1] To be sure this only captures the entanglement under the obvious bipartitioning; we will later be careful to distinguish this from the entanglement contained in further subdivisions of the each system.

statement ER = EPR [29].

One obvious question in this context is the following: is the emergence of geometry simply reliant on the presence or absence of entanglement, or does it depend more crucially on the structure of entanglement? Most discussions in the holographic context presuppose a pure state of a bipartite system whence entanglement entropy suffices. However, we should be able to ask for the emergence of geometry in situations where the configuration in question is more complicated and admits no simple bipartite description. Typical scenarios we have in mind are multipartite systems exemplified by the multi-boundary wormhole geometries of [117–119] in three dimensions. Here the precise manner in which the individual parts are entangled does play a role in the emergence of some sort of semi-classical geometry and indeed previous investigations [50, 51] indicate this to be the case.

The prototype scenario for this discussion is a N-partite system wherein integrating out $(N-3)$ components leads to a density matrix for the residual three components. In this case, it is known following an interesting analysis of [120] that the density matrix of the resulting tripartite system has to have non-positive definite tripartite information (see below) in order to admit a semi-classical geometry as a holographic dual.[2] On the other hand for simple quantum systems the tripartite information can have either sign, so not all states of a tripartite system can a-priori admit a semi-classical gravity dual. This point was already made in [51], cautioning that the ER=EPR statement should be accompanied by some riders. We will take this as sufficient motivation to examine the nature of entanglement in simple systems.

To set the stage for our discussion, let us recall that in the holographic context we are interested in studying continuum quantum field theories in the large central charge limit. While the central charges can be formally defined in terms of conformal anomalies, it is operationally useful to think them as measuring the curvature scale of the holographic dual geometry $\ell_{\rm AdS}$ in units of the Planck constant ℓ_P, viz., $c_{\rm eff} \sim \ell_{\rm AdS}/\ell_P$. Thus $c_{\rm eff} \gg 1$ corresponds to the regime where semi-classical geometry is trustworthy.[3] Heuristically this means that we are interested in considering systems with a large number of degrees of freedom. Given such a theory we want to understand what structures of entanglement are possible.

The canonical route of exploration is to consider various measures of entanglement in continuum QFTs, such as entanglement entropy, Renyi entropies, negativity etc.. However, these quantities are rather difficult to compute generically in interacting systems. If we

[2] As far as we know this condition is necessary but not sufficient to guarantee a semi-classical geometric dual. The constraint was derived in [120] by examining the properties of holographic entanglement entropy, essentially adapting the arguments leading to the proof of strong-subadditivity of holographic entanglement entropy. It appears not to follow simply from strong subadditivity, making it in an independent statement about systems with large numbers of degrees of freedom as is relevant for holography. We thank Matthew Headrick and Veronika Hubeny for an extremely illuminating discussion on this point.

[3] Strictly speaking we also need $\ell_{\rm AdS} \gg \ell_s$ where ℓ_s is the string scale, which requires the field theory coupling being large. If not we end up with a classical theory, but one which involves stringy excitations as well.

start with a pure state in the QFT and demarcate various (disjoint) regions $\mathcal{A}_i$ $i = 1, \cdots, M$, then while it is possible to compute the entanglement entropy for $\cup_i \mathcal{A}_i$ in holographic systems,[4] it is harder to compute the Rényi entropies and negativities.[5]

Entanglement negativity, introduced in [37], is a clean measure of the quantum entanglement even for mixed states, while the usual von Neumann entropy is contaminated by classical correlations. This is particularly pertinent, if we are interested in understanding the entanglement between two of our regions, say $\mathcal{A}_j$ and $\mathcal{A}_k$, after tracing out the state. Entanglement properties of the density matrix $\rho_{\mathcal{A}_j \cup \mathcal{A}_k}$ are more cleanly encoded in the negativity, which bounds the amount of distillable entanglement, so it tells us directly how many Bell pairs are common to this disjoint region. It is however quite hard to compute it in continuum systems.[6]

In a previous work [30], we examined the (logarithmic) negativity in the vacuum state of a CFT (for bipartitionings given by connected regions of spherical topology). We conjectured that the ratio of the universal part of the logarithmic negativity of a pure state with respect to a given bipartitioning was bounded from below by the entanglement entropy of the reduced density matrix obtained by integrating out one of the components.[7] Further analysis of this result for more complicated regions (building on the analysis of [78]) reveals a rather interesting interplay between the central charges of the CFT and the geometry and topology of the entangling surface [77]. Motivated by these observations in the continuum, we introduce a new measure involving negativity, called specific robustness, which is sensitive to the pattern of internal entanglement in simple systems (see below).

To get further insight into features of quantum entanglement we look at a toy problem of non-interacting qubits.[8] Our motivation here is to understand how the measures of entanglement that have been proposed in the quantum information literature serve to help us delineate the entanglement structure of the state. The advantage of working with qubit systems is that we can explicitly compute (at least for small numbers of qubits) various measures of entanglement. Starting with a pure state of N-qubits, we can consider tracing out $k < N$ qubits and examining the entanglement inherent in the remainder $(N-k)$-qubits. Furthermore we can consider different bipartitions (or multi-partitions) of the

[4] Given a collection of boundary regions as above, the [23,39] require one to solve a classical gravitational problem to find an extremal surface in the geometry dual to the state in question. Even in complicated geometries, this is a problem of solving classical partial differential equations, which whilst involved, is nevertheless a lot simpler than the quantum problem (the simplification is made possible by the $c_{\text{eff}} \gg 1$ limit).

[5] Similar statements apply for entangled states in tensor product of CFTs, e.g., [50, 121].

[6] In recent years negativity has been explored quite extensively in pure and thermal states of two dimensional CFTs in a series of works, cf., [31, 49, 84, 85, 122–124]. We should also note that negativity in spin chains has been studied in [125–128].

[7] The universal part here refers to the renormalization scheme independent term; in even dimensional CFTs it is the coefficient of the logarithmically divergent term, while in odd dimensional CFTs it corresponds to the finite part.

[8] Strictly speaking we pick random pure states of a few qubits and are agnostic about the actual Hamiltonian (which may well be the identity operator); hopefully our terminology does not cause confusion.

remaining qubits and investigate how entanglement is distributed among them and what are its properties. We perform some simple numerical experiments starting with randomly chosen pure states of N-qubits (with $N \leq 8$ for computational reasons) and argue that in general the combination of information emerging from different measures of entanglement can give useful insights about the properties of the state. Even for a fixed bipartition of a pure state, where entanglement entropy determines the amount of entanglement, other measures give additional information about the nature of this entanglement. While the holographic systems we are really after are not as simple as non-interacting qubits, it is useful to use this toy model to build some intuition about the nature of entanglement inherent in many-body wavefunctions.[9]

Following our interest for the ratio between the logarithmic negativity and entanglement entropy motivated by field theory arguments [30, 77], we consider a similar (and strictly related) quantity for qubit system, i.e., the ratio $\mathcal{R}$ between the negativity (not logarithmic) and the entropy. Using a known operational interpretation for the negativity in terms of robustness of entanglement against noise, we introduce the concept of *specific robustness* which is measured by the ratio and investigate how this property is related to the pattern of entanglement inside the state. In the case of 4 qubits, where a classification of the possible states under a particular class of operations (called stochastic LOCC, aka, SLOCC) exists, we show how this additional information allows a partial resolution of the classes and investigate the detailed structure of entanglement within this classification scheme.

We also undertake an analysis of mutual information and the monogamy constraint, both for generic states and also for the different classes of 4 qubits. We find that generically the monogamy constraint is not particularly restrictive. However, if we restrict attention to SLOCC classes of states, we find a unique class that respects monogamy.

In [30] part of the motivation for considering negativities as a measure of entanglement in holographic systems was its ability to provide clear distinction between classicality and quantumness. For bipartitions of mixed states the von Neumann entropy mixes classical and quantum correlations, while negativities can distinguish between them. In a multipartite setting the same problem arises for the tripartite information. We use a measure of multipartite entanglement known as tangle in the quantum information literature, as a witness of intrinsically quantum multipartite correlations. Even though its interpretation is somewhat murky and its definition restricted to qubit systems alone, we show that it provides useful information when compared against the tripartite information (and flesh out some connections to the monogamy of mutual information). Armed with these result for qubit systems, we attempt to draw some general lessons for continuum field theories.

The outline of the chapter is as follows: in §4.2 we introduce the measures of bipartite and multipartite entanglement as well as the notation that we will use for our

[9] The entanglement we explore is more closely related to the notion of particle partition entanglement used in certain contexts to gain information complementary to that contained in spatial cuts of the systems, cf., [129–132].

investigations. We then start in §4.3 with the simplest case of 3 qubits, which serves as an introduction to the kind of investigations that we will later conduct on larger systems. §4.4 is the core of the chapter, we first investigate generic states of 4 qubits and then present a detailed analysis of the structure of entanglement for the known equivalence classes. We extend the analysis to generic states of larger systems (6 and 8 qubits) in §4.5 and discuss the main results and potential implication for holography in §4.6. Appendix 4.A, contains additional plots that complete the main results presented in the other sections.

4.2 Measures of entanglement

The problem of quantifying entanglement has been at the center of research in quantum information theory for the last 15 years, nevertheless no conclusive measure has been found so far that enables us to fully capture the structure of entanglement of generic states. Several measures have been proposed in the literature but they are usually strongly dependent on the specificities of the application for which they have been developed, and often very difficult to compute. Alternatively, quantities with the correct mathematical properties to be good candidates for entanglement witness, often lack a clear physical interpretation. In this section we review some properties of entanglement and some measures that can be efficiently used to investigate its structure. In the following we will be careful in distinguishing classical from quantum correlations and reserve the term *entanglement* for the latter.

4.2.1 Bipartite entanglement

In its original formulation entanglement is a form of correlation that is not compatible with local physics. Bell's inequalities impose a bound on the strength of correlations achievable by local physics, the violation of these constraints is a witness of entanglement, which actually serves as its definition. For pure states this is well understood – states which are not products are entangled and always violate some (generalized) Bell's inequality.

This is not always the case for mixed states. A mixed state ρ in a Hilbert space $\mathcal{H}_A \otimes \mathcal{H}_B$ is said to be *separable* if it is a convex combination of product states

$$\rho = \sum_i p_i \, \rho_i^A \otimes \rho_i^B \,, \qquad \sum_i p_i = 1 \,, \qquad p_i \geq 0 \,, \tag{4.2.1}$$

and *entangled* otherwise. Product states contain no correlation, separable states have only classical correlation (i.e., correlations that can be produced by LOCC[10]) and entangled states contain some sort of quantum correlation.[11] It is important to realize that the bipartition of the system is a crucial part of the definition.

[10] LOCC stands for local operations and classical communication, which includes action by unitaries, measurement and information exchange on classical channels.

[11] The question of whether these correlations may or may not be compatible with local physics is still open, see [30] for additional comments and further references.

From a more recent perspective entanglement, can also be interpreted as a powerful resource for specific protocols that are not possible when only classical resources are available. In this context one often would like to be able to manipulate entanglement, convert it into different forms, extract it from a system and transfer it to another and so on. In this context entanglement can be quantified depending on a specific task such as the preparation of a state (*entanglement of formation*), or the extraction of Bell's pairs from a given state (*entanglement of distillation*) (see [133]).

For pure states of a system where a bipartition is specified, it is well known that entanglement entropy is a measure of the amount of entanglement between the subsystems. In a practical situation where two parties only have limited access to the subsystems this is the best measure known so far, as it quantifies both non-locality and the value of entanglement as a resource for specific tasks such as teleportation.[12] Naïvely it is the number of Bell pairs available.[13]

We want instead to investigate how different subsystems are correlated among each other in a state of a given global system, being particularly careful in distinguishing classical from quantum correlations. One natural way to proceed is to consider different bipartitions of the entire system: this would certainly give additional information about the distribution of correlations. If we restrict this analysis to pure states, entanglement entropy is a reasonable way to capture the quantum entanglement inherent in the state.

The problem becomes much more intricate for mixed states, where the relation between non-locality and the "task dependent" formulation of entanglement is in general not clear at present.[14] In this case the von Neumann entropy is not a good measure of entanglement any more.

This is also a problem one faces in the attempt to completely characterize the internal pattern of entanglement in a given state, even if the state is pure. One can use entanglement entropy as long as only bipartitions of the entire state are considered, but this is not enough to describe the state entirely. Given a pure state of a system ABC, if we want to study the entanglement among internal subsystems, for example A and B alone, we first need to trace out the degrees of freedom in C, but the result of this operation is a mixed state. In order to characterize the entanglement between A and B we need some other measure.

In a previous chapter 2 we focused on negativities [37] as the measures of interest. Let us recall their definitions and salient properties for convenience. Given a density matrix

[12] In this case entanglement entropy is known to be equal to both entanglement of formation and distillable entanglement [133].

[13] This is precisely the meaning of distillable entanglement, but it is important to realize that the definition is an asymptotic statement in the limit where an infinite number of copies of the original state is available. In the context of holography one would prefer an interpretation in terms of a single system.

[14] There exist *bound entangled* states which are entangled (i.e., not separable), but at the same time they are of very limited value as resource for typical quantum information (QI) protocols; specifically Bell pairs cannot be distilled from them.

ρ and a bipartition $\mathcal{H}_A \otimes \mathcal{H}_B$ one defines the *partial transpose* ρ^Γ as

$$\langle \mathfrak{r}_i^{(\mathrm{A})} \mathfrak{l}_n^{(\mathrm{B})} | \rho^\Gamma | \mathfrak{r}_j^{(\mathrm{A})} \mathfrak{l}_m^{(\mathrm{B})} \rangle = \langle \mathfrak{r}_i^{(\mathrm{A})} \mathfrak{l}_m^{(\mathrm{B})} | \rho | \mathfrak{r}_j^{(\mathrm{A})} \mathfrak{l}_n^{(\mathrm{B})} \rangle \tag{4.2.2}$$

The *logarithmic negativity* then is defined as

$$\mathscr{E} = \log \|\rho^\Gamma\| , \tag{4.2.3}$$

where $\|...\|$ denotes the trace norm.[15] This is known to be an upper bound to distillable entanglement. It is in general greater or equal to entanglement entropy (for pure bipartite states), with the equality holding for maximally entangled states. It is somewhat natural in continuum systems as one can give a suitable path integral representation [31]. One can also define the *negativity* as

$$\mathscr{N} = \frac{\|\rho^\Gamma\| - 1}{2} . \tag{4.2.4}$$

While simply related to the logarithmic negativity, it is more convenient to consider in simple discrete systems; hence we will focus for the most part on the negativity itself.

Armed with the tools of entanglement entropy for bipartition of pure states and negativity for bipartition of pure or mixed states, one can ask how much information about the structure of entanglement of a given state can be extracted considering different partitionings and comparing the two measures. More specifically [30, 77, 78] considered the ratio between negativity and entanglement entropy for bipartitions of pure states. One of the motivations of the present work is to flesh out a possible interpretation of this quantity.

To this end it turns out it will be useful to interpret the negativity in terms of another measure of entanglement called *robustness* [63]. Given a state ρ and a separable state ρ_s, one can consider mixtures of the two states and ask how much of ρ_s is necessary to completely disentangle ρ. Formally

$$\tilde{\rho} = \frac{1}{1+s} (\rho + s\rho_s) . \tag{4.2.5}$$

The minimal value of s such that $\tilde{\rho}$ is separable is called the robustness of ρ *relative* to ρ_s. One can then ask what is the minimal value of s for all possible choices of ρ_s, this is the robustness of ρ. Intuitively this corresponds to the robustness of ρ against "intelligent jamming"; it is the minimal amount of noise needed to disrupt the entanglement when we have full knowledge about the structure of the state.

For finite dimensional systems the negativity is known to be equal to a half of the robustness

$$\mathscr{N} = \frac{1}{2} \min_{\forall \rho_s} s . \tag{4.2.6}$$

This then provides a potential interpretation of negativity. Note however that this way to quantify entanglement is operational and is quite different from the intuition we have

[15] The trace norm is defined as $\|\mathcal{O}\| = \mathrm{Tr}\left(\sqrt{\mathcal{O}^\dagger \mathcal{O}}\right)$ for any Hermitian operator $\mathcal{O}$.

for the entropy in terms of non-locality and separability. It is interesting to ask if and how the robustness is related to the internal structure of entanglement, namely to the way entanglement is distributed among subsystems.

Inspired by this concept, to get a quantitative handle, we introduce a measure, which we call *specific robustness* $\mathcal{R}$. It is defined as the ratio of the negativity of a given state (and bipartitioning), to the entanglement entropy of the reduced density matrix under the same bipartitioning. Schematically we can write[16]

$$\mathcal{R} = \frac{\mathscr{N}}{S} \tag{4.2.7}$$

Heuristically we want to think of it as a measure of the minimal amount of noise sufficient to disentangle Bell pairs in a given state. More specifically, given two states with the same entropy but different negativity, we will then interpret the entanglement as more or less robust, depending on the ratio $\mathcal{R}$; higher values of $\mathcal{R}$ would correspond to greater robustness of the entanglement pattern. It is worth reiterating that such a notion of robustness captures the operational sense of the concept, as it relies on a procedure that mixes the state with some noise. We want to ask whether (and how) this quantity depends on the internal pattern of entanglement of the state. In particular, given an entangling surface corresponding to a fixed bipartition, one can distinguish entanglement inside the two subsystems or entanglement "across" the entangling surface. In the rest of the chapter we will examine this quantity in simple qubit systems.

Finally, as a measure of bipartite correlations we recall the definition of mutual information

$$I(A|B) = S(A) + S(B) - S(AB) \tag{4.2.8}$$

This has been argued to capture the total amount of correlations, both classical and quantum [134].

In the theory of quantum information it is often useful to consider inequalities that constrain the values of the measure of interest among different subsystems. One such example is a relation called *monogamy*, which is defined for a quantum information theoretic function f as

$$f(A|B) + f(A|C) \leq f(A|BC) \tag{4.2.9}$$

Monogamy is known to be a general feature of quantum entanglement. One can interpret Eq. (4.2.9) as follows: if f is some entanglement measure, and subsystem A is almost maximally entangled both with subsystem B and a larger one BC, then there is almost no entanglement between A and C, i.e., $f(A|C) = 0$. This corresponds to the common intuition for the concept of monogamy. Alternatively, the monogamy relation is the precise statement of the fact that the "union is more than the sum of its parts". Specifically, there is some subtle correlation between A and the pair BC which is lost if one only looks at

[16] In [30, 77] we considered the ratio $\mathcal{X} = \mathscr{E}/S$ which was convenient in continuum systems. For qubit systems the ratio $\mathcal{R}$ seems more appropriate, and one can anyway translate to $\mathcal{X}$ if necessary.

the correlations $A|B$ and $A|C$. The latter interpretation of monogamy will be crucial in the definition of some measures of multipartite entanglement in the following.

We will be interested in exploring monogamy relations as a potential way to constrain the allowed entanglement structures. Specifically, we will have occasion to explore the monogamy relation for the square of the negativity that was proved in [61]. Another monogamy relation involves the mutual information. While $I(A|B)$ is not monogamous in general, it happens to be so for holographic theories, as proved in [120] (this holds asymptotically at large c_{eff}). We note that recently [135–137] used a similar philosophy to derive a set of (inequality) constraints on holographic theories, using strong-subadditivity and relative entropy.

4.2.2 Multipartite entanglement

The definition of entangled and separable states introduced previously can be extended to a multipartite setting. For a system of N parties a state is said to be *fully separable* if it can be written as[17]

$$\rho = \sum_i p_i \, \rho_i^{A_1} \otimes \rho_i^{A_2} ... \otimes \rho_i^{A_N} \,, \qquad \sum_i p_i = 1 \,, \qquad p_i \geq 0 \,, \tag{4.2.10}$$

where the states ρ_i contain no entanglement. If some of the parties contain some entanglement the state is called *m-separable* if it can be similarly decomposed into a convex linear combination of products of m parts only. A state is said to contain genuine N-partite entanglement if it is neither fully separable nor m-separable for any $m > 1$.

We will focus on pure states as in the mixed case the properties of multipartite entanglement are much less understood. The prototype of multipartite entangled states is the well known GHZ state (a.k.a. cat state), whose general expression for N qubits is given by

$$|\,\text{GHZ}_N\rangle = \frac{1}{\sqrt{2}}(|\underbrace{0\cdots0}_{N}\rangle + |\underbrace{1\cdots1}_{N}\rangle) \tag{4.2.11}$$

This is sometimes called a *maximally entangled* state (in an N-partite sense) as it is the state that violates a N-partite generalization of Bell's inequality maximally [139].

The interpretation and quantification of multipartite entanglement is in general difficult and much less understood than in the bipartite case. Some measures exist but their physical meaning is usually not known. In the following our measure of interest for multipartite entanglement of pure states will be the *N-tangle* (τ_N), which was introduced for three qubits by [140]. In the three qubits case τ_3 is known to quantify the residual multipartite entanglement in the state, which is not captured by its bipartite counterpart[18]

$$\tau_2(A|B) + \tau_2(A|C) + \tau_3(ABC) = \tau_2(A|BC) \tag{4.2.12}$$

[17] For more details about multipartite entanglement see [133] and [138].

[18] For pure states the 2-tangle is simply $\tau_2 = 4 \det \rho_A$, where ρ_A is the usual reduced density matrix of the qubit A.

This equation precisely corresponds to the intuition we have from the previous discussion about monogamy and actually serves as the definition of the tripartite entanglement measure τ_3.

A formal generalization of τ_3 to any even number N of qubits was given in [141]

$$\begin{aligned}\tau_N =& 2\Big|\sum a_{\alpha_1\ldots\alpha_N} a_{\beta_1\ldots\beta_N} a_{\gamma_1\ldots\gamma_N} a_{\delta_1\ldots\delta_N} \times \\ & \epsilon_{\alpha_1\beta_1}\epsilon_{\alpha_2\beta_2}\ldots\epsilon_{\alpha_{N-1}\beta_{N-1}}\epsilon_{\gamma_1\delta_1}\epsilon_{\gamma_2\delta_2}\ldots\epsilon_{\gamma_{N-1}\delta_{N-1}}\epsilon_{\alpha_N\gamma_N}\epsilon_{\beta_N\delta_N}\Big| \end{aligned} \tag{4.2.13}$$

where the coefficients correspond to the components of the state vector $|\psi\rangle$ in the conventional computational basis ($|0\cdots00\rangle$,$|0\cdots01\rangle$, $\ldots$). This quantity is known to be an entanglement monotone[19] and invariant under qubits permutation, nevertheless its interpretation for generic N is not fully understood. For $N = 4$ an interpretation in terms of residual entanglement analogous to the three qubits case was given in [142]. Nevertheless it is worth noting that this interpretation has some peculiarities [142]: for example, $\tau_4 = 1$ for a product state of two Bell pairs suggesting that it cannot be interpreted as a measure of genuine 4-partite entanglement. We emphasize that these measures are only defined for qubits – there is no generalization to a continuous setting.

Another measure of mutipartite correlation that we will use is the so called *tripartite* or *interaction* information (I3). This is measure of tripartite correlation which is defined as:

$$\begin{aligned}\mathsf{I3}(A|B|C) =& S(A) + S(B) + S(C) \\ & - S(AB) - S(BC) - S(AC) + S(ABC)\end{aligned} \tag{4.2.14}$$

It is important to notice that this is a combination of mutual informations and hence it mixes classical and quantum correlation. For generic quantum states the tripartite information can be either negative or positive, but one can rephrase the condition for the monogamy of mutual information in terms of I3 simply as [120]:

$$\mathsf{I3}(A|B|C) \leq 0 \tag{4.2.15}$$

In the following we will investigate the relation between monogamy of mutual information and the structure of internal entanglement for simple qubits systems.

4.2.3 Notation

For the convenience of the reader we summarize here the notation that we will use in the sequel. Given a system of N qubits we employ the following notation to denote various partitionings of interest:

- single qubits will be labeled by small letters: $a, b, c, \ldots$.

[19] A measure of entanglement is called an *entanglement monotone* if its value on a given state cannot increase under the effect of LOCC operations performed on the state.

Figure 1: Example of our notation for 6 qubits, the horizontal line represents the entangling surface Σ. (a) Local entanglement, $\mathscr{N}^{\text{loc}}_{1|1}$. (b) Entanglement across the entangling surface, $\mathscr{N}^{\Sigma}_{1|2}$

- capital letters will identify subsets of qubits: $A, B, C, \ldots$.
- partitioning of N-qubits in groups of $m, n, k, \ldots$ etc., with $m+n+k+\cdots \leq N$ will be denoted simply as $m|n|k|\cdots$ when we don't need to specify the particularities of the grouping.

For example $\mathscr{N}_{a|bc}$ denotes the negativity between qubits a and bc, $\mathscr{N}_{A|BC}$ is the negativity between a subset A and a subset BC (further decomposed into B and C), $\mathscr{N}_{1|2}$ is the negativity between a generic single qubit and two other qubits in the system. Fig. 1 shows an example for 6 qubits.

We will often consider averages of different quantities and use an overline to identify them. For example $\overline{\mathscr{N}_{1|2}}$ is the negativity between a single qubit and two qubits, averaged over all the possible choices of three qubits from the original set. In the following we will mostly focus on systems made of an even number of qubits. For this systems it is obviously possible to consider bipartitions into two subsets with $N/2$ qubits each, we will refer to this particular bipartition as the *maximal* one.

Using natural terminology from the context of holography we will call the fiducial surface that specifies a bipartition of a system the *entangling surface* (Σ). We will be interested in the entanglement among qubits that could lie in the two subsystems across the entangling surface Σ, or in the same one, see Fig. 1. Expressions such as $\mathscr{N}^{\Sigma}_{1|1}$ refer to negativity between one qubit in a subset and one qubit in the other subsystem. In this case we use the expression *entanglement across* Σ. We call instead *local entanglement* the correlation between qubits in the same subsystem, and use expressions like $\mathscr{N}^{\text{loc}}_{1|1}$.

In the following sections we investigate the structure of entanglement for pure states of systems composed by few qubits. These are simple toy models where the structure of entanglement can be studied numerically, nevertheless the pattern of entanglement is highly non-trivial. Our goal is twofold, on the one hand we use qubits systems as simple laboratories to investigate the properties of different measures of entanglement and their interpretation. On the other hand we will look for entanglement structures that might be relevant for bulk reconstruction in holography. We start with the simplest case of three qubits, this serves as an introduction to the kinds of investigations which we will later apply to larger and more interesting systems.

4.3 Warm up: Three qubits

We start by recalling the definition of two particular states, the GHZ and the W states of three qubits:[20]

$$|\mathrm{GHZ}_3\rangle = \frac{1}{\sqrt{2}}(|000\rangle + |111\rangle) \qquad |\mathrm{W}_3\rangle = \frac{1}{\sqrt{3}}(|100\rangle + |010\rangle + |001\rangle) \tag{4.3.16}$$

These states are well known in the literature. The GHZ state only carries genuine tripartite entanglement, this is captured by the fact that the value of the 3-tangle is maximal, $\tau_3 = 1$. In particular after tracing out one of the qubits one is left with a system of two qubits in a separable (mixed) state, i.e., not entangled. On the other hand the W state contains the maximal possible amount of bipartite entanglement, i.e., the correlation between any pair of qubits is maximal. It does not contain any tripartite entanglement and $\tau_3 = 0$. This distribution of internal bipartite entanglement corresponds to the known fragility and robustness against qubits removal of the GHZ and W states respectively. An alternative motivation for considering the GHZ state as the maximally entangled state of three qubits (cf., the definition in terms of Bell inequalities in §4.2.2) is precisely this notion of fragility [139].

General pure states of three qubits were classified in [143]. The classification relies on an equivalence relation under a class of operations called SLOCC (stochastic local operation and classical communication). Two states are considered equivalent when there is a non vanishing probability to convert one state into the other using LOCC and a single copy of the state.[21] There is a total number of six classes: the class of product states, three classes of entangled pairs where the third qubit is not entangled, and two classes of states which contain entanglement involving all three qubits. These are the classes we will focus on, they are called GHZ and W classes from the names of their representatives.

Given any pure state it is possible to decide with certainty which class it belongs to using τ_3. When $\tau_3 = 0$ there is no truly 3-partite entanglement in the state, which is then in the W class. We will reverse the process and use instead τ_3 to generate random states in the two classes for which we study the pattern of bipartite entanglement. It should be noted however that the W class has measure zero with respect to the generic class (GHZ), this means that our numerical investigation will not respect the statistics of the two classes.

We label the qubits by abc. There are three possible bipartitions of the entire system which are generally inequivalent, we will denote them by: $a|bc$, $b|ac$, $c|ab$. For such bipartitions one could in principle consider both entanglement entropy and negativity.

[20] The definition of the W state here is given for the case of 3 qubits, but similarly to the GHZ case the generalization to a higher number of qubits is straightforward.

[21] Equivalence under LOCC instead would require the ability to convert one state into the other with certainty. It is known that when only a single copy of a state is available two states are equivalent under LOCC if and only if they are related by local unitaries (LU) [144]. In this case a classification under LOCC would result in an infinite number of inequivalent classes even for a system of only three qubits.

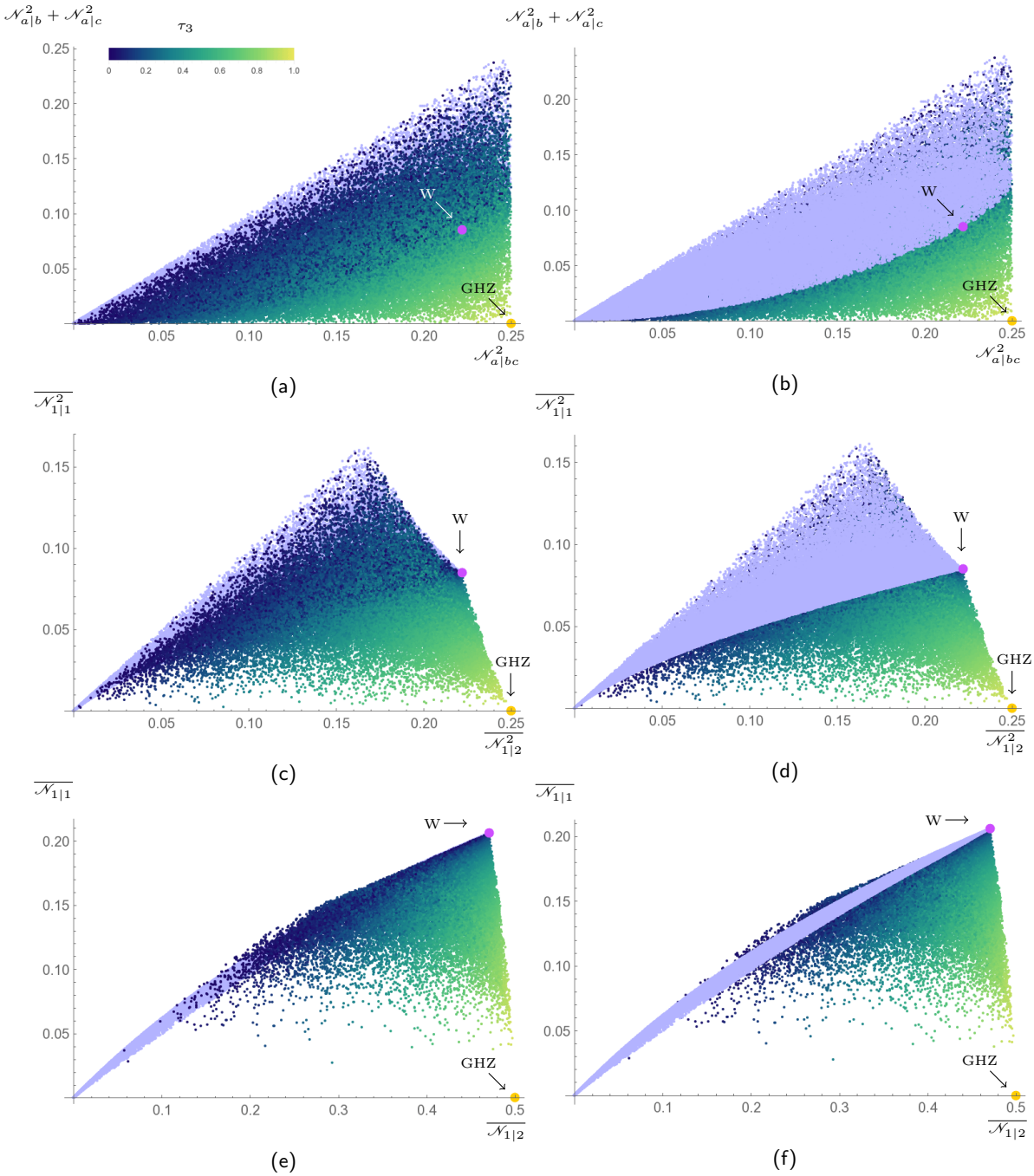

Figure 2: 50000 random states in the W (light violet) and the GHZ (color map) classes. The color map corresponds to the value of τ_3 in the range $(0, 1)$ as shown in panel (a). The GHZ and W states correspond to the orange and purple large dots respectively. Left and right panels show the same plots with different overlay. (a)-(b): Monogamy of the square of the negativity for a specific bipartition of the global system. (c)-(d): Average of the squared negativity over all possible bipartitions. (e)-(f): Average negativity between single qubits compared to the average negativity for bipartitions of the entire system.

Nevertheless since one of the parties only contains a single qubit, its entanglement is completely determined by a single number.[22] This means that if we only look at bipartitions of the entire system there is no additional information carried by a second measure and we can choose to equivalently use either the entropy or the negativity. The negativity being a well defined measure of entanglement, which works well for mixed states, we will prefer it to the entropy and use it to quantify the entanglement between single qubits.

We start by choosing a specific bipartition $(a|bc)$ and computing the following negativities: $\mathscr{N}_{a|bc}$, $\mathscr{N}_{a|b}$, $\mathscr{N}_{a|c}$. As a first exercise we can check the monogamy relation for the square of the negativity which was proved in [61]

$$\mathscr{N}^2_{a|b} + \mathscr{N}^2_{a|c} \leq \mathscr{N}^2_{a|bc} \tag{4.3.17}$$

this is shown in Fig. 2a-2b. We notice that monogamy seems to be saturated more easily by W states. More interestingly we find that there is a lower bound on the internal negativity for W states. Some non-vanishing amount of tripartite correlation is necessary to disentangle pair of qubits while at the same time strongly entangling each qubit with the other pair. An analogous result holds for the average over the three possible bipartitions of the global state, Fig. 2c-2d.

$$2\overline{\mathscr{N}^2}_{1|1} \equiv \frac{2}{3}\left(\mathscr{N}^2_{a|b} + \mathscr{N}^2_{a|c} + \mathscr{N}^2_{b|c}\right) \leq \frac{1}{3}\left(\mathscr{N}^2_{a|bc} + \mathscr{N}^2_{b|ac} + \mathscr{N}^2_{c|ab}\right) \equiv \overline{\mathscr{N}^2}_{1|2} \tag{4.3.18}$$

One can notice how the distribution of the states in the W class is reproduced by the states in the GHZ class with small value of τ_3 (dark blue). It is useful to contrast this behaviour with the saturation of the Arkai-Lieb inequality, but we postpone that discussion till we discuss the situation with more qubits.

As a measure of the strength of correlations in the state it is also interesting to look at the average of the internal negativity between single qubits

$$\overline{\mathscr{N}}_{1|1} \equiv \frac{1}{3}\left(\mathscr{N}_{a|b} + \mathscr{N}_{a|c} + \mathscr{N}_{b|c}\right) \tag{4.3.19}$$

and compare it to the average negativity for bipartitions of the entire state $\overline{\mathscr{N}}_{1|2}$. One clearly sees that the internal negativity is always close to the maximum for states in the W class, Fig. 2e-2f. This corresponds to the common intuition for W-like entanglement as being more robust when a qubit is removed from the system.

Note however that this concept of robustness is different from the definition we gave in the previous section. In that case the robustness is proportional to the negativity for a bipartition of the global state ($\mathscr{N}_{1|2}$), which on average is actually maximized by the GHZ state, and not the W state. The relation between this last concept of robustness and the pattern of internal entanglement will be discussed extensively in the next sections for larger systems. In order to keep this distinction clear we will reserve the expression

[22] Formally a single qubit density matrix has only one non-trivial eigenvalue, the other being determined by the trace normalization.

robustness to the noise-related quantity and refer to the robustness against qubits removal simply as *internal entanglement*.

Finally one can ask for the monogamy of mutual information. It is straightforward to check that for pure states of only three qubits I3 is identically zero; consequently the mutual information is always monogamous.

4.4 Four qubits

In this section we consider the more interesting case of four qubits, we will see that the addition of a single qubits introduces much more structure and correspondingly several new investigations are possible.

For a four qubits system two kinds of bipartitions of the global state are possible, using the notation of the previous section we will refer to them as $(1|3)$ and $(2|2)$. As before, the first case is less interesting as the entropy essentially carries the same information as the negativity. The second case instead is more interesting, for such bipartition we can now compute both the negativity and entanglement entropy and ask what kind of information about the state one can gain by comparing them. More specifically we will consider the specific robustness (4.2.7) and show that it conforms to the interpretation we wish to give it.

A second novelty of a four qubits system is the possibility to investigate the properties of different states with respect to the disentangling theorem for the negativity. In particular, we explore the relation to the saturation of Araki-Lieb inequality for entanglement entropy. This is again inspired from holography owing the occurrence of the entanglement plateaux phenomena [32] there.

Finally, it is now possible to obtain a mixed state of three qubits by simply tracing out a single qubit, the value of I3 is then non-trivial and one can investigate the monogamy of mutual information in relation to the structure of entanglement of the state.

In §4.4.1 we will start these investigation for random generic states. Following this in §4.4.2 we will introduce a SLOCC classification for four qubits systems and apply the extend the consideration to the different classes.

4.4.1 Generic states of 4 qubits

We begin our discussion here by picking out random pure states of 4-qubits. We will subject these to various examinations, testing for the saturation of the AL inequality, the disentangling theorem, and finally explain how the specific robustness can play a useful role in delineating internal entanglement structure.

Monogamy of the negativity and disentangling theorem

Similarly to the three qubits case, it is interesting to ask how the saturation of the monogamy is related to the four-partite entanglement measured by τ_4. There are now

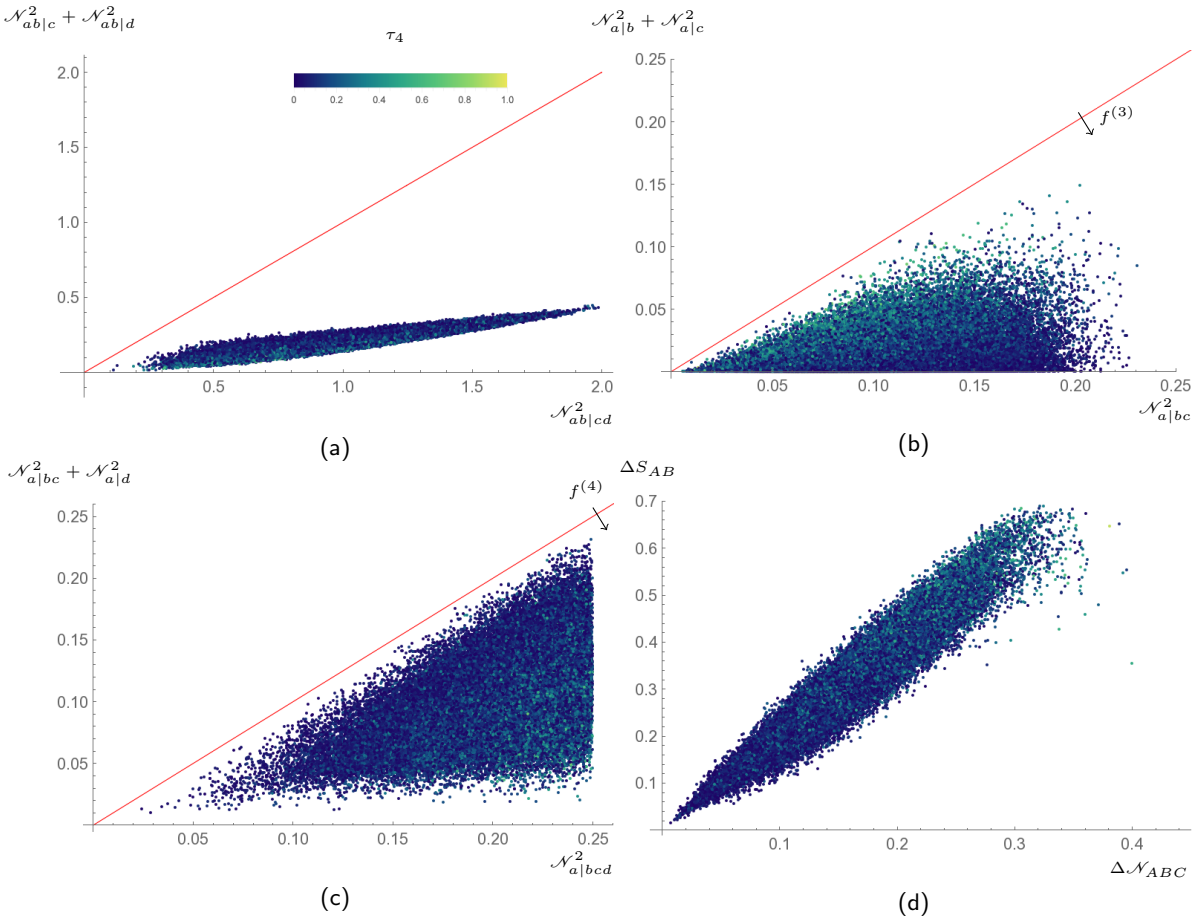

Figure 3: Monogamy of the squared negativity for 100000 random states. (a), (b), (c) show inequalities (4.4.20a), (4.4.20b), (4.4.20c) respectively. (d) Contrasting Araki-Lieb saturation with the disentangling theorem for negativities.

three different kinds of monogamy relations (up to permutation of the qubits), depending on different ways to partition into subsystems:

$$\mathcal{N}^2_{ab|c} + \mathcal{N}^2_{ab|d} \leq \mathcal{N}^2_{ab|cd} \tag{4.4.20a}$$

$$\mathcal{N}^2_{a|b} + \mathcal{N}^2_{a|c} \leq \mathcal{N}^2_{a|bc} \tag{4.4.20b}$$

$$\mathcal{N}^2_{a|bc} + \mathcal{N}^2_{a|d} \leq \mathcal{N}^2_{a|bcd} \tag{4.4.20c}$$

The results are plotted in Fig. 3a-3b-3c; note that the Hilbert space is now much larger and by random sampling one only covers a small portion of the space. Curiously, in the second case (4.4.20b), Fig. 3b, the monogamy relation seems to be saturated more by states with a higher content of multipartite entanglement while in the third case (4.4.20c), Fig. 3c, the states with low tangle saturate monogamy inequality. It is tempting to interpret this result in terms of residual multipartite entanglement (cf., three qubit discussion in §4.3).

Rewriting the saturation of (4.4.20b) as

$$\mathcal{N}^2_{a|b} + \mathcal{N}^2_{a|c} + f^{(3)}_{abc} = \mathcal{N}^2_{a|bc} \tag{4.4.21}$$

where $f^{(3)}$ is some measure of mixed residual tripartite correlation, it is natural to conjecture that high values of τ_4 correspond to small values of bipartite ($\mathcal{N}^2$) and tripartite

($f^{(3)}$) correlation. $\tau_4 \sim 1$ then implies $f^{(3)} \sim 0$ and the saturation of (4.4.20b). Similarly one could rewrite the saturation of (4.4.20c) as

$$\mathcal{N}^2_{a|bc} + \mathcal{N}^2_{a|d} + f^{(4)}_{abcd} = \mathcal{N}^2_{a|bcd} \tag{4.4.22}$$

where now $f^{(4)}$ is some measure of 4-partite correlation related to τ_4. The saturation of (4.4.20c) then corresponds to $\tau_4 \sim 0$.

Let us now turn to the connection between the monogamy of the negativity and the saturation of Araki-Lieb inequality (AL) [74] for entanglement entropy [76]. Recall that the AL inequality reads:

$$|S(A) - S(B)| \leq S(AB) \tag{4.4.23}$$

For a joint system $A \cup B$ in a mixed state, for reasons explained hitherto, it is difficult to interpret AL in terms of quantum correlations. In order to understand what kind of constraint AL implies for the internal structure of entanglement of the state, it is convenient to introduce the purification C of the state AB. Thus for a system U of N qubits we then consider only tripartitions such that $A \cup B \cup C \equiv U$ and the global state is pure. With this choice one can then rewrite (4.4.23) as

$$|S_{A|BC} - S_{B|AC}| \leq S_{C|AB} \tag{4.4.24}$$

where by expressions like $S_{A|BC}$ we mean the entropy of entanglement between A and BC (which of course is $S(A) = S(BC)$), stressing the interpretation of the von Neumann entropy as a measure of entanglement between a subsystem and its complement.

In the case of four qubits then there is only one possible kind of tripartition, up to qubits permutation, i.e., $1|1|2$. We consider the set-up $A = \{a\}$, $B = \{bc\}$, $C = \{d\}$, (4.4.24) then reads

$$|S_{a|bcd} - S_{bc|ad}| \leq S_{d|abc} \tag{4.4.25}$$

Permuting the qubits one obtains a set of constraints on the internal pattern of entanglement of the global state. We want to ask how this set of constraints is related to the one obtained from the monogamy of the negativity. In particular it is known that AL is in general difficult to saturate and it is certainly not saturated by generic states.[23] We want to investigate when this saturation actually happens and for which distribution of internal negativities.

More specifically, we invoke the disentangling theorem for the negativity of [61] for this purpose. For a pure state of $U \equiv A \cup B \cup C$, if $\mathcal{N}_{A|BC} = \mathcal{N}_{A|B}$ then it is possible to partition $B = B_1 \cup B_2$ such that the state factorizes $|\Psi\rangle = |\psi_{AB_1}\rangle \otimes |\psi_{B_2C}\rangle$. For our specific set-up the condition for the disentangling theorem is: $\mathcal{N}_{a|bcd} = \mathcal{N}_{a|bc}$. Eq.(4.4.20c)

[23] For further discussion we refer the reader to [76] for general analysis of AL saturation, [32] for explicit examples where the saturation occurs in holographic systems, and [75] for a general analysis of AL saturation of holographic entanglement entropy. We should note that the saturation of AL in holography is not generic, but does happen in a large class of examples involving bulk spacetimes with horizons.

then implies $\mathscr{N}^2_{a|d} \leq 0$, which is absurd; the only possible solution is saturation of the monogamy relation and in particular $\mathscr{N}_{a|d} = 0$. The consequence of the disentangling theorem is even stronger, not only there is no distillable entanglement between $a|d$, but there is no entanglement at all and the global state factorizes either as $|\psi_{ab}\rangle \otimes |\psi_{cd}\rangle$ or as $|\psi_{ac}\rangle \otimes |\psi_{bd}\rangle$.

The disentangling theorem implies saturation of AL in the following way: because of the factorization of the state one has $S(B) = S(B_1) + S(B_2)$, but since the individual states in the product are pure $S(B) = S(A) + S(C)$. Note that C now is the purification of AB, hence $S(B) = S(A) + S(AB)$ i.e., AL is saturated. We measure the saturation for random states by $\Delta S_{AB} = S(AB) - |S(A) - S(B)| \geq 0$ and correspondingly the amount by which the states match the hypothesis of the disentangling theorem by $\Delta \mathscr{N}_{ABC} = \mathscr{N}_{A|BC} - \mathscr{N}_{A|B} \geq 0$. With our specific choice these quantities are

$$\Delta S_{AB} = S_{d|abc} - |S_{a|bcd} - S_{bc|ad}|\,, \qquad \Delta \mathscr{N}_{ABC} = \mathscr{N}_{a|bcd} - \mathscr{N}_{a|bc} \tag{4.4.26}$$

The results are shown in Fig. 3d. Note that as expected there are no states that saturate AL, while the states that get closer to the saturation correspond to the states that almost satisfy the conditions of the disentangling theorem. This in itself is not particularly surprising, as we discussed AL inequalities are statistically difficult to saturate. Furthermore the result shows that matching the hypothesis of the disentangling theorem is a sufficient conditions for a state to saturate AL. On the other hand it is interesting to ask if these conditions are necessary and what is the meaning of states that saturate AL without factorization. We will comment more on this issue as we investigate further aspects of the relation in greater detail in the following.

Negativity to entanglement ratio

We can now initiate the study of the ratio between entanglement entropy and negativity, which is one of the main motivations of the present work. In order for the entropy to be a sensible measure of quantum entanglement we only consider global bipartition of pure states. Furthermore, for the same reason discussed in the case of three qubits, in the case of a 1—3 bipartition both the entanglement entropy and negativity carry the same information. We will therefore focus on the 2|2 bipartition only, where we can distinguish the negativity and entanglement.

Let us start with a particular partition $(ab|cd)$ and refer to the fiducial separation of the two subsystems (i.e., the symbol "|") as the entangling surface (Σ). One can then compute both negativity and entropy for this particular bipartition. Since the state is pure the entropy is a measure of the amount of entanglement between the subsystems, intuitively the number of Bell's pairs that can be distilled.[24] On the other hand we interpret the negativity as the robustness of the entanglement between the subsystems.

[24] Note however that more precisely this would be an asymptotic statement.

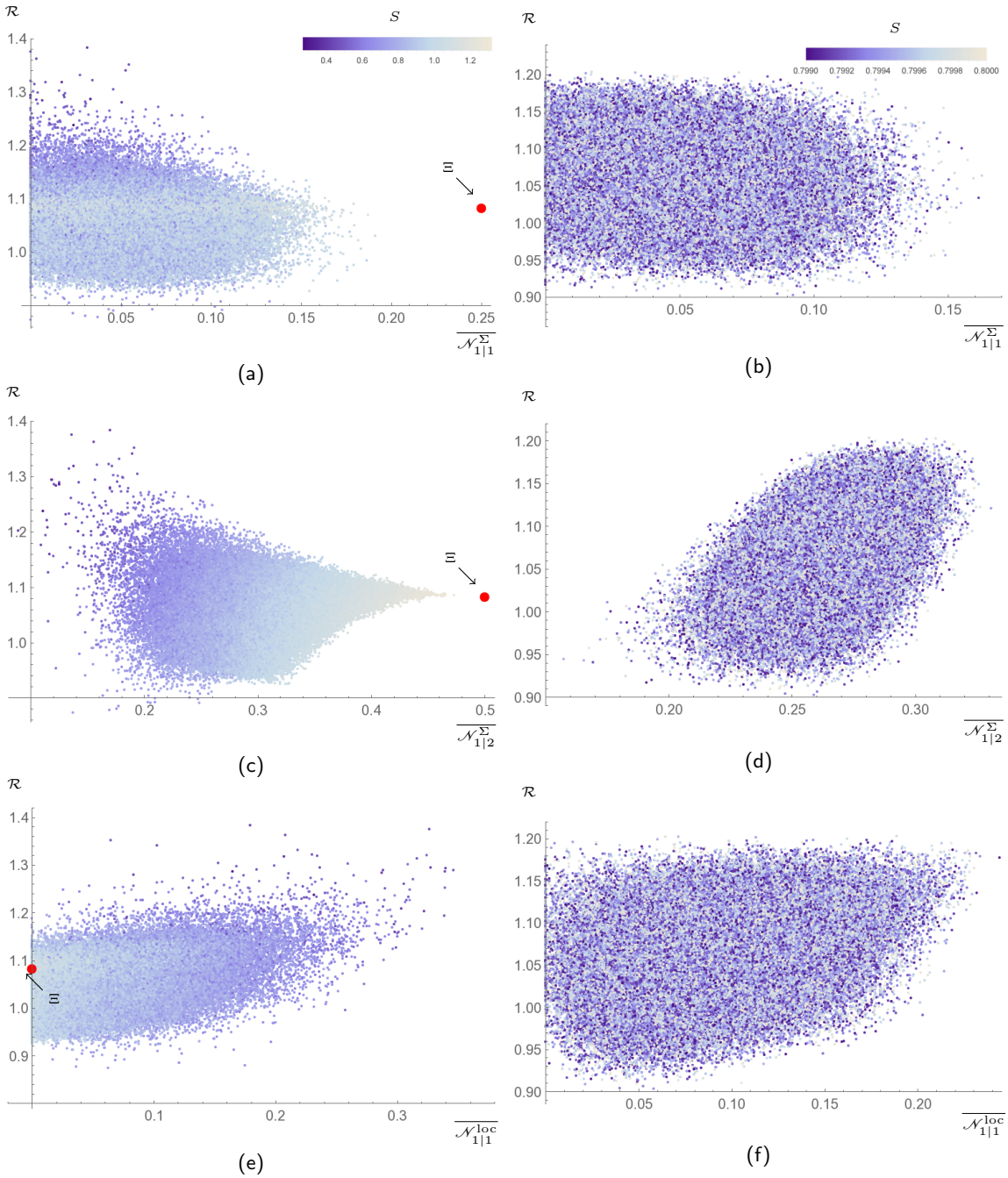

Figure 4: Average negativities across the entangling surface Σ and inside the subsystems for a fixed bipartition (100000 states). The left panels show the results for random states with entropy in the range $(0.27292, 1.32195)$, the large red dots show the maximally entangled state (Ξ). The right panels show states with a constrained value of the entropy $0.799 \leq S(ab) \leq 0.8$.

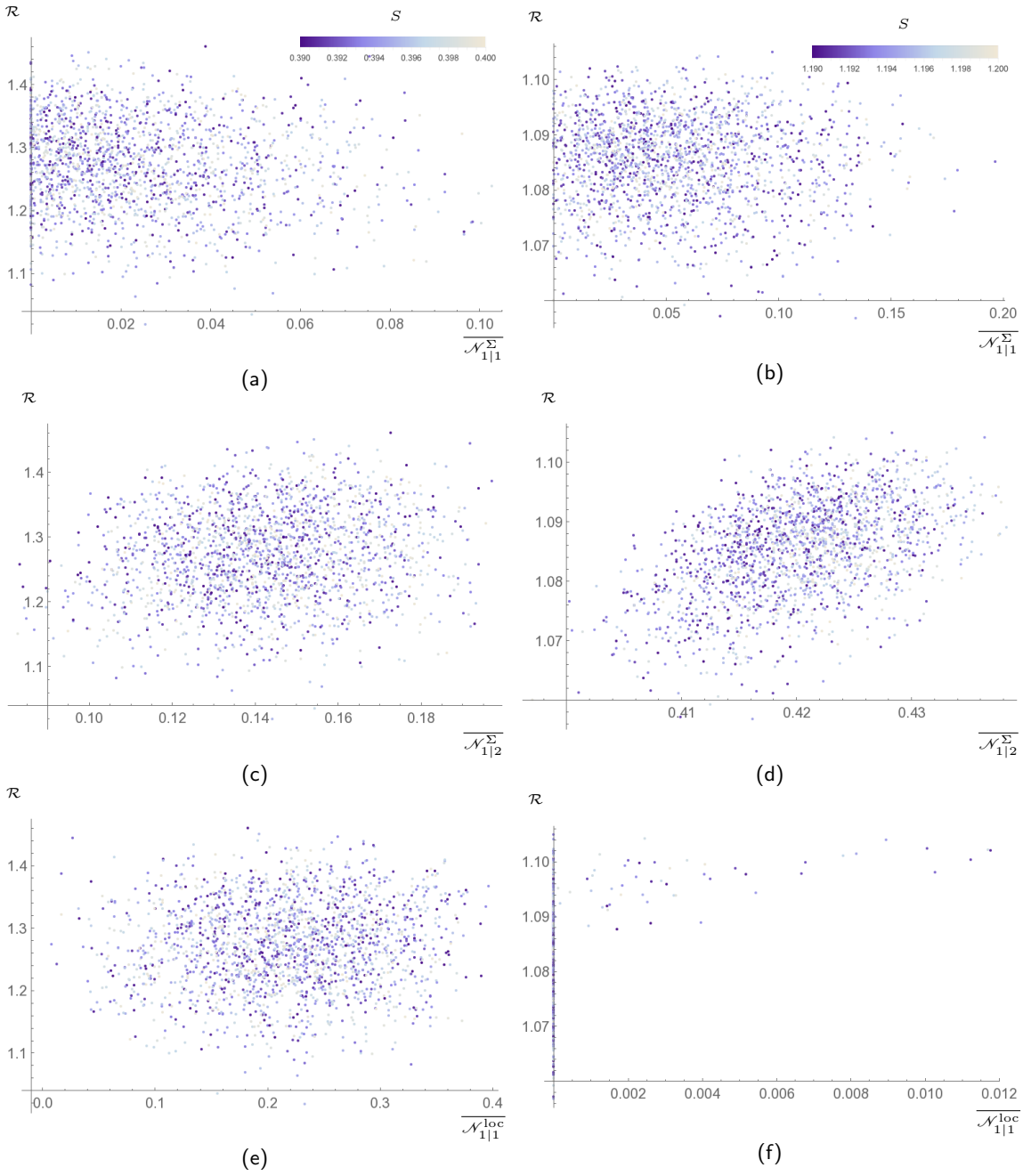

Figure 5: Average negativities across the entangling surface Σ and inside the subsystems for a fixed bipartition (2000 states). The left panels show the results for random states with entropy constrained in the range $0.39 \leq S(ab) \leq 0.4$. The right panels show states with a constrained value of the entropy in $1.19 \leq S(ab) \leq 1.2$.

We stress again that this notion captures the robustness against "intelligent jamming", which is in principle different from the common intuition about the robustness of the W states. In the latter case one actually refers to the amount of internal entanglement. As described in §4.2 we want to interpret the ratio $\mathcal{R}$ as capturing the specific robustness in a given state. We explore the dependence of $\mathcal{R}$ on the entanglement structure of the state focusing on the internal pattern of entanglement.

For the bipartition $ab|cd$ we have $\mathscr{N}^{\text{loc}}_{a|b}$ and $\mathscr{N}^{\text{loc}}_{c|d}$ for local entanglement, while for entanglement across Σ we consider all the possible negativities of the kind $\mathscr{N}^{\Sigma}_{1|1}$ and $\mathscr{N}^{\Sigma}_{1|2}$ where the sets of qubits are subsets of the original subsets of the bipartition. Finally we take the average of all the negativities of a particular kind, keeping the original bipartition fixed. The results are shown in Fig. 4a-4c-4e and show the dependence of the ratio on the internal entanglement with unconstrained value of the entropy across Σ. For states which are almost maximally entangled[25] the spread between possible values of entropy and negativity is very restricted. Interestingly the spread grows considerably for small values of the entropy, which also correspond to a higher value of the ratio. These are states that are less entangled but whose entanglement is particularly robust. In some sense it seems that if a state is highly entangled, its entanglement is more fragile against noise. Larger $\mathcal{R}$ corresponds to greater specific robustness, justifying our terminology.

One can also look for the distribution of the states when the entropy is almost fixed, the results are shown in Fig. 4b-4d-4f. The fixed value is picked to be somewhere in the middle-range of the entanglement spread for our sampling; other choices outside the edge regions lead to similar results. Note that the dependence on the entropy now is completely random. Furthermore the ratio seems to be increasing when the $(1|2)$ entanglement across the entangling surface is higher. On the other hand it seems not to depend on the average $(1|1)$ entanglement. It will be useful to contrast this result against those for larger systems. For now we tentatively interpret the results as suggesting that states with a higher amount of $(1|2)$ entanglement across the entangling surface, but the same value of the entropy, are more robust.

Finally, we look at the average entanglement inside the subsystems specified by Σ. We find that high values of local negativity correspond to high value of the ratio although the converse is not always true. Fig. 5 shows two other slices for different constraints on the entropy. For states which are almost maximally entangled (Fig. 5b-5d-5f) the results agree with the previous analysis. On the other hand when the entropy is fixed but small (Fig. 5a-5c-5e) the dependence of the ratio on $1|2$ entanglement becomes less evident. Furthermore a larger amount of local $1|1$ entanglement is not sufficient any more to produce higher values of the ratio.

[25] By maximally entangled state here we mean the usual state that maximizes entanglement for a given bipartition. For four qubits this is the state which achieves this between two pairs, i.e., $\frac{1}{2}\sum_{i=1}^{4} |\,i\rangle\otimes|\,i\rangle$ where $|\,i\rangle$ is the computational basis for a two-qubits system. We will reserve the symbol $|\,\Xi_N\rangle$ for such states.

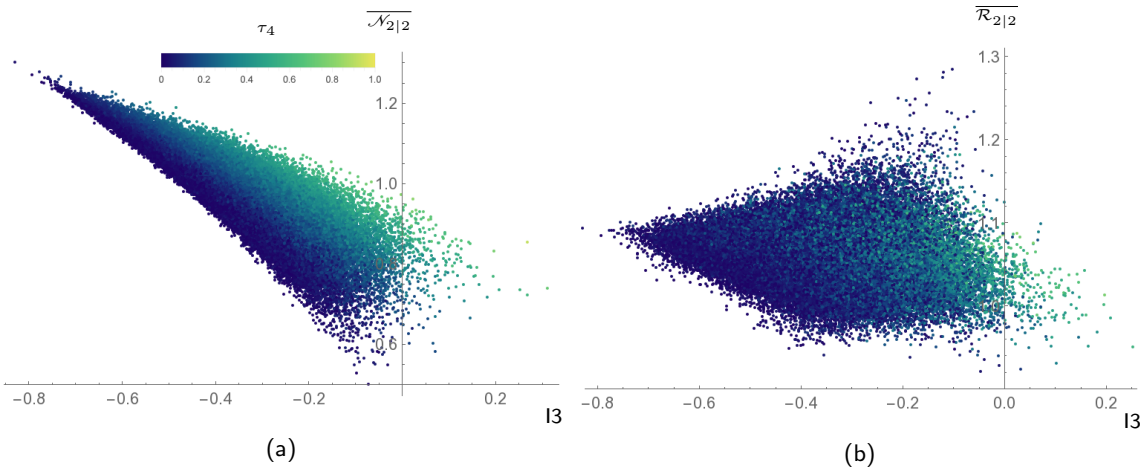

Figure 6: 100000 random generic states to test monogamy of mutual information. (a) Average ratio between negativity and entropy compared to the values of I3 and τ_4 (color map), (b) Average $2|2$ negativity compared to I3 and τ_4 for the same states.

Monogamy of mutual information

For a system of four qubits there are in principle two different kinds of tripartite information one can look at, viz., either $\mathsf{I3}(1|1|2)$, or $\mathsf{I3}(1|1|1)$ after tracing out a single qubit. Since we are only working with pure states, in the first case we have $\mathsf{I3} = 0$, we will instead focus on the second case. There are in principle four different values of I3 depending on which qubit we choose to trace out. Nevertheless it is straightforward to check that they are all equal, there is actually a unique value of I3.

We compare this value to the amount of quantum multipartite entanglement measured by the tangle and the internal entanglement structure. As a measure of the robustness of the state we use the average negativity $\overline{\mathcal{N}_{2|2}}$, the result is shown in Fig. 6a. An evident result is the observation that statistically the monogamy of mutual information is not a very restrictive condition. States with low robustness and high values of τ_4 seem to violate the monogamy of mutual information (positive I3) more easily.

In Fig. 6b we show instead a similar plot for the average ratio $\overline{\mathcal{R}}$. Now we note that the states that violate monogamy and have high value of τ_4, also have quite a small value of the ratio. This correlation is rather suggestive, and if true, implies that the specific robustness measured by $\mathcal{R}$ could be a useful diagnostic vis a vis monogamy of mutual information. However, before we arrive at this conclusion, we should do some more sanity checks, which we now turn to, by considering a classification of four qubit states.

4.4.2 SLOCC classification of 4 qubit states

For four or more qubits it is known that the number of inequivalent SLOCC classes is infinite [143]. Nevertheless, motivated by the result for three qubits, one can still look for special states that maximize mixed internal correlations. These are a higher dimensional generalization of the W states of three qubits. For states of four qubits [145] gave an SLOCC classification into eight special classes of this kind, plus an additional class ([Q1]

in the following) which contains infinitely many SLOCC classes and is related to generic states (see below). Using the standard computational basis for 4-qubits we can write down the classes explicitly as[26]

$$
\begin{aligned}
|[\mathsf{Q1}]\rangle &= \frac{a+d}{2}(|0000\rangle + |1111\rangle) + \frac{a-d}{2}(|0011\rangle + |1100\rangle) + \frac{b+c}{2}(|0101\rangle + |1010\rangle) \\
&\quad + \frac{b-c}{2}(|0110\rangle + |1001\rangle) \\
|[\mathsf{Q2}]\rangle &= \frac{a+b}{2}(|0000\rangle + |1111\rangle) + \frac{a-b}{2}(|0011\rangle + |1100\rangle) + c(|0101\rangle + |1010\rangle) + |0110\rangle \\
|[\mathsf{Q3}]\rangle &= a(|0000\rangle + |1111\rangle) + b(|0101\rangle + |1010\rangle) + |0110\rangle + |0011\rangle \\
|[\mathsf{Q4}]\rangle &= a(|0000\rangle + |1111\rangle) + \frac{a+b}{2}(|0101\rangle + |1010\rangle) + \frac{a-b}{2}(|0110\rangle + |1001\rangle) \\
&\quad + \frac{i}{\sqrt{2}}(|0001\rangle + |0010\rangle + |0111\rangle + |1011\rangle) \\
|[\mathsf{Q5}]\rangle &= a(|0000\rangle + |0101\rangle + |1010\rangle + |1111\rangle) + i\,|0001\rangle + |0110\rangle - i\,|1011\rangle \\
|[\mathsf{Q6}]\rangle &= a(|0000\rangle + |1111\rangle) + |0011\rangle + |0101\rangle + |0110\rangle \\
|[\mathsf{Q7}]\rangle &= |0000\rangle + |0101\rangle + |1000\rangle + |1110\rangle \\
|[\mathsf{Q8}]\rangle &= |0000\rangle + |1011\rangle + |1101\rangle + |1110\rangle \\
|[\mathsf{Q9}]\rangle &= |0000\rangle + |0111\rangle
\end{aligned}
\tag{4.4.27}
$$

Here a, b, c, d are complex numbers which appear as eigenvalues of an operator used in constructing the classification scheme. The classification only includes states where all the qubits are entangled.[27] The first class is the "generic class" in the sense that any generic state of four qubits can be mapped to a state in [Q1] by SLOCC. This class is not unique under SLOCC; as clarified in [142] it is dense in the space of generic states, but it actually contains an infinite number of classes. The remaining classes are thus of measure zero, but contain the maximal amount of internal mixed bipartite or tripartite entanglement (there are some exceptions which we note below). In the following we will focus in particular on the classes [Q1]-[Q6] – the last three only contain exceptional states. The W state of four qubits belongs to [Q4], while the GHZ 4-qubit state is in [Q1] ($a = d$, $b = c = 0$), as expected.

Distinguishing the classes: Given a single state one could ask how it is possible to identify the corresponding class using different measures of entanglement. In principle one could compute the negativity for each bipartiton of the entire system and all bipartitions of each possible subsystem. It is natural to expect that the collection of this data allows some resolution of the classes.

We want instead to ask a different question. As advertised earlier, we are concerned with knowing to what extent it is possible to distinguish states in different classes if one

[26] For simplicity we drop the normalization factor in the definition of the classes.

[27] The class [Q9] is an exception as it can be written as $|0\rangle \otimes |\,\mathrm{GHZ}_3\rangle$. This was indeed one of the motivation for [146] to consider an alternative classification of the four qubits states into eight classes.

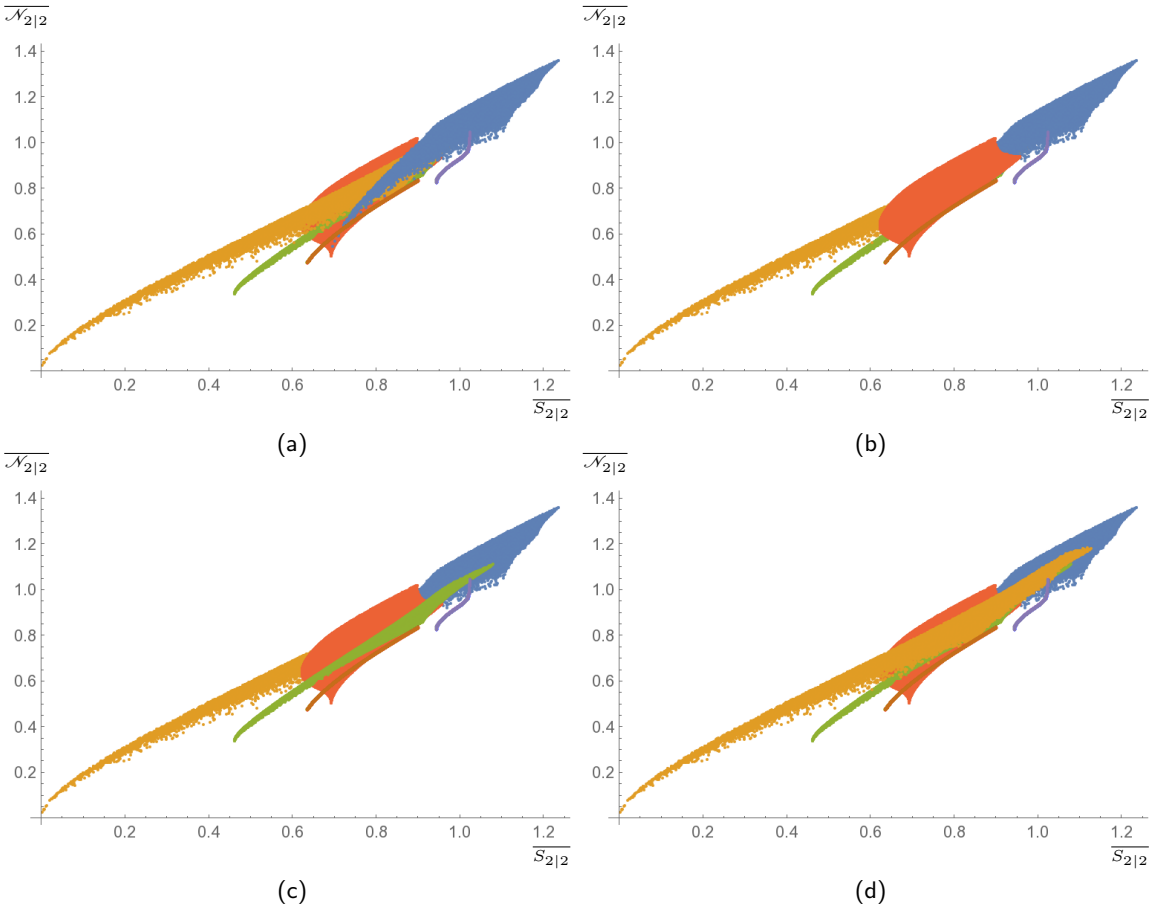

Figure 7: Comparison of the averaged entropy and negativity for the maximal bipartition (50000 random states per class). The four panels show the same plot with different overlap. The color-class correspondence is as follows: ■ = [Q1], ■ = [Q2], ■ = [Q3], ■ = [Q4], ■ = [Q5], ■ = [Q6]. Note that while generic states can be mapped into class [Q1] by a SLOCC, picking states in [Q1] according to the ansatz in (4.4.27) does not sample this genericity. Hence the region covered by ■ = [Q1] is not the entire domain of the plot above, but only a subregion thereof.

is restricted to use measures of entanglement for pure states. Our motivation comes from holography, where at present we only know how to compute the negativity for pure states. We can then combine information one extracts from both negativity and entropy, and see how much we can learn about the entanglement structure.

For simplicity, we focus on the maximal bipartitions, i.e., 2|2. One can easily compute the average negativity and average entropy for random states in the various classes, and average over the three possible inequivalent bipartitions. The results are shown in Fig. 7. One can see that even if the combined information extracted from negativity and entropy is not enough to completely resolve the classes, one can still discriminate them in some ranges of the values of the two measures.

Disentangling theorem and Araki-Lieb: We repeat the analysis of the previous subsection for the disentangling theorem of the negativity and the saturation of AL. In the previous discussion §4.3 the states were generic and all the possible qubits permutations

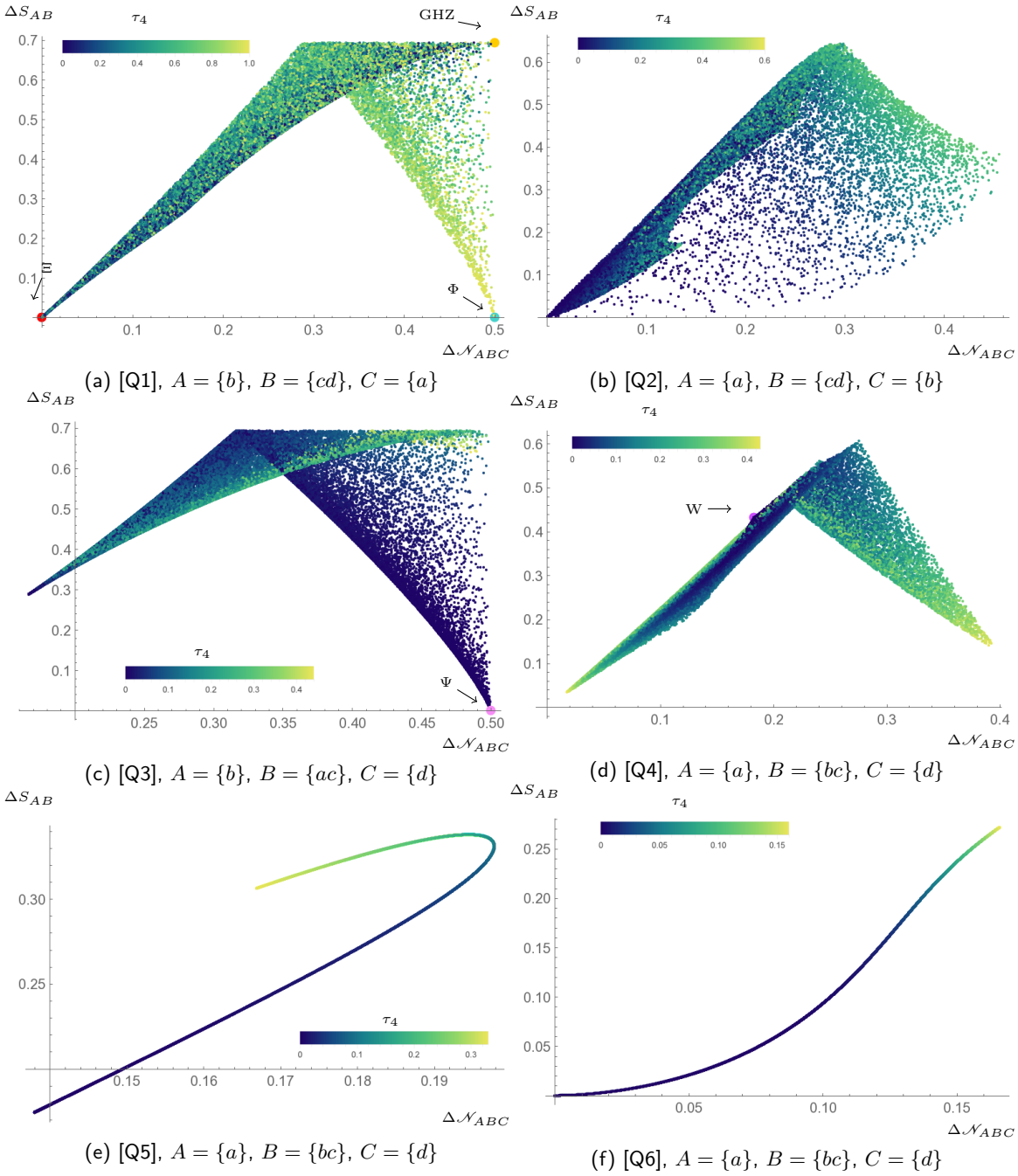

(a) [Q1], $A = \{b\}$, $B = \{cd\}$, $C = \{a\}$

(b) [Q2], $A = \{a\}$, $B = \{cd\}$, $C = \{b\}$

(c) [Q3], $A = \{b\}$, $B = \{ac\}$, $C = \{d\}$

(d) [Q4], $A = \{a\}$, $B = \{bc\}$, $C = \{d\}$

(e) [Q5], $A = \{a\}$, $B = \{bc\}$, $C = \{d\}$

(f) [Q6], $A = \{a\}$, $B = \{bc\}$, $C = \{d\}$

Figure 8: Disentangling theorem and saturation of Araki-Lieb (see Eq. (4.4.26)) for the SLOCC classified 4-qubit states (50000 random states per class). The large dots show the GHZ (orange), $|\Phi\rangle$ (turquoise), $|\Psi\rangle$ (pink), W (purple) and maximally entangled $|\Xi\rangle$ (red) states.

gave the same result. Here we expect the behaviour to be different depending on the specific set-up that we choose – this is manifest in the fact that the classes are not completely symmetric under qubits permutations. In principle there are 12 different situations to consider, but many choices give equivalent results. For each class we report the result for the most interesting partition in Fig. 8. The full list of possible results for each class and the corresponding plots can be found in Appendix 4.A. In each class there are states that get arbitrarily close to saturating AL and respect the conditions for the disentangling theorem, with the only exception of [Q5]. This is the class that will be of particular interest for us in the sequel.

Interestingly, it is worth pointing out that in two classes there are states that saturate AL even without satisfying the conditions for the disentangling theorem. These states have (a) high values of multipartite entanglement in [Q1] and (b) a low value in [Q3] (the color map in the various plots shows the values of τ_4). The specific states (indicated by colored dots in Fig. 8) are respectively a product of two Bell pairs $|\Phi\rangle$, and the product between a Bell pair and two disentangled qubits $|\Psi\rangle$.[28] This means that the hypothesis of the disentangling theorem would be satisfied for a different permutation of qubits. Indeed the tangle is sensitive to the factorization inherent in one of the two subsystems.

AL saturation without factorization ought to be a very restrictive condition on the pattern of internal entanglement. This may exaplain why it hard see the saturation for generic states. Looking at the results one might be tempted to conjecture that such a state could exist in [Q2]. A numerical search for such a state showed that states with $\Delta\mathscr{N} > 0$ and $\Delta S \sim 0$ approach to the product $|0110\rangle$. The reason why these states may be highly shifted to the right of the origin is that their entanglement is particularly robust. An extremely small but non vanishing value of the entropy can produce much higher values of the negativity. We conclude then that in the case of four qubits the saturation of AL only happens if there exists a permutation such that the conditions for disentanglement are matched and factorization actually happens.

Specific robustness $\mathcal{R}$: For generic states we have seen that the most sensible quantity to the internal structure of entanglement is the negativity across Σ between a qubit in a subsystem and the other pair, viz., $\overline{\mathscr{N}^{\Sigma}_{1|2}}$. We now repeat the same analysis for the classes and compare specific robustness (4.2.7) to the negativity $\overline{\mathscr{N}^{\Sigma}_{1|2}}$. The results are shown in Fig. 9; we keep track of the values of the entropy (color map).

States in [Q1] reproduce the behaviour of generic states; similar patterns are visible in [Q2]-[Q4] – see Fig. 9a-9d. On the other hand, for a different choice of Σ, a different pattern manifests itself in classes [Q3] and [Q4], see Appendix 4.A, Figs. 20a and 21a. In this case the highest values of the ratio in the class correspond to states with the highest entropy and negativity. There are no states with small negativity and high value of the

[28] The explicit expressions of these states are: $|\Phi\rangle = |\phi^+\rangle_{ab} \otimes |\phi^+\rangle_{cd}$ and $|\Psi\rangle = |01\rangle_{ac} \otimes |\phi^+\rangle_{bd}$ where $|\phi^+\rangle$ is the maximally entangled two qubits state $|\phi^+\rangle = |01\rangle + |10\rangle$, i.e., a Bell pair.

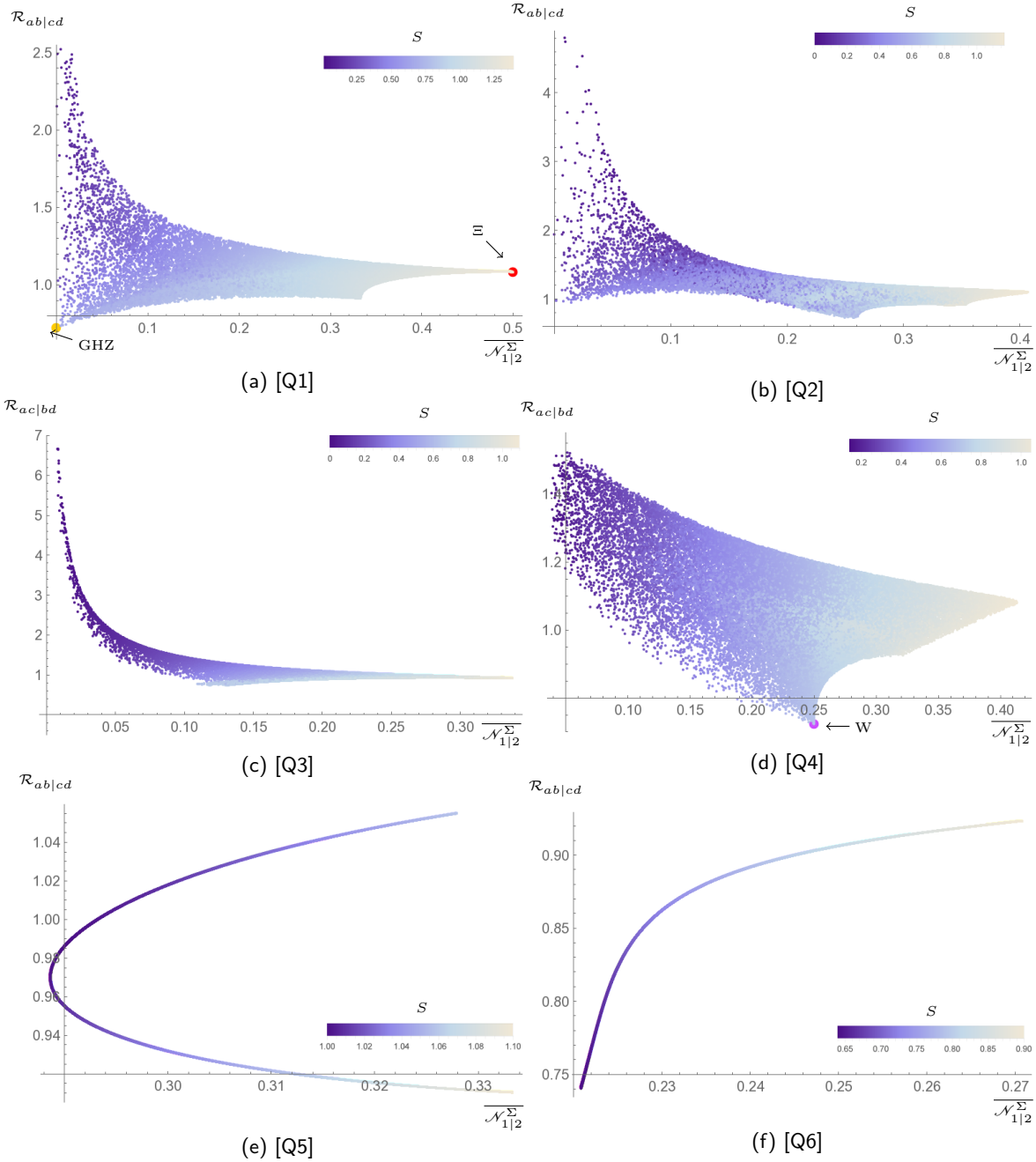

Figure 9: The ratio for a given Σ compared to the average $\mathcal{N}_{1|2}$ across Σ. 50000 random states per class. Panels (a-b) are truncated, few states (not shown) approach the vertical axes with high values of the ratio and small values of the entropy. The large dots show the GHZ (orange), W (purple) and maximally entangled $|\Xi\rangle$ (red) states. (a)(b)(c) are truncated, few states with small values of $\mathcal{N}$ and ratio up to $\mathcal{R} \sim 7.4$ (a), $\mathcal{R} \sim 16$ (b) and $\mathcal{R} \sim 32$ (c), are not shown.

ratio (and small entropy). [Q6] has a similar behaviour as evidenced in Fig. 9f. In contrast, [Q5] instead is quite peculiar, states with high negativity and entropy correspond both to the highest and smallest values of the ratio, cf., Fig. 9e. Highly entangled states in [Q5] are divided in two branches, one with fragile entanglement, the other whose entanglement is more robust. Note however that the three quantities that characterize the state are constrained in a small range of values.

While the behaviour of the various classes is more or less similar to the generic class, the curious feature is the exceptional behaviour in [Q5]. We have previously also seen that this class of 4-qubit states is also peculiar when we analyzed the consequences of the disentangling theorem, vis a vis, saturation of the AL inequality. We shall now compare the ratio to the value of multipartite entanglement and the monogamy of mutual information and find yet another distinguishing feature of this class.

Monogamy of mutual information: Finally, we compare the value of I3, to the tangle, and the average ratio over the three maximal bipartitions. The results for the different classes are shown in Fig. 10. Surprisingly, there is only a single class [Q5] shown in Fig. 10e, whose states always have a negative value of I3.

This the most interesting aspect of our analysis of the SLOCC classified 4-qubit states. What it suggests is the following: in all the other classes [Qk] with $k \neq 5$, a given state with a particular value of I3 can always be turned into a state with positive I3 by SLOCC. Even more strongly, since every generic state of four qubits can be mapped to the first class by SLOCC, the states in [Q5] are the only one that can never violate the monogamy of mutual information. In effect, what this suggests is that the subset of 4-qubit states lying in Class [Q5] are likely to be most holographic. Of course, this statement should be taken with a large grain of salt, for we are discussing here the structure of entanglement in qubit systems with no interactions. Furthermore, it is unclear to us that the holographic map respects the SLOCC operations used to classify states herein.[29] Nevertheless we think the presence of a distinguished class of states suggests that certain patterns of entanglement are more likely than others to play a role in holographic systems (at least for the purposes of building semi-classical geometry).[30]

It is also interesting to look at the result for the generic class [Q1], cf., Fig. 10a. As expected from previous results for generic states the value of I3 is generally negative, in particular for small values of τ_4. Nevertheless states which are strongly entangled in a multipartite sense are divided into two branches. One branch minimizes the average ratio and violates monogamy of mutual information, the other seems to respect monogamy and maximizes the ratio. The states in the latter case asymptotically approach the state Φ

[29] We thank Veronika Hubeny for a discussion on this issue.

[30] For completeness let us also record the values of I3 for the exceptional states [Q7], [Q8], [Q9]:

$$\mathsf{I3}([\mathsf{Q7}]) = -0.356135\,, \qquad \mathsf{I3}([\mathsf{Q8}]) = -0.477386\,, \qquad \mathsf{I3}([\mathsf{Q9}]) = 0\,.$$

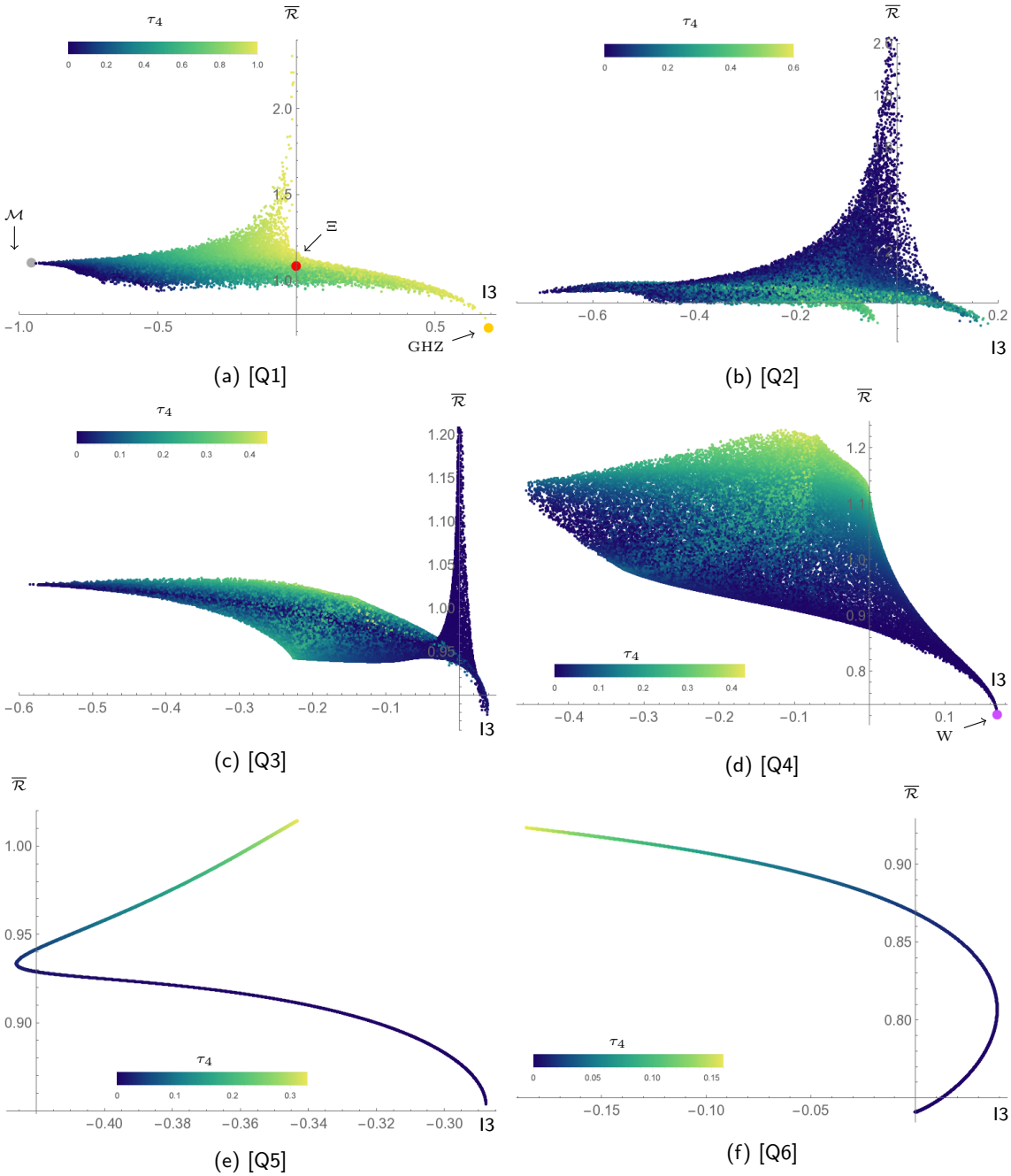

Figure 10: Monogamy of mutual information compared to the average ratio for the maximal bipartitions and mutipartite entanglement τ_4 (color map). The large dots show the GHZ (orange), $|\mathcal{M}\rangle$ (gray), W (purple) and maximally entangled $|\Xi\rangle$ (red) states. 50000 states per class. (b)(c) are truncated, few states with I3 ~ 0 and values of the average ratio up to $\mathcal{R} \sim 8.5$ (b) and $\mathcal{R} \sim 11$ (c) are not shown.

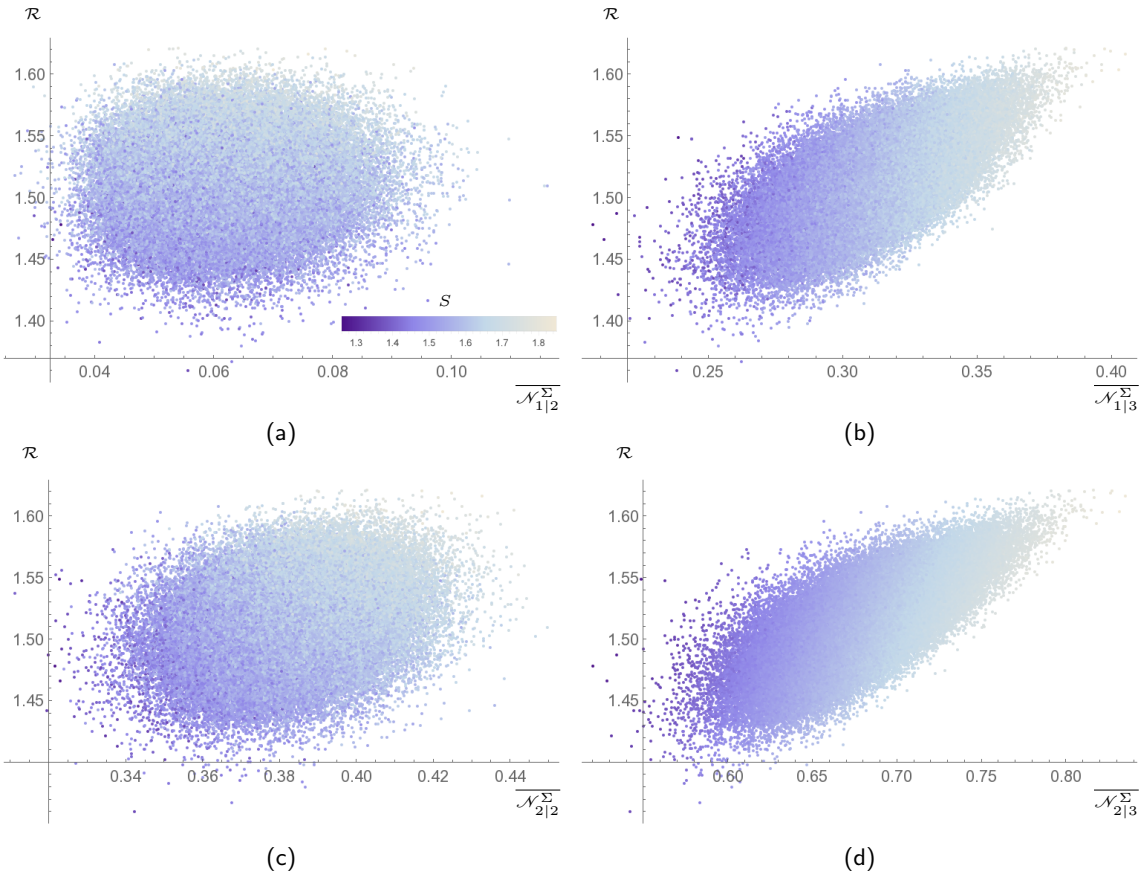

Figure 11: Entanglement across Σ for a system of 6 qubits (100000 random states). The entangling surface Σ is fixed and divides the states into two subsystems of three qubits each. The panels show the dependence of the ratio on the internal negativity. The color map shows the values of the entropy in the range $(1.26147, 1.84577)$.

discussed before in the context of AL inequalities.[31] A numerical search for the states that minimizes the value of I3 gives instead the following state

$$|\mathcal{M}\rangle = |0011\rangle + e^{-\frac{\pi}{3}i}\,|0101\rangle - e^{\frac{\pi}{3}i}\,|0110\rangle - e^{\frac{\pi}{3}i}\,|1001\rangle + e^{-\frac{\pi}{3}i}\,|1010\rangle + |1100\rangle \quad (4.4.28)$$

This state is interesting in its own right; it appears to be a highly scrambled state. It has maximal entanglement under all partitionings of the qubits [142]. Preliminary investigations indicate a similar pattern for higher qubit systems; it would be interesting to explore this class of states further. A behaviour similar to that of [Q1] is manifest for [Q4] (Fig. 10d). On the other hand this should be contrasted with the behaviour of [Q2] and [Q3] (see Fig. 10b and 10c respectively), where the states that maximize the average ratio contain a small amount of multipartite entanglement and can violate monogamy.

4.5 Large N qubit systems

At present no classification is known for pure states of five or more qubits. As a result any analysis of larger number of qubits must necessarily be restricted to generic states. We

[31] This was checked numerically over 1000000 states that maximize the ratio.

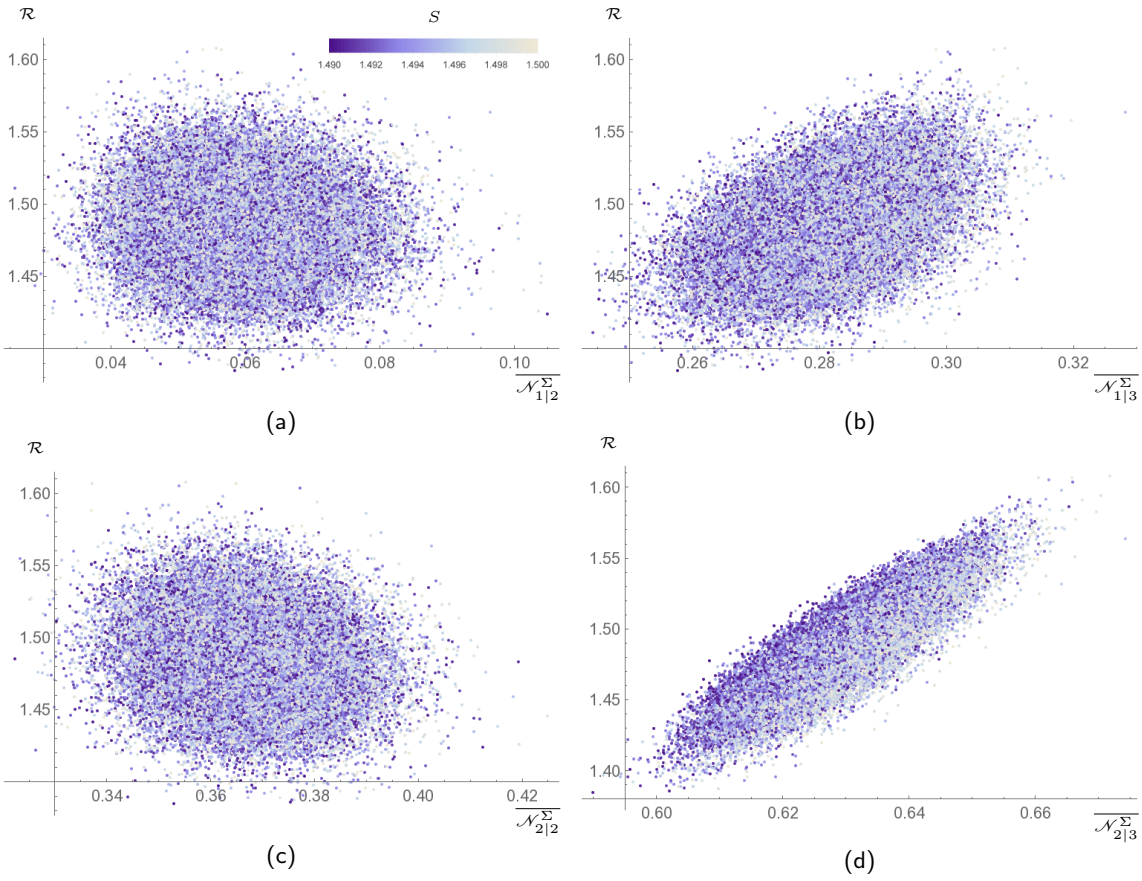

Figure 12: A slice of Fig. 11, for 50000 states, now with a constraint on the entropy which takes values in the interval $(1.49, 1.5)$ and is shown by the color map.

now explore specific robustness characterized by the ratio $\mathcal{R}$, focusing on its dependence on internal entanglement. We also look to examining the relations amongst the ratio, multipartite entanglement and the monogamy of mutual information. We will specifically focus on states of 6 and 8 qubits, primarily because the tangle is only defined for an even number of qubits (for $N > 3$). Much of the other results we derive ought not to change considerably for an odd number of qubits.

4.5.1 Negativity versus entanglement

As in the case of four qubits we want to investigate the dependence of the specific robustness on the internal pattern of entanglement of the system. As before we are interested both in the entanglement between qubits inside a single subsystem and entanglement across the entangling surface Σ. We will choose Σ such that the size of the subsystems is maximal, i.e., commit a 3—3 split for the 6 qubits case, which we keep fixed in what follows.

Let us start by listing all the possible internal negativities we can consider for a pure

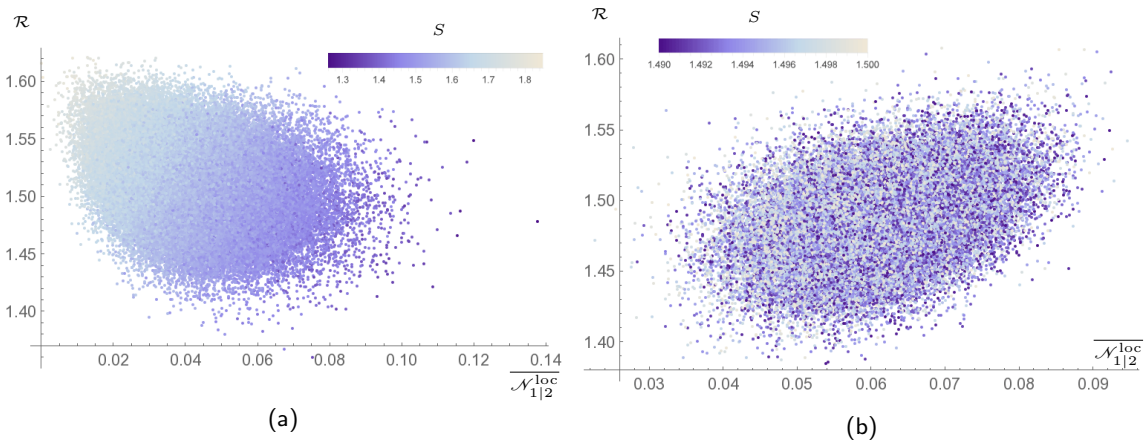

Figure 13: Dependence of the ratio on the average negativity between qubits inside the subsystems specified by Σ for pure states of 6-qubits. (a) no constraint on the entropy (color map), for 100000 states, (b) entropy constrained in the range $(1.49, 1.5)$, for 50000 states.

state of 6-qubits.

$$\begin{array}{lccccc} \text{across } \Sigma: & \overline{\mathcal{N}^{\Sigma}_{2|3}} & \overline{\mathcal{N}^{\Sigma}_{1|3}} & \overline{\mathcal{N}^{\Sigma}_{2|2}} & \overline{\mathcal{N}^{\Sigma}_{1|2}} & \overline{\mathcal{N}^{\Sigma}_{1|1}} \\ \text{local:} & & & & \overline{\mathcal{N}^{\rm loc}_{1|2}} & \overline{\mathcal{N}^{\rm loc}_{1|1}} \end{array} \tag{4.5.29}$$

In the above, averages are computed by considering all possible permutations of qubits (with Σ held fixed).

Of the set of possibilities listed in (4.5.29), $\overline{\mathcal{N}^{\Sigma}_{1|1}}$ is uninteresting, and so we will ignore it from now on. In Fig. 11 we show the results for the other cases. The color map indicates values of the entropy across Σ for the entire system.

We see that the ratio $\mathcal{R}$ clearly increases when $\overline{\mathcal{N}^{\Sigma}_{2|3}}$ or $\overline{\mathcal{N}^{\Sigma}_{1|3}}$ increase. Some dependence is also manifest for $\overline{\mathcal{N}^{\Sigma}_{2|2}}$ while there is no clear dependence on $\overline{\mathcal{N}^{\Sigma}_{1|2}}$. In addition, note that the average negativity is well correlated with the entanglement entropy (they both increase in concert). This should be compared to Fig. 4c for the four qubits case. We just have to bear in mind the obvious fact that random sampling actually covers a larger portion of the space in the 4-qubit case. For system of six qubits the Hilbert space is much larger and random generation only gives access to a small portion of it. We are probably exploring only a region analogous to the one near the tip of Fig. 4c. This is consistent with the fact that statistically we get high values of the entropy.[32] It is entirely possible that as in the four qubits case, $\mathcal{R}$ is maximized by states in another region, again with a much smaller value of the entropy.

Bearing this caveat in mind we can still investigate how the specific robustness depends on internal entanglement for states in this region of the space. In order to understand whether $\mathcal{R}$ increases with the negativity independently of the entropy, we look for random states with the entropy constrained in some small range of values. The results for the

[32] A maximally entangled state of six qubits, in a bipartite 3—3 sense, has entropy $S = 2.079$, specific robustness $\mathcal{R} = 1.683$.

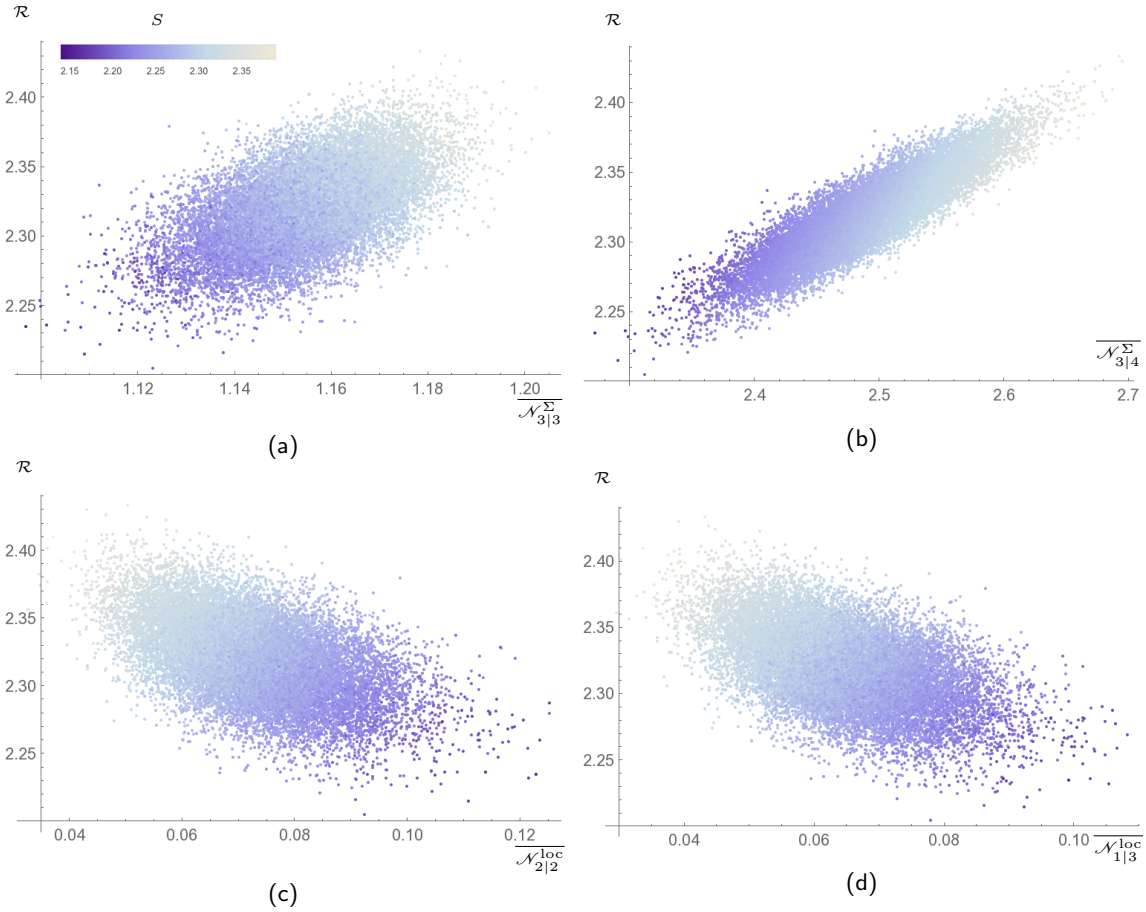

Figure 14: Entanglement across Σ for a system of 8-qubits (20000 random states). The entangling surface Σ is fixed and divides the states into two subsystems of four qubits each. The panels show the dependence of the ratio on the internal negativity. The color map shows the values of the entropy in the range $(2.14035, 2.38651)$. (a)-(b) entanglement across Σ, (c)-(d) entanglement inside subsystems.

same bipartitions as above are shown in Fig. 12. One can see that the weak dependence noticed above in the case $\overline{\mathcal{N}^{\Sigma}_{2|2}}$ actually disappears. On the other hand our suspicions are vindicated for $\overline{\mathcal{N}^{\Sigma}_{1|3}}$ and in particular for $\overline{\mathcal{N}^{\Sigma}_{2|3}}$. In the last case we also notice that for states with a fixed value of the $\mathcal{N}$, the ratio $\mathcal{R}$ seems to be statistically maximized by states with a lower value of the entropy.

We can also look at the local entanglement (again ignoring $\overline{\mathcal{N}^{\mathrm{loc}}_{1|1}}$).The results for $\overline{\mathcal{N}^{\mathrm{loc}}_{1|2}}$ are shown in Fig. 13. Quite curiously the ratio seems to slightly decrease as the internal negativity increases. At the same time the entropy seems to decrease as well. If we look instead at states with a constrained value of the entropy, the ratio seems to increase as the negativity increases.

One lesson that we learn is that the specific robustness $\mathcal{R}$ is particularly sensible if one of subsystems coincides with one of the subsystems of the original bipartition. When we start to trace out qubits, the sensitivity of the ratio progressively fades. Similarly, for the internal entanglement the sensibility of the ratio seems to be higher when do not trace out any qubit.

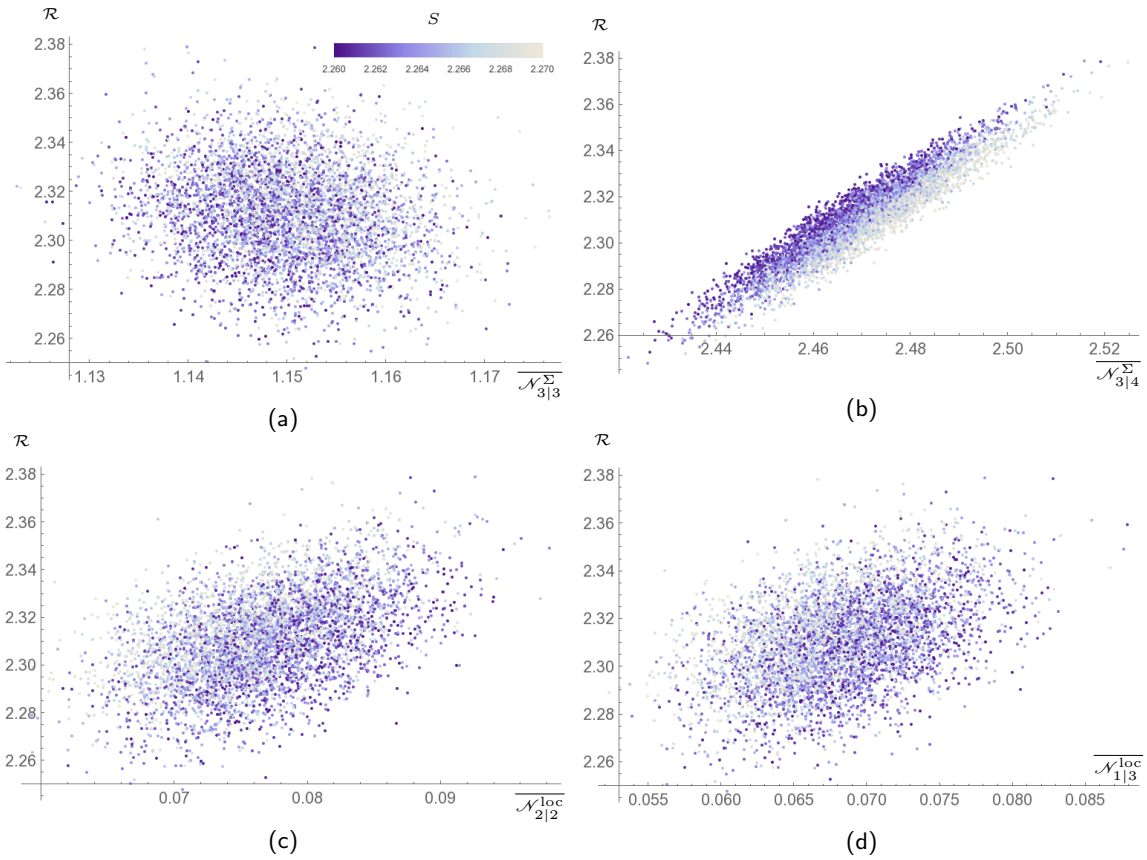

Figure 15: A slice of Fig. 14, now with a constraint on the entropy which takes values in the interval $(2.26, 2.27)$ and is shown by the color map. Plot is for 5000 random states.

We can check this result for an even larger system. For a system of eight qubits the list of all possible negativities we could look at is the following:

$$\begin{array}{lcccccccc} \text{across } \Sigma: & \overline{\mathcal{N}^{\Sigma}_{3|4}} & \overline{\mathcal{N}^{\Sigma}_{2|4}} & \overline{\mathcal{N}^{\Sigma}_{1|4}} & \overline{\mathcal{N}^{\Sigma}_{3|3}} & \overline{\mathcal{N}^{\Sigma}_{2|3}} & \overline{\mathcal{N}^{\Sigma}_{1|3}} & \overline{\mathcal{N}^{\Sigma}_{2|2}} & \overline{\mathcal{N}^{\Sigma}_{1|2}} \\ \text{local:} & & & & & \overline{\mathcal{N}^{\mathrm{loc}}_{1|3}} & \overline{\mathcal{N}^{\mathrm{loc}}_{2|2}} & \overline{\mathcal{N}^{\mathrm{loc}}_{1|2}} & \overline{\mathcal{N}^{\mathrm{loc}}_{1|1}} \end{array} \tag{4.5.30}$$

Fig. 14 shows the results without a constraint on the entropy, the results for states with constrained entropy are shown in Fig. 15. Similar comments as for the 6-qubit case hold.[33]

4.5.2 Exploring multipartite entanglement

We now move to the analysis of multipartite correlations. Consider a pure state of a system U of N-qubits. We can choose subsystems A, B, C such that $A \cup B \cup C \equiv U$. Since the state of U is pure we have $\mathsf{I3} = 0$. We want instead to look at all the possible values of $\mathsf{I3}$, for all the possible inequivalent choices of A, B, C where the total number of qubits k in $A \cup B \cup C$ takes value in $\{3, 4, \cdots, N-1\}$, i.e., subsystems obtained by tracing out at least one and at most $N-3$ qubits of the entire system.

[33] A maximally entangled state of eight qubits, in a bipartite 4—4 sense, has entropy $S = 2.773$, specific robustness $\mathcal{R} = 2.705$.

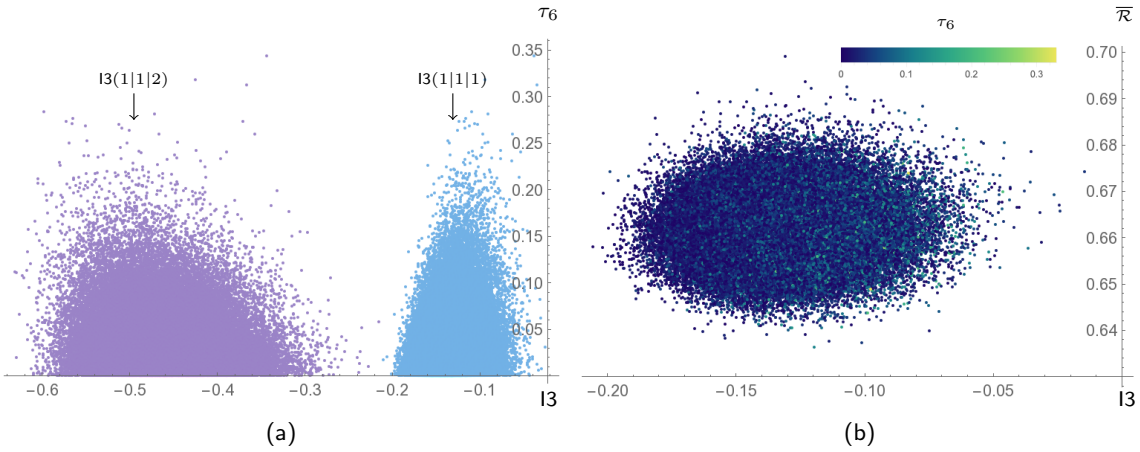

Figure 16: a) Maximal value of I3 for the two inequivalent kinds of partitionings of 4.5.33, from right to left. The values of I3 are compared to the tangle, 100000 states per class, b) Max value of $I3(1|1|1)$ compared to tangle and the average ratio (color map), 100000 states.

We follow the following canonical algorithm for computing the tripartite mutual information. For a given value of k we consider all the possible ways to partition the qubits into three subsystems (up to qubit permutations), this is given by the list of possible decompositions of k into three integers. Fixing k and the type of tripartition chosen, we compute all the possible values of I3 considering the full set of qubits permutations, and retain the maximal value. The choice is inspired by the fact that its sign clearly tells us whether there is a violation of the monogamy of mutual information for at least one permutation of the qubits. To wit,

$$\begin{aligned} &I3(k_1|k_2|k_3) = \max_{\text{perms}} I3\left(a_{\alpha_1}\cdots a_{\alpha_{k_1}}|b_{\beta_1}\cdots b_{\beta_{k_2}}|c_{\gamma_1}\cdots a_{\gamma_{k_3}}\right) \\ &\text{for } \; A=\{a_{\alpha_i}\},\; B=\{b_{\beta_i}\},\; C=\{c_{\gamma_i}\}\,, \\ &k_1+k_2+k_3=k\in\{3,4,\cdots,N-3\}\,. \end{aligned} \tag{4.5.31}$$

Since the global state is pure, we will find certain equivalences among values of I3 for different kinds of partitions $\{k_1,k_2,k_3\}$ and different values of k.

We start with a system of six qubits, where k takes values in $\{3,4,5\}$. The possible kinds of partitions for different values of k are easily listed:

$$\begin{aligned} k=3 \qquad & I3(1|1|1) \\ k=4 \qquad & I3(1|1|2) \\ k=5 \qquad & I3(1|1|3)\,, \quad I3(1|2|2) \end{aligned} \tag{4.5.32}$$

Moreover, as promised it is simple to check the following equivalence relations:

$$\begin{aligned} I3(1|1|1) &\equiv I3(1|1|3) \\ I3(1|1|2) &\equiv I3(1|2|2) \end{aligned} \tag{4.5.33}$$

We remind the reader that expressions like $I3(1|1|1)$ here represent the set of values of I3 for a particular tripartition and all the possible choices of the qubits.

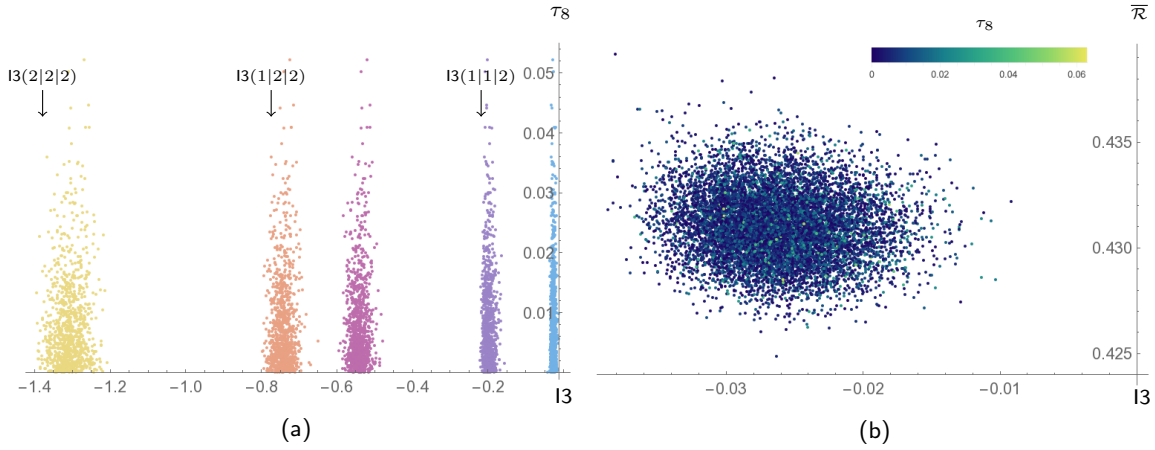

Figure 17: a) Maximal value of I3 for the five inequivalent kinds of partitionings of 4.5.34, from right to left. The values of I3 are compared to the tangle, 1000 states per class, b) Max value of $I3(1|1|1)$ compared to tangle and the average ratio (color map), 10000 states.

Fig. 16a shows the maximal value of I3 for these two classes of equivalent partitionings, one can notice that $I3(1|1|1)$ is the quantity that get closer to the violation of monogamy. For such a partitioning we then compare the maximal value of I3 to the value of the averaged specific robustness and the tangle, see Fig. 16b.

We can repeat this analysis for the eight qubits case. The list of all the equivalence classes of I3 for different values of k is:

$$\begin{aligned} &I3(1|1|1) \equiv I3(1|1|5) \\ &I3(1|1|2) \equiv I3(1|1|4) \equiv I3(1|2|4) \\ &I3(1|1|3) \equiv I3(1|3|3) \\ &I3(1|2|2) \equiv I3(1|2|3) \equiv I3(2|2|3) \\ &I3(2|2|2) \end{aligned} \tag{4.5.34}$$

Fig. 17a shows the results for the five inequivalent values of I3. As for the six qubit case, we also report the relation with the average ratio and the tangle, see Fig. 17b.

As expected from the results for four qubits, the monogamy of mutual information appears to be generically satisfied. Thus the monogamy of mutual information in these systems is not particularly restrictive vis a vis applications to holographic considerations. We expect the result to be true for larger systems as well.

From the eight qubits case another suggestive pattern appears to emerge. The values of I3 that get closer to zero correspond to the case where single qubits are involved, eg., $I3(1|1|1)$. On the other hand tripartitions into larger subsystems seem to produce the lowest values of I3, eg., $I3(2|2|2)$. The result seems to suggest that mutual information is essentially monogamous for large regions and that in search of a violation one should look at regions of the smallest possible size.

4.6 Discussion: Lessons for holography

The main message of our discussion has been to demonstrate how several measures of quantum entanglement (more generally correlations) can be used to investigate the *structure of entanglement* of pure states of non-interacting qubits. Specifically, we examined the properties of this entanglement that are captured by (a) the monogamy of negativity, (b) the specific robustness, (c) tripartite mutual information, and (d) the tangles. Our primary interest was to use these measures to delineate the distribution of entanglement inside a given pure state of N-qubits. For the most part we resorted to random sampling from the space of states, though in specific circumstances (e.g., 3 and 4 qubit systems) we did make use of available classification schemes.

Even if the systems under consideration were a vast oversimplification of continuum QFTs, we believe that they have rather useful message to impart in the context of holography. This should in part be attributed to the non-trivial structure entanglement inherent in them, coupled with their eminent tractability. Let us therefore try to abstract some general lessons for holographic systems.

Consider a state of a holographic QFT (assuming $c_{\text{eff}} \gg 1$) which is dual to a classical bulk geometry. This state can be pure or mixed (eg., the thermal density matrix which is dual to a black hole). We pick a spatial region $\mathcal{A}$ on the background geometry where the QFT resides, to make up our subsystem. The holographic entanglement entropy prescriptions of [20, 23, 39] associate the area of an extremal surface to the von Neumann entropy $S_{\mathcal{A}}$.

There are two interpretation of $S_{\mathcal{A}}$, which are sometimes called *objective* and *subjective* in the literature. The objective interpretation, which is perhaps more physical, relies on the intuition of entropy as measure of disorder of the system. The subjective point of view, on the other hand, is typical of information theory. If the entropy of $\mathcal{A}$ is thermal there is still no correlation among degrees of freedom inside $\mathcal{A}$, but the system contains complete information about some other system, i.e., its purification. It is in this second case that the von Neumann entropy can be interpreted as a measure of entanglement between the two parties, namely entanglement entropy. From the point of view of understanding the structure of quantum entanglement, the subjective viewpoint is more appropriate. We will therefore focus on pure states of some extended system; e.g., instead of the thermal density matrix we pick the thermofield double state [121]. Given a subregion $\mathcal{A}$, it should therefore be borne in mind that the complement $\mathcal{A}^c$ could include the purifying degrees of freedom.

Given this configuration, lets say that we are handed an algorithm for reconstructing the bulk geometry from the information theoretic content of the field theory. To be sure, such an algorithm does not exist to date, but it has been speculated that the picture is somewhat akin to tensor networks which encapsulate the entanglement pattern of the state [26, 42]. The closest one gets is the error correction model discussed recently in [28] (see [11] for the genesis of this set of ideas). In this context, the extremal surface and spacetime regions associated with it, such as the entanglement wedge are distinguished, in

that they capture the long range correlations of the degrees of freedom contained in the subregion $\mathcal{A}$ of interest and its complement.

Per se tensor networks or other models are but a tool to characterize the structure of correlations of a state. We want to analyse the entanglement pattern from a more operational perspective. Given a global pure state of a system U consider N-parties $\mathcal{O}_i$, each of which has access only to some subregion $\mathcal{A}_i$ of U (in general $\cup_{i=1}^{N} \mathcal{A}_i \subseteq U$) and suppose that all the parties are allowed to perform operations on their subsystems and are also allowed to communicate through classical channels.[34] The entanglement amongst these subregions is the resource that $\mathcal{O}_i$'s can use to implement typical tasks that would not be achievable if they were restricted to classical correlations. A common intuitive procedure for example would be the distillation of Bell pairs (for two parties) or GHZ_N states (for $N > 2$) which can be stored and later used for other purposes. Entanglement measures, both bipartite and multipartite, are designed to quantify this resource and characterize its properties. As mentioned earlier, in the case of two parties the logarithmic negativity provides an upper bound to distillable entanglement.[35] Unfortunately this being hard to compute in all but the simplest cases, we resorted to qubit experiments to gain some intuition; likewise to our knowledge there is no clean measure of multipartite entanglement defined for continuous systems. Effectively, we are making the approximation $\mathcal{A}_i = \text{span}\{|\,0\rangle, |\,1\rangle\}$, which is dramatic but useful truncation.[36]

Alternatively, imagine an external agent that knowns the detailed properties of the state and wants to disrupt the entanglement for a particular bipartition. As far as only bipartitions of the entire state are concerned, the minimal amount of noise that she has to inject into the system is captured by the negativity. A question we want to ask is to what extent is the dual geometry stable against these operations. Similarly one may also ask what is the consequence of the distillation procedure on the state. It would be nice to have a model where one could test the effect of different protocols explicitly. In its absence, we limited our analysis to the minimal sufficient condition for the disruption of the state, namely the violation of monogamy of mutual information.

The first lesson one learns from our study of $\mathsf{I3}$ in qubit systems is that the monogamy constraint for mutual information, which is known to be satisfied by holographic states [120], is not a particularly restrictive condition. Statistically, random states of four qubits tend in general to satisfy monogamy; this only strengthens as the number of qubits increases. We discussed how for a given number of qubits, the possible values of $\mathsf{I3}$ for

[34] This is a cartoon of the typical quantum information set-up where different parties are allowed to perform LOCC. We ignore any causal constraint (note that actually these regions live on a time-slice of the theory). This is somewhat akin to the discussions of [147] who attempt to give an operational definition to the concept of differential entropy.

[35] As explained hitherto we used instead the negativity because of its interpretation for pure states, but one can map from one quantity to the other.

[36] It would be interesting to upgrade our explorations where we replace a single qubit by a composite system of many qubits; ramping up the internal dimension could allow exploration of free vector or matrix like models. We thank Don Marolf for a discussion on this issue.

different choices of the three subregions are related. When large regions are involved, I3 becomes more and more negative and, statistically, the matching of the monogamy restriction becomes even more favoured. This in particular suggests that in search of a violation of monogamy one should look at the smallest possible regions. This would for instance suggest that in multiboundary wormhole spacetimes of [117, 119], which was analyzed in [50], one should retain the domain of outer communication of the smallest set of black holes.

Being a linear combination of mutual informations, I3 mixes quantum and classical correlations. We compared its behaviour to the multipartite entanglement captured by the tangle. Our results suggest that states with high values of quantum multipartite entanglement have a higher probability to violate monogamy of mutual information. For the GHZ_4 state this is a known result, which was used in [51] to argue that a 4-boundary state built from many copies of GHZ_4 cannot be dual to a smooth classical geometry (see also [50, 148]). Our result extends this argument to generic states with a high multipartite entanglement. We discussed a possible interpretation of multipartite entanglement that relies on the residual entanglement which is left after one takes into account all the (mixed) bipartite and tripartite entanglement in the state. A small value of 4-partite entanglement then corresponds to strong correlation among internal parties. This may suggest that special states with high internal correlation are then more suitable for holography. Nevertheless it is immediate to check that even the W_4 state violates monogamy. More generally, the states of 4-qubits with the strongest internal correlations are precisely those belonging to the special classes [Q2]-[Q6]. Under the effect of SLOCC operations a state in a class can evolve to a new state that violates monogamy. The one exception are states in class [Q5] which always respect $\mathsf{I3} < 0$. This class of 4-qubit states is in a natural sense most suitable to be "holographic". In any event it is tempting to conjecture that states with geometric duals in holography have strong bipartite (or tripartite) correlations.

For larger qubit systems, there isn't a statistically significant correlation between the N-partite entanglement and the tripartite mutual information. In fact, in our analysis it appears that increasing the number of qubits is sufficient to ensure that the $\mathsf{I3} < 0$. However, absent a classification, we have been forced to examine generic states in these systems, so it would be interesting to further analyze if there is a special sub-class of states with a specific pattern that mimics the class [Q5] of 4-qubits.

We then argued that for pure states with a given bipartitioning, even if the amount of entanglement is measured by the entropy, other measures can provide further resolution of the entanglement structure. Negativity is good measure of quantum entanglement (which can be computed in the continuum) – it allows for some resolution of the pattern of entanglement inherent in the state. We showed that for 4-qubits states the internal pattern of negativity allows for a partial resolution of the classes.

In particular, we looked at the ratio between these two quantities for bipartitions of a pure state, which we called *specific robustness*. We proposed that this captures the minimal amount of noise necessary to disentangle Bell pairs in the bipartition. We further

demonstrated how it is related to the distribution of internal entanglement. When a state is highly entangled (vis a vis S), the specific robustness is highly constrained. On the other hand when S is small the behaviour depends on the specific details of the state. In general one could say that large values of specific robustness correspond to nematic type order: the local entanglement for the bipartitioning across some entangling surface is large, but the entanglement entropy for the reduced density matrices themselves is small.

On a slightly different note, holographic states are known to satisfy other interesting constraints on the distribution of internal correlations. There are situations where the Araki-Lieb inequality (AL) can be saturated to leading order in c_{eff}, leading to the entanglement plateaux phenomena [32]. The prototypical example is a thermofield double state (a pure state in $\mathcal{H} \otimes \mathcal{H}$), where for a subsystem $\mathcal{A} \in \mathcal{H}$ one finds $S_{\mathcal{A}} = S_{\mathcal{H}\backslash\mathcal{A}} + S_{\text{thermal}}$. As described there (and further explained in [30,75]), one can visualize this as saying that the degrees of freedom in $\mathcal{A}$ can be decomposed in two groups; one that carries entanglement across the entangling surface in $\mathcal{H}$ and the other carries the thermal correlations built into the thermofield state.[37] This implies a factorization of the global state into two components.

We explained how the AL can be interpreted as a constraint on the internal pattern of entanglement of the state and related its saturation to the disentangling theorem for the negativity (cf., [30]). When the conditions for the disentangling theorem are matched then the degrees of freedom satisfy the factorization mentioned above. Curiously, it was possible to see such behaviour in special states of even small numbers of qubits. Our analysis demonstrates conclusively that the conditions for the disentangling theorem are not only sufficient, but also necessary for the saturation of Araki-Lieb, strengthening thus the entropic results of [76].

All in all, qubit systems appear to provide an excellent playground for understanding the general properties of entanglement that one might hope to understand in holographic contexts. While our analysis has been restricted to the simplest of possible scenarios, the rich structure seen in the qubit states, leads us to believe that one could extract general lessons from examining them closely. It would be interesting to build in minimal dynamics and or consider networks of qubits as in graph states or tensor type networks [28], to gain more insight into the interplay of entanglement and geometry.

[37] Geometrically this is realized when the extremal surface associated with a region $\mathcal{A}$ splits up into a disjoint union of a small surface that is anchored on $\mathcal{A}^c = \mathcal{H}\backslash\mathcal{A}$ and the bifurcation surface of a black hole, see [32] for illustrative examples.

4.A Four qubit states: Detailed analysis of SLOCC classes

In this appendix we collect the results for the SLOCC classes of 4-qubit states. These complement the discussion of §4.4.2 in that they encompass the partitions of qubits we did not consider in the main text.

[Q1]

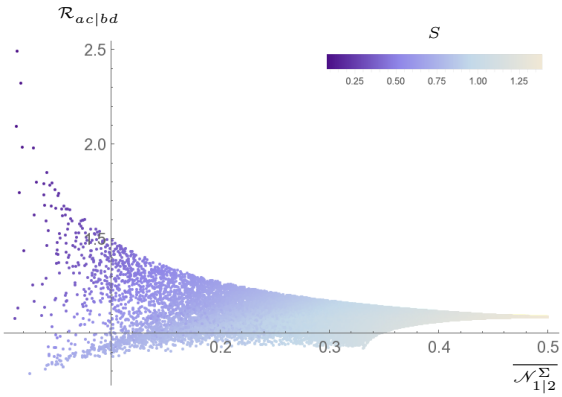

(a) The result for the cut $\mathcal{R}_{ad|bc}$ is equivalent.

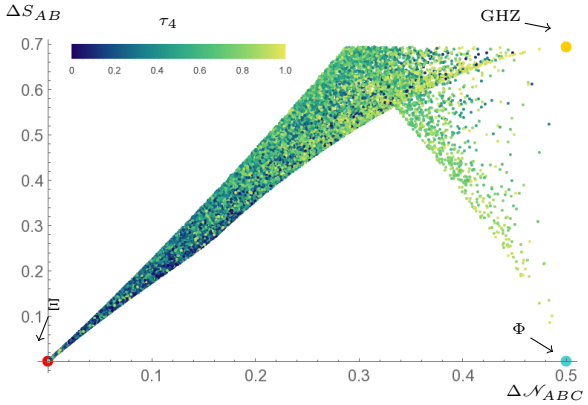

(b) $A = \{a\}$, $B = \{bc\}$, $C = \{d\}$

Figure 18: (a) Specific robustness for different choices of Σ. (b) Saturation of AL for alternative permutation of qubits, see Tab. 4.1 for the full list of possible cases.

$A = \{b\}\,,\ B = \{cd\}\,,\ C = \{a\}$	$A = \{a\}\,,\ B = \{bc\}\,,\ C = \{d\}$
$A = \{a\}\,,\ B = \{cd\}\,,\ C = \{b\}$	$A = \{a\}\,,\ B = \{bd\}\,,\ C = \{c\}$
$A = \{d\}\,,\ B = \{ab\}\,,\ C = \{c\}$	$A = \{b\}\,,\ B = \{ac\}\,,\ C = \{d\}$
$A = \{c\}\,,\ B = \{ab\}\,,\ C = \{d\}$	$A = \{b\}\,,\ B = \{ad\}\,,\ C = \{c\}$
	$A = \{d\}\,,\ B = \{ac\}\,,\ C = \{b\}$
	$A = \{d\}\,,\ B = \{bc\}\,,\ C = \{a\}$
	$A = \{c\}\,,\ B = \{ad\}\,,\ C = \{b\}$
	$A = \{c\}\,,\ B = \{bd\}\,,\ C = \{a\}$

Table 4.1: Possible permutations of qubits for the disentangling theorem of the negativity and the saturation of AL inequality. The left column shows the choices which give the result shown in the main text, the right column corresponds to Fig. 18b.

[Q2]

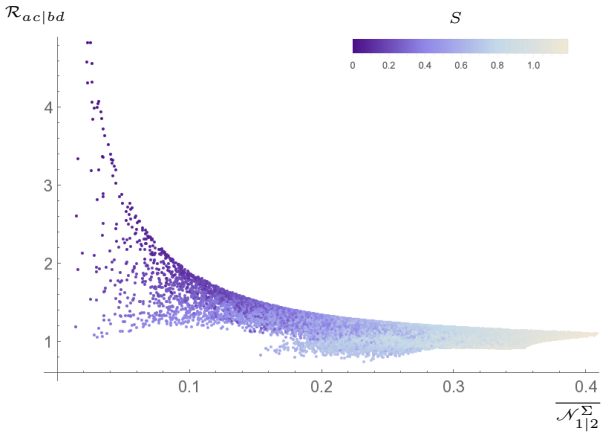

(a) The result for the cut $\mathcal{R}_{ad|bc}$ is equivalent. The plot is truncated, few states with small values of $\mathcal{N}$ and ratio up to $\mathcal{R} \sim 7.2$ are not shown ($\mathcal{R} \sim 4.8$ for the other cut).

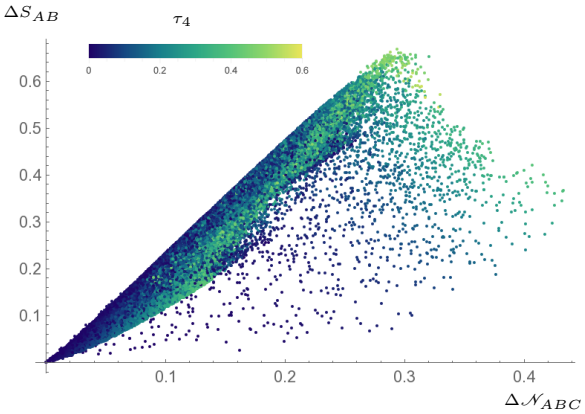

(b) $A = \{a\}$, $B = \{bc\}$, $C = \{d\}$

Figure 19: (a) Specific robustness for different choices of Σ. (b) Saturation of AL for alternative permutation of qubits, see Tab. 4.2 for the full list of possible cases.

$A = \{a\}\,,\ B = \{cd\}\,,\ C = \{b\}$	$A = \{a\}\,,\ B = \{bc\}\,,\ C = \{d\}$
$A = \{b\}\,,\ B = \{cd\}\,,\ C = \{a\}$	$A = \{a\}\,,\ B = \{bd\}\,,\ C = \{c\}$
$A = \{d\}\,,\ B = \{ab\}\,,\ C = \{c\}$	$A = \{b\}\,,\ B = \{ac\}\,,\ C = \{d\}$
$A = \{c\}\,,\ B = \{ab\}\,,\ C = \{d\}$	$A = \{b\}\,,\ B = \{ad\}\,,\ C = \{c\}$
	$A = \{d\}\,,\ B = \{ac\}\,,\ C = \{b\}$
	$A = \{d\}\,,\ B = \{bc\}\,,\ C = \{a\}$
	$A = \{c\}\,,\ B = \{ad\}\,,\ C = \{b\}$
	$A = \{c\}\,,\ B = \{bd\}\,,\ C = \{a\}$

Table 4.2: Possible permutations of qubits for the disentangling theorem of the negativity and the saturation of AL inequality. The left column shows the choices which give the result shown in the main text, the right column corresponds to Fig. 19b.

[Q3]

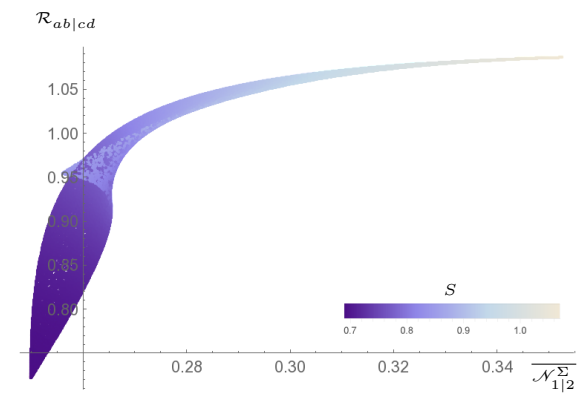

(a) The result for the cut $\mathcal{R}_{ad|bc}$ is equivalent.

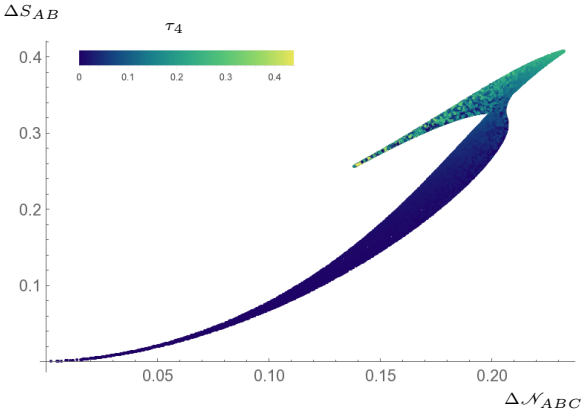

(b) $A = \{a\}$, $B = \{bc\}$, $C = \{d\}$

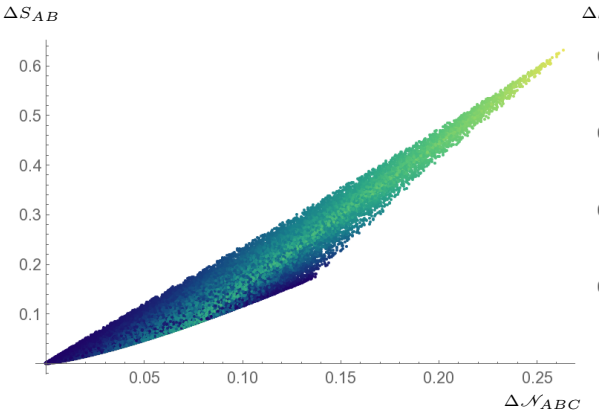

(c) $A = \{a\}$, $B = \{bd\}$, $C = \{c\}$

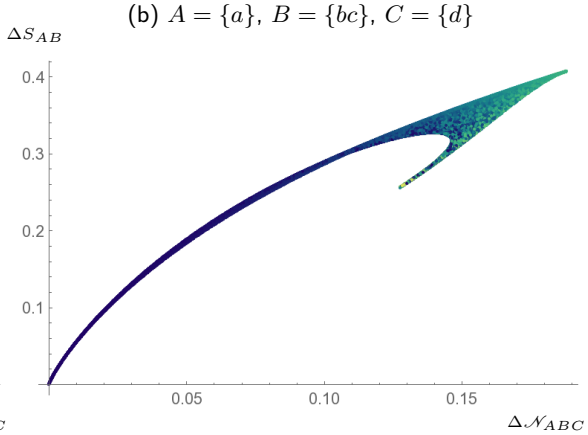

(d) $A = \{b\}$, $B = \{ad\}$, $C = \{c\}$

Figure 20: (a) Specific robustness for different choices of Σ. (b)(c)(d) Saturation of AL for alternative permutations of qubits, see Tab. 4.3 for the full list of possible cases.

$A = \{b\}\,,\ B = \{ac\}\,,\ C = \{d\}$	$A = \{a\}\,,\ B = \{bc\}\,,\ C = \{d\}$
$A = \{d\}\,,\ B = \{ac\}\,,\ C = \{b\}$	$A = \{a\}\,,\ B = \{cd\}\,,\ C = \{b\}$
	$A = \{c\}\,,\ B = \{ab\}\,,\ C = \{d\}$
	$A = \{c\}\,,\ B = \{ad\}\,,\ C = \{b\}$
$A = \{a\}\,,\ B = \{bd\}\,,\ C = \{c\}$	$A = \{b\}\,,\ B = \{ad\}\,,\ C = \{c\}$
$A = \{c\}\,,\ B = \{bd\}\,,\ C = \{a\}$	$A = \{b\}\,,\ B = \{cd\}\,,\ C = \{a\}$
	$A = \{d\}\,,\ B = \{ab\}\,,\ C = \{c\}$
	$A = \{d\}\,,\ B = \{bc\}\,,\ C = \{a\}$

Table 4.3: Possible permutations of qubits for the disentangling theorem of the negativity and the saturation of AL inequality. The top left cases give the result shown in the main text. Top right, Fig. 20b. Bottom left, Fig. 20c. Bottom right, Fig. 20d.

[Q4]

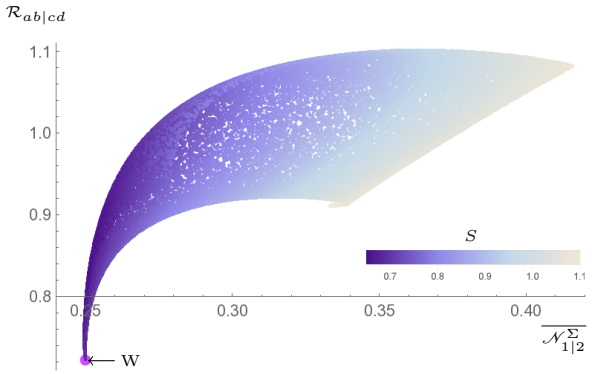

(a) The result for the cut $\mathcal{R}_{ad|bc}$ is equivalent to the one shown in the main text.

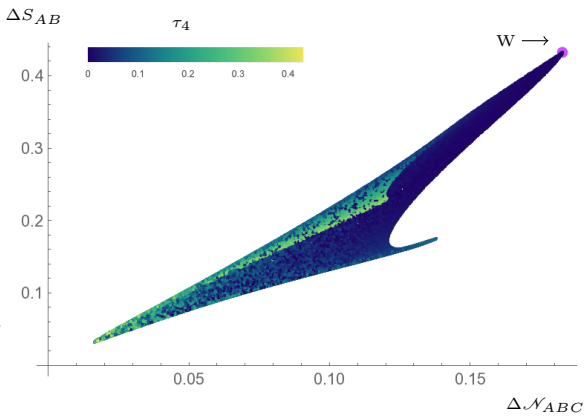

(b) $A = \{a\}$, $B = \{cd\}$, $C = \{b\}$

Figure 21: (a) Specific robustness for different choices of Σ. (b) Saturation of AL for alternative permutation of qubits, see Tab. 4.4 for the full list of possible cases.

$A = \{a\}\,,\ B = \{bc\}\,,\ C = \{d\}$	$A = \{a\}\,,\ B = \{cd\}\,,\ C = \{b\}$
$A = \{a\}\,,\ B = \{bd\}\,,\ C = \{c\}$	$A = \{b\}\,,\ B = \{cd\}\,,\ C = \{a\}$
$A = \{b\}\,,\ B = \{ac\}\,,\ C = \{d\}$	$A = \{d\}\,,\ B = \{ab\}\,,\ C = \{c\}$
$A = \{b\}\,,\ B = \{ad\}\,,\ C = \{c\}$	$A = \{c\}\,,\ B = \{ab\}\,,\ C = \{d\}$
$A = \{d\}\,,\ B = \{ac\}\,,\ C = \{b\}$	
$A = \{d\}\,,\ B = \{bc\}\,,\ C = \{a\}$	
$A = \{c\}\,,\ B = \{ad\}\,,\ C = \{b\}$	
$A = \{c\}\,,\ B = \{bd\}\,,\ C = \{a\}$	

Table 4.4: Possible permutations of qubits for the disentangling theorem of the negativity and the saturation of AL inequality. The left column shows the choices which give the result shown in the main text, the right column corresponds to Fig. 21b.

[Q5]

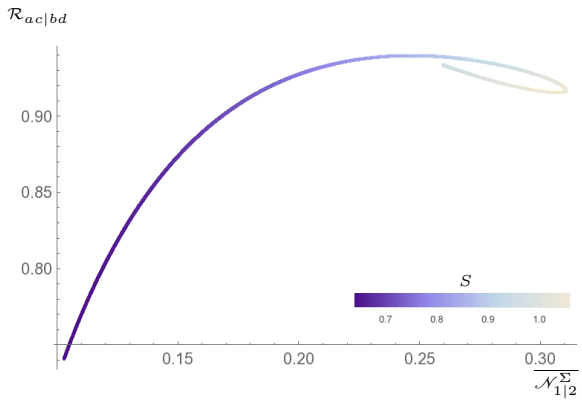

(a) The result for the cut $\mathcal{R}_{ad|bc}$ is equivalent to the one shown in the main text.

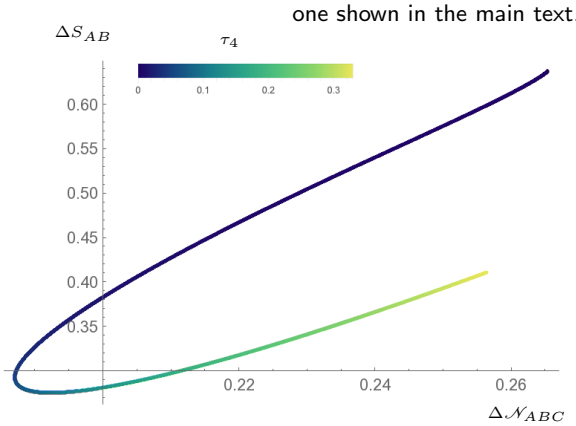

(b) $A = \{a\}$, $B = \{bd\}$, $C = \{c\}$

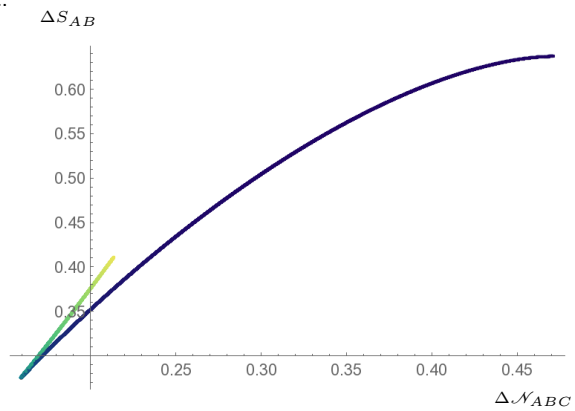

(c) $A = \{b\}$, $B = \{ac\}$, $C = \{d\}$

Figure 22: (a) Specific robustness for different choices of Σ. (b)(c) Saturation of AL for alternative permutations of qubits, see Tab. 4.5 for the full list of possible cases.

$A = \{a\}\,,\ B = \{bc\}\,,\ C = \{d\}$	$A = \{a\}\,,\ B = \{bd\}\,,\ C = \{c\}$	$A = \{b\}\,,\ B = \{ac\}\,,\ C = \{d\}$
$A = \{a\}\,,\ B = \{cd\}\,,\ C = \{b\}$	$A = \{c\}\,,\ B = \{bd\}\,,\ C = \{a\}$	$A = \{d\}\,,\ B = \{ac\}\,,\ C = \{b\}$
$A = \{b\}\,,\ B = \{ad\}\,,\ C = \{c\}$		
$A = \{b\}\,,\ B = \{cd\}\,,\ C = \{a\}$		
$A = \{d\}\,,\ B = \{ab\}\,,\ C = \{c\}$		
$A = \{d\}\,,\ B = \{bc\}\,,\ C = \{a\}$		
$A = \{c\}\,,\ B = \{ab\}\,,\ C = \{d\}$		
$A = \{c\}\,,\ B = \{ad\}\,,\ C = \{b\}$		

Table 4.5: Possible permutations of qubits for the disentangling theorem of the negativity and the saturation of AL inequality. The left column shows the choices which give the result shown in the main text. The center column corresponds to Fig. 22b, the right one to Fig. 22c.

[Q6]

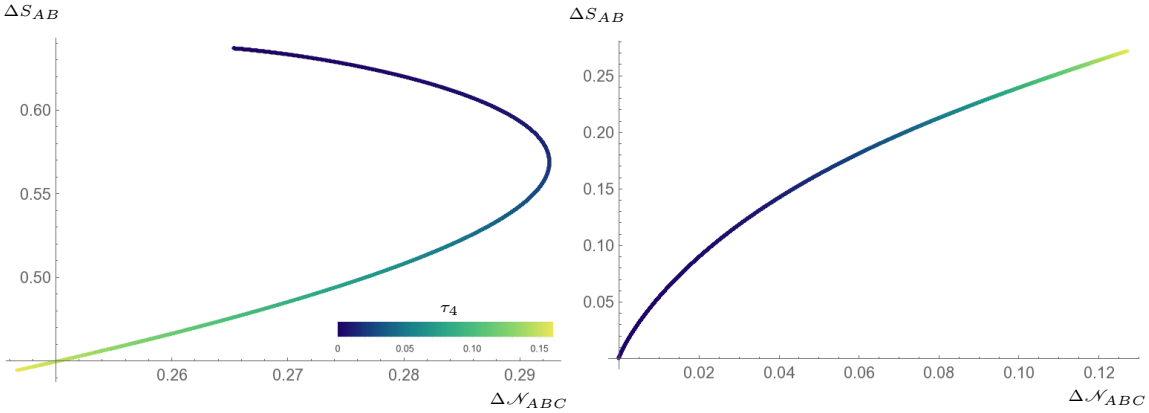

(a) $A = \{b\}$, $B = \{ac\}$, $C = \{d\}$ (b) $A = \{b\}$, $B = \{cd\}$, $C = \{a\}$

Figure 23: Saturation of AL for alternative permutations of qubits, see Tab. 4.6 for the full list of possible cases.

$A = \{a\}\,,\ B = \{bc\}\,,\ C = \{d\}$	$A = \{b\}\,,\ B = \{ac\}\,,\ C = \{d\}$	$A = \{b\}\,,\ B = \{cd\}\,,\ C = \{a\}$
$A = \{a\}\,,\ B = \{bd\}\,,\ C = \{c\}$	$A = \{b\}\,,\ B = \{ad\}\,,\ C = \{c\}$	$A = \{d\}\,,\ B = \{bc\}\,,\ C = \{a\}$
$A = \{a\}\,,\ B = \{cd\}\,,\ C = \{b\}$	$A = \{d\}\,,\ B = \{ab\}\,,\ C = \{c\}$	$A = \{c\}\,,\ B = \{bd\}\,,\ C = \{a\}$
	$A = \{d\}\,,\ B = \{ac\}\,,\ C = \{b\}$	
	$A = \{c\}\,,\ B = \{ab\}\,,\ C = \{d\}$	
	$A = \{c\}\,,\ B = \{ad\}\,,\ C = \{b\}$	

Table 4.6: Possible permutations of qubits for the disentangling theorem of the negativity and the saturation of AL inequality. The left column shows the choices which give the result shown in the main text. The center column corresponds to Fig. 23a, the right one to Fig. 23b.

Chapter 5

Tripartite information of highly entangled states

This chapter is a reproduction of the paper *Tripartite information of highly entangled states* [149].

The Ryu-Takayanagi prescription for the computation of holographic entanglement entropy implies that for states which have a classical geometric dual the sign of the tripartite information is non-positive. In the previous chapter the behaviour of the tripartite information was analysed for states of systems containing up to eight qubits. In this chapter this investigation is extended to larger systems for some particular states.

We first look at states with a large amount of multipartite entanglement. We explore the behaviour of the tripartite information for states obtained in various ways starting from GHZ states and propose a particular construction that we conjecture generates global maxima of the tripartite information. The result of this analysis suggests that 4-partite quantum entanglement is an essential ingredient for states with positive value of the tripartite information.

Next, we look at states with a large amount of bipartite entanglement. States which are exactly maximally entangled for each possible bipartitions of the system where introduced recently in the literature and are known as *perfect states*. They can be built using a particular kind of tensors, the *perfect tensors*, as building blocks of a tensor network. States realized by these networks have been used in [28] as a toy model to sharpen the connection between AdS/CFT and quantum error correction. We compute the tripartite information for perfect states of an arbitrary number of qubits and all possible partitionings of the system.

The results of the previous chapter suggest that from an operational perspective, one should ask how stable the sign of the tripartite information is under different operations performed on the constituents of the system. This is particularly interesting in the case of perfect states, as for some partitionings the tripartite information vanishes exactly. We can hence look for small perturbations which are able to produce a positive value. Here we comment on the case of $N = 6$ qubits, the only possible perfect state for qubits.

Finally, recent work suggested that the tripartite information can be used as a parameter to detect scrambling of information. Indeed, perfect states are by definition scrambled states, and they are minimizers of the tripartite information. We comment on this proposal building some counterexamples explicitly and showing that for the purpose of detecting scrambling, the tripartite information is a sensible quantity only for states which are symmetric under all possible qubits permutations. We argue that the average of the tripartite information over qubits permutations could be a more sensible quantity.

Notation: throughout this chapter we slightly change the notation for the tripartite information that we used previously, and keep instead the notation used in the original paper. While in the previous chapter we wrote $I3(A|B|C)$ we now use the expression $I3(A:B:C)$ instead.

5.1 Introduction

The *tripartite information* ($I3$) was introduced in [150], under the name topological entropy, as a quantity to characterize entanglement in states of many-body systems with topological order. Given three subsystems A, B, C it is defined by the following expression: $I3(A:B:C) = S_A + S_B + S_C - S_{AB} - S_{AC} - S_{BC} + S_{ABC}$, where S is the von Neumann entropy.

For arbitrary states of many-body systems $I3$ has no definite sign. This is true also in field theory, cf., [151]. On the contrary, within the context of the gauge gravity duality, it was shown in [120] that for states of CFTs with a classical holographic dual, $I3$ is always non-positive. This sign definiteness is a direct consequence of the Ryu-Takayanagi prescription [20] for the computation of the von Neumann entropy in holography, and it implies that the holographic mutual information is monogamous.

As consequence of this constraint imposed by holography, the sign of $I3$ has been used in various works to explore what states might be good candidates to encode the properties of classical geometries. In the framework of the ER=EPR[1] proposal [29] for example, it was argued in [51] that black holes obtained by "collapsing" multiple copies of GHZ states of 4 qubits (for which $I3 = +1$) cannot be connected by classical Einstein-Rosen bridges.[2] The sign of $I3$ was an important consistency check also in the work of [28], which within the context of the quantum-error-correction interpretation of AdS/CFT of [11], built a toy model of holographic states and codes using tensor network constructions.

For qubits systems, the behaviour of $I3$ was explored in [116], where it was shown that random states typically have negative value of $I3$, suggesting that the holographic

[1] A conjectured equivalence between entanglement (EPR for Einstein-Podolsky-Rosen) and geometric connectedness (ER for Einstein-Rosen bridges).

[2] Strictly speaking this was not an holographic argument, as ER=EPR is a general proposal about quantum gravity, nevertheless one can imagine an analogue version of this argument where the geometry is dual to the mentioned qubits state.

constraint is not particularly restrictive. Results also indicated that one has to be careful about the particular choices of subsystems for which $I3$ is computed, as some partitionings might be more suitable than others to detect violation of monogamy. Furthermore having holography in mind, the authors proposed that we should look not only at the values of $I3$ for a specific state, but also at how stable this sign is against small deformations or operations performed on it. This proposal was motivated by the finding that for states of 4 qubits, there is only one class of states with definite sign of $I3$.[3]

Another interesting property of $I3$ which was found in [116] is the fact that its absolute value seems to be minimized by states which are highly entangled for all bipartitions. In the case of 4 qubits, a numerical search for the minimum of $I3$ approaches a state, known as M-state in the quantum information literature [152], which is the maximally entangled state of 4 qubits. Indeed it was recently shown in [153] that the "perfect states" of [28] are the minimizers of $I3$ and that due to this property $I3$ can be used as a measure of information scrambling [8] [154] [155] and quantum chaos [156].

In this chapter we explore the behaviour of $I3$ for some highly entangled states in a bipartite or multipartite sense. In §5.2 we review the definition of $I3$ and discuss some of its general properties. In §5.3 we focus on qubits systems with maximal multipartite entanglement. We explore products of GHZ states and their perturbations in arbitrary directions in Hilbert space, for all possible partitionings of the systems. We move then to the case of states with maximal bipartite entanglement in §5.4, where we extend the result of [153] to different partitioning of perfect states and comment about their deformations. We conclude in §5.5 with a summary and interpretation of the results, together with a discussion about open questions and future directions.

5.2 General properties

Definitions and notation

To simplify the discussion in the following we will focus on generic pure states for systems of an arbitrary number of qu-b-its, nevertheless most of the results naturally extend to systems of qu-d-its. The fact that we are only looking at pure states will not be a restriction, because for any mixed state one can always consider some purification by enlarging the system.

Pure states of a system U of N qubits live in a 2^N dimensional Hilbert space $\mathcal{H}_{(2^N)}$ with structure $\mathcal{H}_{(2)}^{\otimes N}$, where $\mathcal{H}_{(2)}$ is the two-dimensional Hilbert space of each individual qubit. We will consider subsets of U such that $A \cup B \cup C \subseteq U$ and $A \cap B \cap C = \emptyset$. The Hilbert space corresponding to this partitioning then is $\mathcal{H}_A \otimes \mathcal{H}_B \otimes \mathcal{H}_C$, and the tripartite

[3] States of 4 qubits can be classified into 9 equivalence classes. States within a class are equivalent in the sense that they can be mapped to each other using operations known as SLOCC (stochastic local operations and classical communication). We refer the reader to the original paper for further details.

information is defined as

$$I3(A:B:C) \equiv S_A + S_B + S_C - S_{AB} - S_{AC} - S_{BC} + S_{ABC} \tag{5.2.1}$$

Since we are only considering pure states of U, in the case $A \cup B \cup C = U$ one trivially has $I3 \equiv 0$, so in the following we will restrict to $A \cup B \cup C \subset U$. We will use the notation $\mathcal{P} = (A : B : C)$ for a particular partitioning and $I3(\mathcal{P})$ for the tripartite information, stressing that the latter is not only a function of a state but also of a specific partitioning.

Oftentimes the specific choice of the qubits belonging to the subsets A, B, C will not be important and we will only need to consider the cardinality of the subsystems. In this case we will write $\mathcal{P} = (a : b : c)$ where a, b, c refer to the cardinalities of A, B, C respectively. Ignoring the case $a + b + c = N$ (for which $I3 = 0$) we then have the conditions

$$\begin{aligned} &1 \leq a \leq N-3, \quad 1 \leq b \leq N-3, \quad 1 \leq c \leq N-3, \\ &3 \leq a+b+c \leq N-1 \end{aligned} \tag{5.2.2}$$

We will use the expression $I3(a : b : c)$ to denote the *set* of all values of $I3(\mathcal{P})$, with $\mathcal{P} = (A : B : C)$, that can be obtained by permuting the specific choice of the qubits in each subset, while keeping a, b and c fixed.

For a given state, or class of states, we want to explore the behaviour of $I3(\mathcal{P})$ for all possible partitionings $\mathcal{P}$.

Equivalences among partitionings

For each partitioning $\mathcal{P} = (A : B : C)$ we will call D the complement of $A \cup B \cup C$ in U. As a consequence of the purity of the state of U, the entropy of each subsystem is equal to the entropy of the corresponding complementary subsystem. This implies that the tripartite information has the following symmetry [153]

$$I3(A:B:C) = I3(A:B:D) = I3(A:C:D) = I3(B:C:D) \tag{5.2.3}$$

As a consequence of Eq. (5.2.3) then, some of the sets introduced before are actually equivalent. For example, $I3(a:b:c) = I3(N-(a+b+c):b:c)$, see also [116]. Notice in particular that for the case where N is a multiple of 4, the set $I3(\frac{N}{4} : \frac{N}{4} : \frac{N}{4})$ is unique.

Product states

We now explore the behaviour of the tripartite information for states that are obtained by taking products of states of smaller systems. Consider two Hilbert spaces $\mathcal{H}_1, \mathcal{H}_2$ associated to systems U_1, U_2 of respectively N_1 and N_2 qubits. Starting from the states $|\,\psi\rangle_1 \in \mathcal{H}_1$ and $|\,\phi\rangle_2 \in \mathcal{H}_2$ we build the state $|\,\chi\rangle_{12} = |\,\psi\rangle_1 \otimes |\,\phi\rangle_2$. We choose then a partitioning $\mathcal{P}_1 = (A_1 : B_1 : C_1)$ of U_1 and ask how the values of $I3(\mathcal{P})$ for partitionings of the joint system depend on $I3(\mathcal{P}_1)$ and how the subsets of U_1 in $\mathcal{P}_1$ are "contaminated"

by qubits of U_2. This means that we will not change the partitioning of the system U_1 but only add qubits of U_2 into one or more subsystems of $\mathcal{P}_1$.

Due to the additivity of the entropy for product states, one can check that the following cases are possible

$$\begin{aligned}
&\mathcal{P} = (A_1X : B_1 : C_1) && \Rightarrow && I3(\mathcal{P}) = I3(\mathcal{P}_1) && \text{for } X \subseteq U_2 \\
&\mathcal{P} = (A_1X : B_1Y : C_1) && \Rightarrow && I3(\mathcal{P}) = I3(\mathcal{P}_1) && \text{for } X \cup Y \subseteq U_2 \\
&\mathcal{P} = (A_1X : B_1Y : C_1Z) && \Rightarrow && I3(\mathcal{P}) = I3(\mathcal{P}_1) + I3(\mathcal{P}_2) && \text{for } X \cup Y \cup Z \subset U_2 \\
&\mathcal{P} = (A_1X : B_1Y : C_1Z) && \Rightarrow && I3(\mathcal{P}) = I3(\mathcal{P}_1) && \text{for } X \cup Y \cup Z = U_2
\end{aligned} \tag{5.2.4}$$

where $\mathcal{P}_2 = (X : Y : Z)$. In this set-up then, $I3(\mathcal{P})$ is either invariant or additive. We will come back to this property and some of its consequences in the following sections.

General bounds

We first look at general bounds for $I3(\mathcal{P})$ that are satisfied by all states and partitionings. In the next sections we will explore further bounds that apply to specific partitionings for different classes of states. The fact that $I3(\mathcal{P})$ is in general bounded is an obvious consequence of the bound of the entropy.

A lower bound for the tripartite information was given in [153] and can be found by rewriting $I3(\mathcal{P})$ as[4]

$$I3(A : B : C) = I(A : B) + I(A : C) - I(A : BC) \tag{5.2.5}$$

where $I(X : Y) = S_X + S_Y - S_{XY}$ is the mutual information. From the non-negativity of mutual information it follows then that $I3(A : B : C) \geq -I(A : BC)$. Furthermore $I(A : BC) \leq 2\min(S_A, S_{BC})$ which implies $I3(A : B : C) \geq 2\min(S_A, S_{BC})$. One can then repeat the same argument using the symmetry Eq. (5.2.3), getting

$$I3(A : B : C) \geq -2\min(S_A, S_B, S_C, S_D, S_{AB}, S_{AC}, S_{AD}, S_{BC}, S_{BD}, S_{CD}) \tag{5.2.6}$$

Note that the minimal value of $I3(\mathcal{P})$ is attained for states such that $S_{XY} \geq S_X \ \forall X, Y$. In this case the bound is the one reported in [153].

$$I3(A : B : C) \geq -2\min(S_A, S_B, S_C, S_D) \tag{5.2.7}$$

When N is a multiple of 4, $I3(\mathcal{P})$ is minimized by states such that all the entropies S_X are maximal and $\mathcal{P} = (\frac{N}{4} : \frac{N}{4} : \frac{N}{4})$; in this case $I3(\mathcal{P}) = -\frac{N}{2}$. We will analyse the behaviour of $I3(\mathcal{P})$ for these states in more detail in §5.4. For $N = 1, 2, 3 \pmod 4$ instead, the bound would be tighter.

[4] We thank Beni Yoshida for a clarification about this point.

To derive an upper bound one could start again from Eq. (5.2.5), but using strong subadditivity (SSA)[5] the bound is more restrictive. We can simply rewrite the tripartite information as

$$\begin{aligned} I3(A:B:C) \equiv & \frac{1}{2}\left(S_A + S_B - S_{AC} - S_{BC}\right) + \frac{1}{2}\left(S_A + S_B - S_{AC} - S_{BC}\right) \\ & + \frac{1}{2}\left(S_A + S_B - S_{AC} - S_{BC}\right) + S_{ABC} \equiv \Sigma_{ABC} + S_{ABC} \end{aligned} \tag{5.2.8}$$

SSA implies then $\Sigma_{ABC} \leq 0$. Using purity of the global state (which implies $S_{ABC} = S_D$) and the symmetry Eq. (5.2.3) one gets

$$I3(A:B:C) \leq \min(S_A, S_B, S_C, S_D) \tag{5.2.9}$$

Similarly to before, when N is a multiple of 4, $I3(\frac{N}{4}:\frac{N}{4}:\frac{N}{4})$ is maximal for states with maximal entropies S_X. In this case $I3(\mathcal{P}) \leq \frac{N}{4}$.

5.3 States with maximal multipartite entanglement

The GHZ state of N qubits is defined as

$$|\,\mathrm{GHZ}_N\rangle = \frac{1}{\sqrt{2}}\left(|0...0\rangle + |1...1\rangle\right) \tag{5.3.10}$$

and it is a well known example of a state for which $I3(\mathcal{P}) \geq 0$. Ignoring the trivial case $N = 3$ for which $I3(\mathcal{P}) = 0$, an immediate calculation shows that for any subsystem X of the N qubits, the entropy is $S_X = 1$. This implies that for any partitioning $\mathcal{P}$, one has $I3(\mathcal{P}) = 1$ for any N. For the case $N = 4$ this immediately implies that the state GHZ_4 is the global maximum of $I3(\mathcal{P})$, because it saturates the bound Eq. (5.2.9).

Consider now the state $|\,\mathrm{GHZ}_4\rangle^{\otimes k}$, obtained by taking a tensor product of k copies of the state GHZ_4. For this state of the new $N = 4k$ qubits system we look at the partitioning defined as follows: take one qubit for each copy of the GHZ_4 state and put it into the subsystem A of the larger system, then repeat the same procedure for subsystems B and C. For this particular partitioning it follows from Eq. (5.2.4) that $I3(\mathcal{P}) = k = \frac{N}{4}$. As before, this value saturates the bound Eq. (5.2.9), implying that these product states are the global maxima of $I3(\frac{N}{4}:\frac{N}{4}:\frac{N}{4})$ for $4k$ qubits.

In this section we discuss how the values of $I3(\mathcal{P})$ depend on the different partitionings $\mathcal{P}$ for deformations of GHZ_N states. In particular we present an algorithmic construction that we conjecture can be used to build local maxima of $I3(\mathcal{P})$ for arbitrary N and any given $\mathcal{P}$. In the particular case $N = 4k$ this construction recovers the previous result for the state $|\,\mathrm{GHZ}_4\rangle^{\otimes k}$ and generates an entire new family of states that saturate the bound.

[5] For the convenience of the reader we report here the definition of strong subadditivity $S_A + S_B \leq S_{AC} + S_{BC}$.

$S_1(\epsilon)$	both I_X and I_{X^c} are Hom in η	$\lambda_1 = \frac{(1+2\mathrm{Re}\epsilon+\lvert\epsilon\rvert^2)}{1+\lvert 1+\epsilon\rvert^2},\ \lambda_2 = \frac{1}{1+\lvert 1+\epsilon\rvert^2}$
$S_2(\epsilon)$	I_X is Hom in η and I_{X^c} in $\bar{\eta}$	$\lambda_{12} = \frac{(2+\lvert\epsilon\rvert^2 \pm \lvert\epsilon\rvert\sqrt{4+\lvert\epsilon\rvert^2})}{2(2+\lvert\epsilon\rvert^2)}$
$S_3(\epsilon)$	either I_X or I_{X^c} is Hom	$\lambda_1 = \frac{1}{2+\lvert\epsilon\rvert^2},\ \lambda_2 = \frac{1+\lvert\epsilon\rvert^2}{2+\lvert\epsilon\rvert^2}$
$S_4(\epsilon)$	both I_X and I_{X^c} are not Hom	$\lambda_1 = \frac{1}{2+\lvert\epsilon\rvert^2},\ \lambda_2 = \frac{1}{2+\lvert\epsilon\rvert^2},\ \lambda_3 = \frac{\lvert\epsilon\rvert^2}{2+\lvert\epsilon\rvert^2}$

Table 5.1: The table shows the four possible configurations of the strings of digits I_X and I_{X^c} and the set of eigenvalues of the corresponding expression for the reduced density matrix ρ_X. The functions $S_i(\epsilon)$ are the entropies, for the various cases labelled by i. The parameters $\eta, \bar{\eta}$ are mutually exclusive variables, when $\eta = 0$, $\bar{\eta} = 1$, and vice versa.

Deformations of GHZ_N states

We start by considering the following deformation of the GHZ_N state

$$|\,\mathrm{GHZ}_N\rangle \to |\,\psi_I^\epsilon\rangle = \begin{cases} \frac{1}{\sqrt{1+|1+\epsilon|^2}}\left(|\,0...0\rangle + |\,1...1\rangle + \epsilon\,|\,I\rangle\right) & \text{if } |\,I\rangle \in \{|\,0...0\rangle, |\,1...1\rangle\} \\ \frac{1}{\sqrt{2+|\epsilon|^2}}\left(|\,0...0\rangle + |\,1...1\rangle + \epsilon\,|\,I\rangle\right) & \text{otherwise} \end{cases} \tag{5.3.11}$$

where $|\,I\rangle$ is an element of the computational basis $\{|\,0...0\rangle, |\,0...1\rangle, ...\ |\,1...1\rangle\}$. Consider then a generic bipartition of the system into a subsystem X of size x and its complement X^c of size $N-x$. The reduced density matrix ρ_X associated to the subsystem X is given by (up to the normalization factor)

$$\begin{aligned} \rho_X(\epsilon, I) \equiv \mathrm{Tr}_{X^c}\rho_I^\epsilon = |\,0...0\rangle\langle\,0...0\,| + |\,1...1\rangle\langle\,1...1\,| + |\epsilon|^2\,|\,I_X\rangle\langle\,I_X\,| \\ + \begin{cases} \epsilon^*\,|\,0...0\rangle\langle\,I_X\,| + \epsilon\,|\,I_X\rangle\langle\,0...0\,| & \text{if } |\,I_{X^c}\rangle \text{ is Homogeneous in 0's} \\ \epsilon^*\,|\,1...1\rangle\langle\,I_X\,| + \epsilon\,|\,I_X\rangle\langle\,1...1\,| & \text{if } |\,I_{X^c}\rangle \text{ is Homogeneous in 1's} \\ 0 & \text{if } |\,I_{X^c}\rangle \text{ is not Homogeneous} \end{cases} \end{aligned} \tag{5.3.12}$$

where $|\,I_X\rangle$ and $|\,I_{X^c}\rangle$ are the states of subsystems X and X^c when the global system is in the state $|\,I\rangle$. By the expression "Homogeneous in 0's" we mean $|\,I_{X^c}\rangle = |\,0\rangle^{\otimes N-x}$ (and similarly for 1's). $|\,I_{X^c}\rangle$ instead is not Homogeneous if $|\,I_{X^c}\rangle = |\,0\rangle^{\otimes\gamma} \otimes |\,1\rangle^{\otimes\delta}$ for any γ, δ such that $\gamma + \delta = N - x$. In the following we will use short expressions like "I_{X^c} is Hom" to indicate these cases (eventually dropping also the "ket", as we think about I_{X^c} simply as a string of digits).

Depending on the homogeneity properties of $|\,I_X\rangle$ we then have four possibilities for the final expression of the reduced density matrix. We list the possible cases, together with the corresponding eigenvalues of $\rho_X(\epsilon, I)$, in Tab. 5.1. This is an exact result, not only perturbative in ϵ.

The functions $S_i(\epsilon)$ that give the entropy of $\rho_X(\epsilon, I)$ depending on its possible structures, all have vanishing first derivative at $\epsilon = 0$. This shows that in the Hilbert space of

ϕ	Details of I_A, I_B, I_C, I_D	$I3(\mathcal{P})$
0	X is not Hom, $\forall X$	$S_4(\epsilon)$
1	$\exists!\, X$ that is Hom	$S_3(\epsilon)$
2	X, Y are Hom in λ	$S_3(\epsilon)$
	X is Hom in η and Y is Hom in $\bar{\eta}$	$2S_3(\epsilon) - S_4(\epsilon)$
3	X is not Hom and X^c is Hom	$S_3(\epsilon)$
	X is not Hom and X^c is not Hom	$2S_3(\epsilon) - S_4(\epsilon)$
4	$I_A \cup I_B \cup I_C \cup I_D \equiv I$ is Hom	$S_1(\epsilon)$
	X is Hom in η and X^c is Hom in $\bar{\eta}$	$S_2(\epsilon)$
	$X \cup Y$ is Hom in η and $(X \cup Y)^c$ is Hom in $\bar{\eta}$	$4S_3(\epsilon) - 2S_4(\epsilon) - S_2(\epsilon)$

Table 5.2: The table lists the possible behaviour of $I3(\mathcal{P})$ for different $\mathcal{P}$ and a fixed direction of deformation $|I\rangle$. The parameter ϕ is the number of strings among I_A, I_B, I_C, I_D which are Hom in 1's or 0's. Again η and $\bar{\eta}$ are mutually exclusive variables, when $\eta = 0$, $\bar{\eta} = 1$, and vice versa.

N qubits, and for any N, the state GHZ_N is a saddle point of $I3(\mathcal{P})$ for all $\mathcal{P}$.[6] Furthermore, the functions $S_1(\epsilon)$, $S_2(\epsilon)$ and $S_3(\epsilon)$ are all decreasing, while $S_4(\epsilon)$ is increasing. In particular $S_3(\epsilon)$ decreases only at order ϵ^4.

With the set of possible entropies at hand, we now want to classify the possible behaviours of the tripartite information of $|\psi_I^\epsilon\rangle$, depending on the partitioning and the direction of the deformation $|I\rangle$. A natural classification would proceed by first fixing a partitioning $\mathcal{P}$, and then looking at the behaviour of $I3(\mathcal{P})$ in all possible directions $|I\rangle$. Nevertheless, due to the nature of the problem, it is more natural to proceed in the opposite way. We first fix a direction $|I\rangle$ of deformation and then derive the behaviour of $I3(\mathcal{P})$ for all possible $\mathcal{P}$. This is more natural because the behaviour of $I3(\mathcal{P})$ will just depend on the homogeneity properties of the strings I_A, I_B, I_C, I_D derived from $|I\rangle$ under $\mathcal{P}$, and the analogous properties for their unions.[7] The possible cases are shown in Tab. 5.2 and are classified using a parameter ϕ that counts the number of strings $X \in \{I_A, I_B, I_C, I_D\}$ which are Hom.

The results of Tab. 5.2 show that for a given direction $|I\rangle$, $I3(\mathcal{P})$ of GHZ_N can increase only for those $\mathcal{P}$ such that all the strings I_A, I_B, I_C, I_D are not Hom. Since a string made of a single digit is always Hom, the following lemma follows

Lemma: *For any N, the GHZ_N state is a local maximum of $I3(\mathcal{P})$ for any $\mathcal{P}$ such that at least one of the subsystems contains only a single qubit.*

Since for $N \leq 7$ this always happens, in this case the GHZ_N state is a local maximum of $I3(\mathcal{P})$ for all $\mathcal{P}$.

[6] This result immediately follows from the fact that for any $\mathcal{P}$ the tripartite information is just a linear combination of entropies.

[7] Recall that for two Hom strings X, Y the union is not Hom if X is Hom in 1's (or 0's) and Y in 0's (1's).

For arbitrary N and $\mathcal{P}$ instead, the GHZ_N states are not local maxima. Nevertheless, since we know exactly how the value of $I3(\mathcal{P})$ behaves along each direction (not only perturbatively), for fixed $\mathcal{P}$ we can choose a direction $|I_1\rangle$ along which $I3(\mathcal{P})$ grows and follow it until we reach a maximum in that direction. One can check that the function $S_4(\epsilon)$ reaches a maximum along $|I_1\rangle$ for $|\epsilon| = 1$. We can then build the new state

$$|\mathrm{GHZ}_N\rangle \rightarrow |\psi_1\rangle = \frac{1}{\sqrt{3}}\left(|0...0\rangle + |1...1\rangle + e^{i\theta_1}|I_1\rangle\right) \tag{5.3.13}$$

This new state of course is not guaranteed to be a local maximum of $I3(\mathcal{P})$. To investigate whether this is the case or not, we can again look at deformations along all possible directions. We then build the new state

$$|\psi_1\rangle \rightarrow |\psi_2^\epsilon\rangle = \frac{1}{\sqrt{\mathcal{N}}}\left(|0...0\rangle + |1...1\rangle + e^{i\theta_1}|I_1\rangle + \epsilon|I_2\rangle\right) \tag{5.3.14}$$

For an arbitrary bipartition of the system into X and X^c, the reduced density matrix $\rho_X(\epsilon, I_1, I_2)$ will have the following structure (up to normalization factors)

$$\rho_X(\epsilon, I_1, I_2) = \rho_X(e^{i\theta_1}, I_1) + \rho_X(\epsilon, I_2) + e^{i\theta_1}\epsilon^* |I_X^1\rangle\langle I_X^2| + e^{-i\theta_1}\epsilon |I_X^2\rangle\langle I_X^1| \tag{5.3.15}$$

In Eq. (5.3.15) the expressions $\rho_X(e^{i\theta_1}, I_1)$ and $\rho_X(\epsilon, I_2)$ correspond to matrices of the form Eq. (5.3.12), with deformations along $|I_1\rangle, |I_2\rangle$ and coefficients respectively $e^{i\theta_1}$ and ϵ. The last two terms are "interference" terms that survive only when $|I_X^1\rangle, |I_X^2\rangle$ (defined as in Eq. (5.3.12)) are not orthogonal.

We check numerically for many examples that the interference terms reduce the entropy, while the entropy increases if these terms disappear. This observation motivates the following construction. Given a partitioning $\mathcal{P} = (A : B : C : D)$ for a system of N qubits, start with the GHZ_N state. Then pick a direction $|I_1\rangle$ with the property that all the strings $I_A^1, I_B^1, I_C^1, I_D^1$ are not Hom, such that $I3(\mathcal{P})$ will grow, and build the new state Eq. (5.3.13). Then look for a second possible direction $|I_2\rangle$ such that $I_A^2, I_B^2, I_C^2, I_D^2$ are again not Hom and $\langle I_A^1|I_A^2\rangle = \langle I_B^1|I_B^2\rangle = \langle I_C^1|I_C^2\rangle = \langle I_D^1|I_D^2\rangle = 0$, and build the new state Eq. (5.3.14) with $\epsilon = e^{i\theta_2}$. Finally iterate this construction for all possible directions that satisfy these conditions. This procedure is limited by the subset $X \in \{A, B, C, D\}$ which has minimal size x, and will stop at some point. We then conjecture the following

Conjecture: *All the states that can be built following this algorithmic construction are local maxima of* $I3(A : B : C : D)$.

On can check for example that in the case $N = 4k$, for specific permutation of the qubits in the partitioning $\mathcal{P} = (\frac{N}{4} : \frac{N}{4} : \frac{N}{4} : \frac{N}{4})$, and picking all the phases to be $e^{i\theta_i} = 1$, the procedure starts with the state $|\mathrm{GHZ}_N\rangle$ and ends with the state $|\mathrm{GHZ}\rangle_4^{\otimes k}$, recovering the result stated before. We leave the general proof of this conjecture as an open problem for future work.

$\exists X,\ \lvert X\rvert \geq \frac{N}{2}$	$I3(\mathcal{P}) = 0,\ \forall \mathcal{P}$					
	χ	$I3$	$\mathcal{P}_{\min}$	$I3_{\min}$	$\mathcal{P}_{\max}$	$I3_{\max}$
$\lvert X\rvert < \frac{N}{2},\ \forall X$	0	-2α	$a = b = c = \frac{N}{4}$	$-\frac{N}{2}$	$\alpha = 1$	-2
	1	$-2c$	$a = b - 1 = c + 1 = \frac{N}{4}$	$-\frac{N}{2} + 2$	$c = 1$	-2
	2	$-N + 2a$	$a - 1 = b = c = \frac{N}{4}$	$-\frac{N}{2} + 2$	$a = \frac{N}{2} - 1$	-2
	3	$2\alpha - N$	$a - 1 = b - 1 = c = \frac{N}{4}$	$-\frac{N}{2} + 4$	$\alpha = \frac{N}{2} - 1$	-2

Table 5.3: The table shows the classification of the values of $I3(\mathcal{P})$ for perfect states, for all possible partitionings of the system. When a subsystem X (possibly also $X = D$) contains at least half of the qubits, $I3(\mathcal{P})$ vanishes. The other cases are classified according to the parameter χ. For each case the value of $I3(\mathcal{P})$ is given as a function of (a, b, c). Maximal and minimal values of $I3(\mathcal{P})$ and the corresponding partitionings are also shown for each case. The parameter α is defined as $\alpha = a + b + c - \frac{N}{2}$.

.

5.4 States with maximal bipartite entanglement

In this section we focus on bipartite entanglement and investigate the behaviour of the tripartite information for states that are highly entangled for all possible bipartitions of the system. The search for this kind of states, usually called MMES (maximal multi-qubit entangled states),[8] is an important problem in quantum information theory [157], where entanglement is a resource for the implementation of many protocols.

A particularly interesting subclass of MMES are the *perfect* MMES, for which the entropy of each subsystem is exactly maximal; these are indeed the *perfect states* of [28] and [153]. In the case of qubits it is known that they do not exist for $N \geq 8$ [158]. For qudits, examples can be found using stabilizer code [159] techniques [153] [160].

We want to explore the behaviour of $I3(\mathcal{P})$ for different partitionings of these states. We start with perfect states, for which a classification of the possible values of $I3(\mathcal{P})$ is possible even without knowing an explicit expression. Next we investigate some examples of MMES for $N = 2, 4, 6, 8$ and some other states that can be built from them.

Perfect states

Perfect states are defined as those states for which each subsystem $X \subseteq U$ (with $|X| = x$) has exactly maximal entropy

$$S_x = \begin{cases} x & \text{for } x \leq \frac{N}{2} \\ N - x & \text{for } x > \frac{N}{2} \end{cases} \tag{5.4.16}$$

Since perfect states are symmetric under permutations of the qubits, we can classify the behaviour of $I3(\mathcal{P})$ looking at the sets $I3(a : b : c)$ with constraints Eq. (5.2.2) on a, b and

[8] They are sometimes called *maximal multipartite entangled states*, but this denomination might be misleading, suggesting some connection to multipartite entanglement. Instead, "multipartite" here refers to the fact that we are looking not only at entanglement for one particular bipartition of the system, but for all bipartitions.

c. Once the sizes of subsystems are specified, the entropies are given by Eq. (5.4.16) and we can immediately compute the value of $I3(\mathcal{P})$. For simplicity, in the following we will assume that N is a multiple of 4.

When $a+b+c < \frac{N}{2}$, or when any of the subsystems contains $\frac{N}{2}$ qubits or more, one has $I3(\mathcal{P}) = 0$. The two cases are equivalent because of Eq. (5.2.3), indeed when $a+b+c < \frac{N}{2}$, it follows that $d \geq \frac{N}{2}$. To classify all other possible cases we will use a parameter χ, defined as the number of unions of two subsystems X, Y that contain at least $\frac{N}{2}$ qubits, i.e. $|X \cup Y| \geq \frac{N}{2}$. To simplify the notation, and without loss of generality, we assume that $a \geq b \geq c$, such that

$$\chi = \begin{cases} 0 & \text{for } |X \cup Y| < \frac{N}{2},\ \forall X, Y \\ 1 & \text{for } |A \cup B| \geq \frac{N}{2} \text{ but } |A \cup C|, |B \cup C| < \frac{N}{2} \\ 2 & \text{for } |A \cup B|, |A \cup C| \geq \frac{N}{2} \text{ but } |B \cup C| < \frac{N}{2} \\ 3 & \text{for } |X \cup Y| \geq \frac{N}{2},\ \forall X, Y \end{cases} \tag{5.4.17}$$

The classification of the possible values of $I3(\mathcal{P})$ is summarized in Tab. 5.3, where we also indicate the specific partionings that maximize or minimize the value of $I3(\mathcal{P})$ in each case.

Note that the partitioning $\mathcal{P} = (\frac{N}{4} : \frac{N}{4} : \frac{N}{4})$ is the minimizer of $I3(\mathcal{P})$ for perfect states. Furthermore, since in this case $I3(\mathcal{P}) = -\frac{N}{2}$, perfect states saturate the bound Eq. (5.2.7) and are absolute minima of $I3(\mathcal{P})$. Indeed, this motivated the proposal of [153] that $I3(\mathcal{P})$ can be used as a parameter for scrambling.

Suppose now that for some value of N (again multiple of 4), a perfect state $|\,\mathrm{P}_N\rangle$ exists. Then we can take two copies of this state and build a new state of a system of size $2N$ taking the product $|\,\mathrm{P}_N\rangle \otimes |\,\mathrm{P}_N\rangle$. This new state would not be a perfect state any more, nevertheless according to the additivity of $I3(\mathcal{P})$ shown in Eq. (5.2.4), there is some partitioning that gives $I3(\mathcal{P}_{2N}) = 2 \times I3(\mathcal{P}_N) = -\frac{(2N)}{2}$. This simple fact shows that although it is true that a scrambled state would minimize $I3(\mathcal{P})$ of a partitioning $\mathcal{P} = (\frac{N}{4} : \frac{N}{4} : \frac{N}{4})$, the converse is not true. Only if we know that the state we are dealing with is completely symmetric under all permutations, the value of $I3(\mathcal{P})$ is sufficient to imply scrambling.

Finally, we comment on another interesting property that emerges from the results of Tab. 5.3. Note that while the lower bound of $I3(\mathcal{P})$ for different partitionings scales with N, the upper bound does not. In particular there are partitionings for which $I3(\mathcal{P}) = 0$. In the holographic perspective, these are the ones we should be more careful about, as they get closer to the violation of monogamy for mutual information. It would be interesting to study the behaviour of perfect states for such partitionings under the effect of arbitrary operations performed on the constituents of the system. We leave the general question for future work, while in the next section we explore the example of $N = 6$, for which a perfect state of qubits exists and is known explicitly.

Some examples of MMES states

We now explore the behaviour of the tripartite information for systems of $N = 2, 4, 6, 8$ qubits, focusing on highly entangled states and some deformations of them. We also compare the value of $I3(\mathcal{P})$ to the value obtained for particular product states, suggesting that the average $\overline{I3(\mathcal{P})}$ over permutation of the qubits could be a more sensible measure to evaluate scrambling.

N=2 Obviously $I3(\mathcal{P})$ for states of just 2 qubits is nonsense. Starting with maximally entangled states $|\,M_2\rangle$ of 2 qubits (Bell pairs), we can build maximally entangled states of an arbitrary even number of qubits by simply taking the product $|\,M_2\rangle^{\otimes k}$. These states are indeed maximally entangled but only for certain bipartitions. In particular there is only one subsystem containing $\frac{N}{2}$ qubits which has maximal entropy. For the case $k = 2$ one gets a maximally entangled state of 4 qubits for which $I3(\mathcal{P}) = 0$. As a consequence of Eq. (5.2.4) when we take a product with a new copy of $|\,M_2\rangle$, $I3(\mathcal{P})$ is invariant. By induction one has $I3(\mathcal{P}) = 0$ for arbitrary k. In other words, any "distilled" state[9] has $I3(\mathcal{P}) = 0$ for all $\mathcal{P}$. The converse is obviously not true, a product state for all qubits contains no entanglement and would equally have $I3 \equiv 0$.

N=4 The MMES of 4 qubits was found in [152] and is known as M state. It has the form

$$|\,M_4\rangle = |0011\rangle + e^{-\frac{\pi}{3}i}\,|0101\rangle - e^{\frac{\pi}{3}i}\,|0110\rangle - e^{\frac{\pi}{3}i}\,|1001\rangle + e^{-\frac{\pi}{3}i}\,|1010\rangle + |1100\rangle \quad (5.4.18)$$

Although this is the maximally entangled state of 4 qubits, it is not a perfect state as the entropies of one and two qubits are respectively $S_{\{1\}} = 1$, $S_{\{2\}} = \frac{1}{2}\log_2 12 \approx 1.79248 < 2$. The tripartite information for this state has value $I3(\mathcal{P}) = 4 - \frac{3}{2}\log_2 12 \approx -1.37744$. By deforming the state with a small pertubation in any direction in Hilbert space, one can check numerically that this state is a local minimum for $I3(\mathcal{P})$.

N=6 In the particular case of 6 qubits the perfect state $|\,\mathrm{P}_6\rangle$ is known explicitly,[10] it was found in [161]. We can then investigate the effect of deformations of the state on the sign of $I3(\mathcal{P})$. Following the classification of Tab. 5.3, we can look for the partitionings for which $I3(\mathcal{P}) = 0$. We have the possible cases $\mathcal{P} = (1:1:1)$ or $\mathcal{P} = (3:1:1)$, but they are equivalent according to Eq. (5.2.3). Starting with the state $|\,\mathrm{P}_6\rangle$ we can deform it in the directions labelled by the computational basis: $|\,\psi_I^\epsilon\rangle = |\,\mathrm{P}_6\rangle + \epsilon\,|I\rangle$. A numerical check shows that $I3(1:1:1)$ decreases in all directions; small perturbations cannot change its sign. We can also explore the effect of measurements performed on some of the qubits of the system. We can for example measure a single qubit with any of $\sigma_x, \sigma_y, \sigma_z$ or we can do a Bell measurement and project two qubits onto a maximally entangled state. In both

[9] Distillation is the process of extraction of Bell pairs from a given state using LOCC operations.
[10] We refer the reader to the original paper for its expression.

these cases one can check that for the states obtained under these operations it is still true that $I3(\mathcal{P}) \leq 0$ for all $\mathcal{P}$.

N=8 An 8 qubits MMES was found in [162], we will refer to it as the $|\,\mathrm{M}_8\rangle$ state. As for $N = 4$, a numerical check shows that this state is a local minimum of $I3(2:2:2)$ in Hilbert space. In particular $I3(2:2:2)[\mathrm{M}_8] \approx -1.35458$, while for a perfect state of 8 qubits ($|\,\mathrm{P}_8\rangle$ which does not exist) it would have been $I3(2:2:2)[\mathrm{P}_8] = -4$. We can now compare this result with the value of $I3(2:2:2)$ for the state $|\,\mathrm{M}_4\rangle\otimes|\,\mathrm{M}_4\rangle$, where $|\,\mathrm{M}_4\rangle$ is the MMES of 4 qubits introduced before. In this case one has $I3(2:2:2)[\mathrm{M}_4\otimes\mathrm{M}_4] \approx -2.75489 < -1.35458$. This simple observation suggests again[11] that one should be careful in using $I3(\mathcal{P})$ as a parameter of scrambling. On the other hand, since this value of $I3(2:2:2)[\mathrm{M}_4\otimes\mathrm{M}_4]$ is only attained for some permutations of the qubits, one can ask whether the average value $\overline{I3(2:2:2)}$ over all permutation is a more sensible measure. The state $|\,\mathrm{M}_8\rangle$ is completely symmetric under permutations of the qubits, so that the average tripartite information has the same value obtained before. This is not true for the state $|\,\mathrm{M}_4\rangle\otimes|\,\mathrm{M}_4\rangle$ in which case, taking into account the combinatorics,[12] one gets $\overline{I3(2:2:2)}[\mathrm{M}_4\otimes\mathrm{M}_4] \approx -0.62969 > -1.35458$. For $N = 8$ a perfect state does not exist and it is natural to consider the MMES as the scrambled state in this Hilbert space. This example then shows that the MMES is not the absolute minimizer for a single value of $I3(\mathcal{P})$ corresponding to a specific permutation of the qubits . On the other hand the average $\overline{I3(\mathcal{P})}$ seems to be minimized by the MMES.

5.5 Discussion

In this chapter we explored the behaviour of the tripartite information for different partitionings of systems in highly entangled states. For simplicity we focused in particular on systems of qubits, but most of the result can be generalized to constituents that live in a higher dimensional Hilbert space, i.e. qudits.

After a discussion about general properties of $I3(\mathcal{P})$, we started by looking at states that maximize multipartite entanglement, namely GHZ_N states. We showed how $I3(\mathcal{P})$ changes for deformations of the states in various directions in Hilbert space, depending on the different partitionings of the system. Then we proposed an algorithmic construction that we conjectured can be used to build local maxima of $I3(\mathcal{P})$ for arbitrary N and $\mathcal{P}$. We leave the proof of this conjecture and the extension to higher dimensional generalizations of GHZ_N states for future work.

Next we moved to states that manifest a high amount of bipartite entanglement for all possible bipartitions of the system. We explored the general behaviour of the perfect

[11] See also the discussion about perfect states.

[12] For the state $|\,\mathrm{M}_4\rangle\otimes|\,\mathrm{M}_4\rangle$, the tripartite information is either -2.75489 or 0. There are in general 420 possible qubits permutations corresponding to the partitioning $\mathcal{P} = (2:2:2)$ of the system, 96 of which give the non vanishing value.

states of [28] for all possible partitionings and then looked at some examples of qubits states which although not perfect, are known to be highly entangled for all bipartitions.

Our main motivation for studying the tripartite information came from holography, where $I3(\mathcal{P})$ has definite non-positive sign and captures the monogamy of mutual information [120]. Drawing from the results of the previous sections, we conclude with some observations which are relevant in the holographic context, posing some open questions that we leave to future investigations.

The sign of the tripartite information The work of [116] asked the question of how generic is monogamy of mutual information, and consequently how restrictive is the constraint imposed by holography. It was found numerically that for random states of 6 and 8 qubits it is extremely difficult to obtain states with positive value of $I3(\mathcal{P})$. Furthermore, it was observed that when $\mathcal{P} = (1:1:1)$, the values of $I3(\mathcal{P})$ for random states, although still negative, approach $I3(\mathcal{P}) = 0$. This matches with the behaviour of perfect states shown in Tab. 5.3, which under the same assumptions for $\mathcal{P}$, have precisely $I3(\mathcal{P}) = 0$.

This similarity between the distribution of random states for different choices of $\mathcal{P}$ and the values of $I3(\mathcal{P})$ for perfect states, extends to all cases where the size of subsystems in $\mathcal{P}$ is much smaller (or much larger) than half of the size of the entire system. This can be interpreted as a consequence of Page theorem [163], which precisely under the same assumptions for the size of subsystems, implies that random states are almost maximally entangled. It would be interesting to explore further the relation between random and perfect states. In particular, since as far as entropies are concerned, they generically have a similar behaviour, one could try to make this connection quantitative by introducing a notion of "typicality"[13] for perfect states.

Next, since for certain partitionings of perfect states one gets $I3(\mathcal{P}) = 0$, it is natural to ask how stable is the sign definiteness of $I3(\mathcal{P})$ for these particular partitionings when we deform the states either by some perturbation or by some operation performed on the constituents. Without a general expression at hand for perfect states, we focused on the example of the 6 qubits systems, for which the perfect state is known explicitly. We checked numerically that any deformation in any direction in Hilbert space can only decrease the value of $I3(\mathcal{P})$, suggesting that in general perfect states are local maxima of $I3(\mathcal{P})$ for these partitionings. Furthermore we explored the effect of different measurements on one and two of the qubits of the system, but even in this case we did not get any new state with positive value of $I3(\mathcal{P})$. It would be interesting to explore these results for larger systems, higher dimensional generalizations of the constituents and different classes of operations.

Finally, considering also the results from investigations of GHZ_N states, it seems natural to expect that some amount of 4-partite quantum entanglement is really crucial for the violation of monogamy of mutual information. Unfortunately, no measure of 4-partite

[13] *Typicality* here has to be interpreted in the sense of [164]. According to some measure, the distance between the behaviour of random and perfect states would be exponentially suppressed for large N.

quantum entanglement for mixed state is available to investigate this expectation quantitatively.

The tripartite information as a parameter for scrambling Since perfect states might be thought as the result of scrambling, and they correspond to global minima of $I3(\mathcal{P})$, it was proposed in [153] that the tripartite information can be used as a parameter for scrambling. In our analysis of perfect states, we showed that for some permutation of the constituents of the system, the same value of $I3(\mathcal{P})$ can in principle be attained by products of perfect states of smaller systems. Since these product states are not perfect states of the larger system, one can conclude that the value of $I3(\mathcal{P})$ can be an appropriate measure of scrambling only under the assumption that the state under consideration is completely symmetric under permutations of the qubits. We propose that in general, as a measure of scrambling, one should use instead the average of the tripartite information ($\overline{I3(\mathcal{P})}$) over all possible permutations of the qubits.

Furthermore, since perfect states do not always exist, one can ask if for a given value of N, the state which contain the maximal possible amount of entanglement for all bipartitions (MMES) is the minimizer of $I3(\mathcal{P})$. A counterexample to this expectation seems to derive from the highly entangled state of 8 qubits found in [162], which is conjectured to be a MMES state. We showed that the value of $I3(\mathcal{P})$ obtained for this state is smaller than the one obtained from the product of two copies of MMES of 4 qubits. On the contrary, when we take the average of $I3(\mathcal{P})$ over all permutations of the qubits, the situation is reversed. This is a further argument in support of our proposal that $\overline{I3(\mathcal{P})}$ is a more appropriate parameter for scrambling.

Chapter 6

Outlook

We conclude this work with some comments about open questions and future possible directions of investigation towards a deeper understanding of operational aspects of entanglement in holography.

An information theory for quantum fields: as we discussed in the introduction, a satisfactory operational interpretation of entanglement measures together with a theory of quantum information along the lines of quantum mechanics still have to be developed for quantum fields. While field theory is usually viewed as the continuous limit of quantum mechanics, the Tsirelson problem suggests that the difference in the two formalisms might have radical implications. Similarly, it is not clear whether the notion of causality in field theory is fully equivalent to the no-signaling condition defined by PR-boxes and we do not know if there is a field theory version of the Tsirelson bound, i.e. if the strength of correlations in field theory is bounded as in quantum mechanics. The situation is even worst in the case of gauge fields, where even for theories which are regularized on a lattice one could not expect factorization of the Hilbert space. While a deeper understanding of these problems in field theory is of great interest on its own right, it could also sharpen what would be the most appropriate definition of entanglement in that context. This is crucial for developing an operational interpretation of computable measures. The algebraic formulation is perhaps the most natural framework for this kind of investigations, but it would be desirable to translate to a more practical language, such as that of correlation functions. As in the quantum mechanical case, it would also be interesting to explore the possibility of manipulating quantum fields for practical purposes. Perhaps the entanglement of ground states which is evident from the Reeh-Schlieder theorem can be used to implement teleportation or to run some form of quantum computation. To answer all these questions, a deeper understanding of the effect of measurements in field theory will probably be vital.

New measures of entanglement: in our investigations involving qubits systems, we used negativity to explore in detail all possible entanglement structures and the dependence of the ratio between negativity and entropy on the pattern of entanglement. Next,

we looked for an interpretation of this ratio in terms of robustness of the entanglement and explored the relation between the disentangling theorem and the entanglement plateaux phenomenon. It would be very interesting to extend this analysis to quantum field theory, but new tools are necessary, in particular techniques to compute negativity for mixed states. Recently there have been some progress in this direction, but only for few special cases. For mixed states, negativity has been computed for a thermal state, but only for a single interval in $1+1$ dimensions [85]. Some progress has also been made towards the calculation of negativity between two intervals, but so far there is no conclusive answer [165].

A particularly interesting situation where such tools could be useful are geometries with multiple boundaries, such as the eternal black hole geometry. For this geometry the field theory on a single boundary is in the thermal state and quantum correlations are expected to decay very quickly when the temperature increases. On the other hand there are geometries with a different topology behind the horizon that can purify the state on one boundary. An example is Wheeler's Bag of Gold, where the geometry behind the horizon is that of a Friedmann-Robertson-Walker universe. In this case, since the state on one boundary is excited, but pure, one could expect larger quantum correlations between subregions. It is then interesting to ask whether a quantity like negativity, measured between two "small" subregions, would be able to detect some feature of the topology behind the horizon. In principle this could be difficult, since for highly entangled states like perfect states, quantum correlations between subregions are very small. Nevertheless it would be interesting to quantify what is the minimal size of regions which are sensible to topology behind the horizon and compare the result to what we expect from the entropy.

Finally the state of affairs for measures in field theory is even worst for multipartite entanglement. As we have seen this is difficult to measure and characterise even in quantum mechanics and so far there is no proposal which could be applied to field theory. On the other hand investigations presented in chapters 4 and 5 seem for example to suggest that some form of 4-partite entanglement is crucial for violation of monogamy of mutual information. It would be interesting to check whether this is true also in field theory and understand why this pattern of entanglement is not allowed by holographic field theories.

Discrete toy models for holography: given the difficulties described above, one can follow the strategy of chapter 4 and focus on quantum mechanics. If one could extend investigations to systems where the number N of qubits is large, it is natural to expect that the analysis would become sensible to field theory properties. For some special states this can be done, as in chapter 5, but in general the treatment becomes infeasible for arbitrary states because the dimension of the Hilbert space grows exponentially with N. Nevertheless, only a small portion of this huge Hilbert space is of physical interest. Indeed it was shown in [166] that systems governed by k-body Hamiltonians, if evolved for an amount of time which scales polynomially with N, can only explore an exponentially small region of the Hilbert space. One can then restrict attention to special states of interest. For a generic state in $\mathcal{H}$ the entropy of a subsystem scales with the number of constituents,

on the other hand for ground states of local field theory entanglement usually satisfies an area law. This fact justifies the use of tensor networks to investigate the entanglement structure of holographic states [26] [27] [28] [160]. We explored the behaviour of the tripartite information for the tensor networks of [28] in chapter 5.

The program of modelling the holographic mapping using tensor networks is still at its infancy. One limitation is the fact that it is not fully understood which tensor networks describe "good" candidates for holographic states. In this respect the Ryu-Takayanagi prescription and in particular the sign definiteness of the tripartite information are an important consistency check. Interestingly, it has been shown recently [167] that this constraint is not the only one imposed by holographic entanglement entropy. As the number of subsystems grows it is known that the von Neumann entropy satisfies additional inequalities that define what is called an *entropy cone*. The results of [167] show that holographic entanglement entropy has to satisfy more restrictive inequalities and that the *holographic entropy cone* is contained in the previous one. The investigations of chapter 5 could then in principle be extended to all the inequalities that define this region of Hilbert space which is of interest for holography. In particular, we could ask what kind of entanglement structures are typical of states within this cone, and for states on the faces of the cone, investigate the stability under different classes of operations.

Another limitation of current proposals for "holographic" tensor networks is the inability to do time evolution. To this end other special states might be useful and in particular *graph states* are particularly appealing. As the name suggests, these are states which can be identified by a graph structure. The graph can be viewed as a preparation procedure that starting from a product state builds a particular entangled state according to an Ising-like interaction. Graph states can be evolved more naturally, even under the effect of measurements, and are a resource for one way quantum computation. Their entanglement structures have been classified under SLOCC operations as presented in chapter 4 even for larger systems. Furthermore, graph state are also important for quantum error correction, which make them interesting for holography also in the perspective of [28]. Finally, the structure of graph states have been combined to that of tensor networks in [168] to build a particular variational ansatz that can be used for time evolution.

It would be very interesting to build a discrete toy model of holography using these quantum mechanical structures. This would be of paramount importance for example to investigate questions about locality and causality, and in particular to compare the definitions which are natural in quantum mechanics and gravitational physics. Finally, it would be interesting to see some feature of geometry emerging from such models. This would be perhaps a concrete realization of a discrete version of ER=EPR, in particular one that could be analysed more naturally from an operational perspective.

Foundations of quantum mechanics: as mentioned in the introduction, it is conceivable that the formulation of a theory of quantum gravity will require at some level a departure from conventional quantum mechanics. This has been noticed in [169], which

discussed what could be the most general postulates of such a theory. Unitary evolution of closed systems is a fundamental axiom of the Copenhagen formulation, nevertheless deformations of quantum theory exist where this fundamental assumption is relaxed to some extent (see for example the discussion in [170]). Long standing questions of quantum theory have recently entered into discussions concerning quantum gravity. The role played by measurements for example is discussed in [148]. A possible violation of the Born rule in the proposal of [171] to reconstruct the black hole interior is presented in [172]. Post-selection, another interesting feature of quantum theory is the mechanism behind the black hole final state proposal of [10]. It is also in this respect that quantum information theory could shed new light on important features of quantum gravity.

Bibliography

[1] J. Bell, *On the Einstein-Podolsky-Rosen paradox*, *Physics* **1** (1964) 195.

[2] S. Popescu and D. Rohrlich, *Causality and nonlocality as axioms for quantum mechanics*, *Fundamental Theories of Physics* **97** (1994) 383.

[3] J. F. Clauser, M. A. Horne, A. Shimony and R. A. Holt, *Proposed experiment to test local hidden variable theories*, *Phys. Rev. Lett.* **23** (1969) 880–884.

[4] B. S. Cirelson, *Quantum generalizations of bell's inequality*, *Lett. Math. Phys.* **4** (1980) 93–100.

[5] S. Popescu, *Nonlocality beyond quantum mechanics*, *Nature Phys.* **10** (2014) 264–270.

[6] A. Almheiri, D. Marolf, J. Polchinski and J. Sully, *Black Holes: Complementarity or Firewalls?*, *JHEP* **02** (2013) 062, [1207.3123].

[7] R. Raussendorf", *A one-way quantum computer*, *Physical Review Letters* **86** (2001) 5188–5191.

[8] P. Hayden and J. Preskill, *Black holes as mirrors: Quantum information in random subsystems*, *JHEP* **09** (2007) 120, [0708.4025].

[9] D. Gottesman and I. L. Chuang, *Quantum teleportation is a universal computational primitive*, quant-ph/9908010.

[10] G. T. Horowitz and J. Maldacena, *The black hole final state*, hep-th/0310281.

[11] A. Almheiri, X. Dong and D. Harlow, *Bulk Locality and Quantum Error Correction in AdS/CFT*, *JHEP* **04** (2015) 163, [1411.7041].

[12] B. Czech, P. Hayden, N. Lashkari and B. Swingle, *The information theoretic interpretation of the length of a curve*, 1410.1540.

[13] M. B. Plenio and S. Virmani, *An introduction to entanglement measures*, *Quant.Inf.Comput.* **7** (2007) 1–51, [quant-ph/0504163].

[14] M. Horodecki, J. Oppenheim and R. Horodecki, *Are the laws of entanglement theory thermodynamical?*, *Phys. Rev. Lett. 89 240403 (2002)* (2002) , [quant-ph/0207177].

[15] S. J. Summers and R. Werner, *Bell's Inequalities and Quantum Field Theory. 1. General Setting*, *J. Math. Phys.* **28** (1987) 2440–2447.

[16] N. Brunner, D. Cavalcanti, S. Pironio, V. Scarani and S. Wehner, *Bell nonlocality*, 1303.2849.

[17] P. Calabrese and J. Cardy, *Entanglement entropy and quantum field theory*, hep-th/0405152.

[18] M. Srednicki, *Entropy and area*, *Phys.Rev.Lett.* **71** (1993) 666–669, [hep-th/9303048].

[19] J. M. Maldacena, *The large n limit of superconformal field theories and supergravity*, hep-th/9711200.

[20] S. Ryu and T. Takayanagi, *Holographic derivation of entanglement entropy from AdS/CFT*, *Phys.Rev.Lett.* **96** (2006) 181602, [hep-th/0603001].

[21] M. Headrick and T. Takayanagi, *A holographic proof of the strong subadditivity of entanglement entropy*, 0704.3719.

[22] A. Lewkowycz and J. Maldacena, *Generalized gravitational entropy*, *JHEP* **1308** (2013) 090, [1304.4926].

[23] V. E. Hubeny, M. Rangamani and T. Takayanagi, *A Covariant holographic entanglement entropy proposal*, *JHEP* **0707** (2007) 062, [0705.0016].

[24] R. Orus, *A practical introduction to tensor networks: Matrix product states and projected entangled pair states*, 1306.2164.

[25] G. Vidal, *Entanglement renormalization*, cond-mat/0512165.

[26] B. Swingle, *Entanglement Renormalization and Holography*, *Phys.Rev.* **D86** (2012) 065007, [0905.1317].

[27] X.-L. Qi, *Exact holographic mapping and emergent space-time geometry*, 1309.6282.

[28] F. Pastawski, B. Yoshida, D. Harlow and J. Preskill, *Holographic quantum error-correcting codes: Toy models for the bulk/boundary correspondence*, 1503.06237.

[29] J. Maldacena and L. Susskind, *Cool horizons for entangled black holes*, *Fortsch.Phys.* **61** (2013) 781–811, [1306.0533].

[30] M. Rangamani and M. Rota, *Comments on Entanglement Negativity in Holographic Field Theories*, *JHEP* **1410** (2014) 60, [1406.6989].

[31] P. Calabrese, J. Cardy and E. Tonni, *Entanglement negativity in quantum field theory*, *Phys.Rev.Lett.* **109** (2012) 130502, [1206.3092].

[32] V. E. Hubeny, H. Maxfield, M. Rangamani and E. Tonni, *Holographic entanglement plateaux*, *JHEP* **1308** (2013) 092, [1306.4004].

[33] R. Werner, *Quantum states with Einstein-Podolsky-Rosen correlations admitting a hidden-variable model*, *Phys. Rev. A* **40** (1989) 4277–4281.

[34] S. Popescu, *Bell's inequalities versus teleportation: What is nonlocality?*, *Phys. Rev. Lett.* **72** (1994) 797–799.

[35] S. Popescu, *Bell's inequalities and density matrices: Revealing "hidden" nonlocality*, *Phys. Rev. Lett.* **74** (1995) 2619–2622.

[36] C. H. Bennett, G. Brassard, S. Popescu, B. Schumacher, J. A. Smolin et al., *Purification of noisy entanglement and faithful teleportation via noisy channels*, *Phys.Rev.Lett.* **76** (1996) 722–725, [quant-ph/9511027].

[37] G. Vidal and R. Werner, *Computable measure of entanglement*, *Phys.Rev.* **A65** (2002) 032314.

[38] R. Verch and R. F. Werner, *Distillability and positivity of partial transposes in general quantum field systems*, *Rev.Math.Phys.* **17** (2005) 545–576, [quant-ph/0403089].

[39] S. Ryu and T. Takayanagi, *Aspects of Holographic Entanglement Entropy*, *JHEP* **0608** (2006) 045, [hep-th/0605073].

[40] M. Van Raamsdonk, *Comments on quantum gravity and entanglement*, 0907.2939.

[41] M. Van Raamsdonk, *Building up spacetime with quantum entanglement*, *Gen.Rel.Grav.* **42** (2010) 2323–2329, [1005.3035].

[42] T. Hartman and J. Maldacena, *Time Evolution of Entanglement Entropy from Black Hole Interiors*, *JHEP* **1305** (2013) 014, [1303.1080].

[43] M. Nozaki, T. Numasawa, A. Prudenziati and T. Takayanagi, *Dynamics of Entanglement Entropy from Einstein Equation*, *Phys.Rev.* **D88** (2013) 026012, [1304.7100].

[44] N. Lashkari, M. B. McDermott and M. Van Raamsdonk, *Gravitational dynamics from entanglement 'thermodynamics'*, *JHEP* **1404** (2014) 195, [1308.3716].

[45] J. Bhattacharya and T. Takayanagi, *Entropic Counterpart of Perturbative Einstein Equation*, *JHEP* **1310** (2013) 219, [1308.3792].

[46] T. Faulkner, M. Guica, T. Hartman, R. C. Myers and M. Van Raamsdonk, *Gravitation from Entanglement in Holographic CFTs*, *JHEP* **1403** (2014) 051, [1312.7856].

[47] B. Swingle and M. Van Raamsdonk, *Universality of Gravity from Entanglement*, 1405.2933.

[48] H. Casini, M. Huerta and R. C. Myers, *Towards a derivation of holographic entanglement entropy*, *JHEP* **1105** (2011) 036, [1102.0440].

[49] P. Calabrese, J. Cardy and E. Tonni, *Entanglement negativity in extended systems: A field theoretical approach*, *J.Stat.Mech.* **1302** (2013) P02008, [1210.5359].

[50] V. Balasubramanian, P. Hayden, A. Maloney, D. Marolf and S. F. Ross, *Multiboundary Wormholes and Holographic Entanglement*, 1406.2663.

[51] H. Gharibyan and R. F. Penna, *Are entangled particles connected by wormholes? Evidence for the ER=EPR conjecture from entropy inequalities*, *Phys.Rev.* **D89** (2014) 066001, [1308.0289].

[52] A. Peres, *Separability criterion for density matrices*, *Phys.Rev.Lett.* **77** (1996) 1413–1415, [quant-ph/9604005].

[53] M. Horodecki, P. Horodecki and R. Horodecki, *On the necessary and sufficient conditions for separability of mixed quantum states*, *Phys. Lett.* **A 223** (11, 1996) 1–8, [quant-ph/9605038].

[54] M. Horodecki, P. Horodecki and R. Horodecki, *Mixed-state entanglement and distillation: Is there a "bound" entanglement in nature?*, *Phys. Rev. Lett.* **80** (Jun, 1998) 5239–5242.

[55] A. Peres, *All the Bell inequalities*, *Foundations of Physics* **29** (1999) 589.

[56] R. Werner and M. Wolf, *Bell's inequalities for states with positive partial transpose*, *Physical Review A* **61** (2000) .

[57] B. Terhal, A. Doherty and D. Schwab, *Symmetric extensions of quantum states and local hidden variable theories*, *Phys. Rev. Lett.* **90** (2003) .

[58] T. Vértesi and N. Brunner, *Disproving the Peres conjecture: Bell nonlocality from bipartite bound entanglement*, 1405.4502.

[59] K. Audenaert, M. B. Plenio and J. Eisert, *Entanglement cost under positive-partial-transpose-preserving operations*, *Phys. Rev. Lett.* **90** (Jan, 2003) 027901.

[60] M. Plenio, *The logarithmic negativity: A full entanglement monotone that is not convex*, *Phys. Rev. Lett.* **95** (2005) 090503, [quant-ph/0505071].

[61] H. He and G. Vidal, *Disentangling theorem and monogamy for entanglement negativity*, 1401.5843.

[62] Y.-C. Ou and H. Fan, *Monogamy inequality in terms of negativity for three-qubit states*, *Physical Review A* **75** (2007) 062308, [quant-ph/0702127].

[63] G. Vidal and R. Tarrach, *Robustness of entanglement*, *Phys.Rev.* **A59** (1999) 141–155, [quant-ph/9806094].

[64] M. Headrick, V. E. Hubeny, A. Lawrence and M. Rangamani, *Causality and holographic entanglement entropy*, *to appear* (2014) .

[65] S. A. Gentle and M. Rangamani, *Holographic entanglement and causal information in coherent states*, *JHEP* **1401** (2014) 120, [1311.0015].

[66] H. Casini and M. Huerta, *Entanglement entropy for the n-sphere*, *Phys.Lett.* **B694** (2010) 167–171, [1007.1813].

[67] I. R. Klebanov, S. S. Pufu, S. Sachdev and B. R. Safdi, *Renyi Entropies for Free Field Theories*, *JHEP* **1204** (2012) 074, [1111.6290].

[68] D. Fursaev, *Entanglement Renyi Entropies in Conformal Field Theories and Holography*, *JHEP* **1205** (2012) 080, [1201.1702].

[69] R. Emparan, *AdS / CFT duals of topological black holes and the entropy of zero energy states*, *JHEP* **9906** (1999) 036, [hep-th/9906040].

[70] L.-Y. Hung, R. C. Myers, M. Smolkin and A. Yale, *Holographic Calculations of Renyi Entropy*, *JHEP* **1112** (2011) 047, [1110.1084].

[71] D. A. Galante and R. C. Myers, *Holographic Renyi entropies at finite coupling*, *JHEP* **1308** (2013) 063, [1305.7191].

[72] M. Headrick, *Entanglement Renyi entropies in holographic theories*, *Phys.Rev.* **D82** (2010) 126010, [1006.0047].

[73] T. Hartman, *Entanglement Entropy at Large Central Charge*, 1303.6955.

[74] H. Araki and E. Lieb, *Entropy inequalities*, *Commun.Math.Phys.* **18** (1970) 160–170.

[75] M. Headrick, *General properties of holographic entanglement entropy*, *JHEP* **1403** (2014) 085, [1312.6717].

[76] L. Zhang and J. Wu, *On Conjectures of Classical and Quantum Correlations in Bipartite States*, *J.Phys.* **A45** (2012) 025301.

[77] E. Perlmutter, M. Rangamani and M. Rota, *Positivity, negativity, and entanglement*, *to appear* (2015) .

[78] A. Lewkowycz and E. Perlmutter, *Universality in the geometric dependence of Rényi entropy*, *JHEP* **1501** (2015) 080, [1407.8171].

[79] J. Lee, A. Lewkowycz, E. Perlmutter and B. R. Safdi, *Renyi entropy, stationarity, and entanglement of the conformal scalar*, 1407.7816.

[80] X. Dong, *Shape dependence of holographic renyi entropy in conformal field theories*, 1602.08493.

[81] S. N. Solodukhin, *Entanglement entropy, conformal invariance and extrinsic geometry*, *Phys.Lett.* **B665** (2008) 305–309, [0802.3117].

[82] R. C. Myers and A. Sinha, *Holographic c-theorems in arbitrary dimensions*, *JHEP* **1101** (2011) 125, [1011.5819].

[83] D. L. Jafferis, I. R. Klebanov, S. S. Pufu and B. R. Safdi, *Towards the F-Theorem: N=2 Field Theories on the Three-Sphere*, *JHEP* **1106** (2011) 102, [1103.1181].

[84] M. Kulaxizi, A. Parnachev and G. Policastro, *Conformal Blocks and Negativity at Large Central Charge*, *JHEP* **1409** (2014) 010, [1407.0324].

[85] P. Calabrese, J. Cardy and E. Tonni, *Finite temperature entanglement negativity in conformal field theory*, *J.Phys.* **A48** (2015) 015006, [1408.3043].

[86] A. Allais and M. Mezei, *Some results on the shape dependence of entanglement and Rényi entropies*, *Phys.Rev.* **D91** (2015) 046002, [1407.7249].

[87] M. Mezei, *Entanglement entropy across a deformed sphere*, *Phys.Rev.* **D91** (2015) 045038, [1411.7011].

[88] A. F. Astaneh, G. Gibbons and S. N. Solodukhin, *What surface maximizes entanglement entropy?*, *Phys.Rev.* **D90** (2014) 085021, [1407.4719].

[89] T. J. Willmore, *Note on embedded surfaces*, *An. St. Univ. Iasi, sIa Mat. B* **11B** (1965) 493–496.

[90] D. M. Hofman and J. Maldacena, *Conformal collider physics: Energy and charge correlations*, *JHEP* **0805** (2008) 012, [0803.1467].

[91] J. Lee, L. McGough and B. R. Safdi, *Rényi entropy and geometry*, *Phys.Rev.* **D89** (2014) 125016, [1403.1580].

[92] K. Zyczkowski, *Renyi extrapolation of Shannon entropy*, *Open Syst. Inf. Dyn.* **10** (2003) 297, [0305062].

[93] F. C. Marques and A. Neves, *Min-Max theory and the Willmore conjecture*, *Annals of Mathematics* **179** (02, 2014) 683–782, [1202.6036].

[94] H. B. Lawson, *Complete minimal surfaces in s3*, *Annals of Mathematics* (1970) 335–374.

[95] R. Kusner, *Comparison surfaces for the willmore problem.*, *Pacific J. Math.* **138** (1989) 317–345.

[96] L. Simon, *Existence of willmore surfaces*, in *Miniconference on Geometry and Partial Differential Equations*, (Canberra AUS), pp. 187–216, Centre for Mathematical Analysis, The Australian National University, 1986.

[97] P. Joshi and C. Séquin, *Energy minimizers for curvature-based surface functionals*, *Computer-Aided Design and Applications* **4** (2007) 1.

[98] S. Heller and N. Schmitt, *Deformations of symmetric cmc surfaces in the 3-sphere*, *Experimental Mathematics* **24** (2015) 65–75.

[99] S. Brendle, *Minimal surfaces in S^3: a survey of recent results*, *Bull. Math. Sciences* **3** (2013) 133–171, [1307.6938].

[100] W. Kuhnel and U. Pinkall, *On total mean curvatures.*, *Quart. J. Math. Oxford* **37** (1986) 437–447.

[101] W. Donnelly and A. C. Wall, *Entanglement entropy of electromagnetic edge modes*, *Phys.Rev.Lett.* **114** (2015) 111603, [1412.1895].

[102] K.-W. Huang, *Central Charge and Entangled Gauge Fields*, 1412.2730.

[103] J. Dowker, *Entanglement entropy for even spheres*, 1009.3854.

[104] K. A. Intriligator, N. Seiberg and S. Shenker, *Proposal for a simple model of dynamical SUSY breaking*, *Phys.Lett.* **B342** (1995) 152–154, [hep-ph/9410203].

[105] D. Gaiotto, *N=2 dualities*, *JHEP* **1208** (2012) 034, [0904.2715].

[106] I. Bah, C. Beem, N. Bobev and B. Wecht, *Four-Dimensional SCFTs from M5-Branes*, *JHEP* **1206** (2012) 005, [1203.0303].

[107] D. Gaiotto and J. Maldacena, *The Gravity duals of N=2 superconformal field theories*, *JHEP* **1210** (2012) 189, [0904.4466].

[108] A. Buchel, R. C. Myers and A. Sinha, *Beyond eta/s = 1/4 pi*, *JHEP* **0903** (2009) 084, [0812.2521].

[109] D. Anselmi, D. Freedman, M. T. Grisaru and A. Johansen, *Nonperturbative formulas for central functions of supersymmetric gauge theories*, *Nucl.Phys.* **B526** (1998) 543–571, [hep-th/9708042].

[110] L. Di Pietro and Z. Komargodski, *Cardy formulae for SUSY theories in $d = 4$ and $d = 6$*, *JHEP* **1412** (2014) 031, [1407.6061].

[111] A. A. Ardehali, J. T. Liu and P. Szepietowski, *c - a from the $\mathcal{N} = 1$ superconformal index*, *JHEP* **1412** (2014) 145, [1407.6024].

[112] M. Beccaria and A. A. Tseytlin, *Higher spins in AdS_5 at one loop: vacuum energy, boundary conformal anomalies and AdS/CFT*, *JHEP* **1411** (2014) 114, [1410.3273].

[113] P. Kovtun, D. T. Son and A. O. Starinets, *Viscosity in strongly interacting quantum field theories from black hole physics*, *Phys.Rev.Lett.* **94** (2005) 111601, [hep-th/0405231].

[114] M. Brigante, H. Liu, R. C. Myers, S. Shenker and S. Yaida, *Viscosity Bound Violation in Higher Derivative Gravity*, *Phys.Rev.* **D77** (2008) 126006, [0712.0805].

[115] X. O. Camanho, J. D. Edelstein, J. Maldacena and A. Zhiboedov, *Causality Constraints on Corrections to the Graviton Three-Point Coupling*, 1407.5597.

[116] M. Rangamani and M. Rota, *Entanglement structures in qubit systems*, *J. Phys.* **A48** (2015) 385301, [1505.03696].

[117] D. R. Brill, *Multi - black hole geometries in (2+1)-dimensional gravity*, *Phys.Rev.* **D53** (1996) 4133–4176, [gr-qc/9511022].

[118] S. Aminneborg, I. Bengtsson, D. Brill, S. Holst and P. Peldan, *Black holes and wormholes in (2+1)-dimensions*, *Class.Quant.Grav.* **15** (1998) 627–644, [gr-qc/9707036].

[119] D. Brill, *Black holes and wormholes in (2+1)-dimensions*, *Lect.Notes Phys.* **537** (2000) 143, [gr-qc/9904083].

[120] P. Hayden, M. Headrick and A. Maloney, *Holographic Mutual Information is Monogamous*, *Phys.Rev.* **D87** (2013) 046003, [1107.2940].

[121] J. M. Maldacena, *Eternal black holes in anti-de Sitter*, *JHEP* **0304** (2003) 021, [hep-th/0106112].

[122] A. Coser, E. Tonni and P. Calabrese, *Entanglement negativity after a global quantum quench*, *J.Stat.Mech.* **1412** (2014) P12017, [1410.0900].

[123] M. Hoogeveen and B. Doyon, *Entanglement negativity and entropy in non-equilibrium conformal field theory*, 1412.7568.

[124] X. Wen, P.-Y. Chang and S. Ryu, *Entanglement negativity after a local quantum quench in conformal field theories*, 1501.00568.

[125] H. Wichterich, J. Molina-Vilaplana and S. Bose, *Scaling of entanglement between separated blocks in spin chains at criticality*, *Physical Review A* **80** (2009) 010304.

[126] P. Calabrese, L. Tagliacozzo and E. Tonni, *Entanglement negativity in the critical ising chain*, *Journal of Statistical Mechanics: Theory and Experiment* **2013** (2013) P05002.

[127] V. Eisler and Z. Zimborás, *On the partial transpose of fermionic gaussian states*, *New Journal of Physics* **17** (2015) 053048.

[128] A. Coser, E. Tonni and P. Calabrese, *Partial transpose of two disjoint blocks in xy spin chains*, .

[129] K. Eckert, J. Schliemann, D. Bruß and M. Lewenstein, *Quantum Correlations in Systems of Indistinguishable Particles*, *Annals of Physics* **299** (jul, 2002) 88–127, [quant-ph/0203060].

[130] M. Haque, O. Zozulya and K. Schoutens, *Entanglement entropy in fermionic laughlin states*, *Phys. Rev. Lett.* **98** (Feb, 2007) 060401.

[131] O. S. Zozulya, M. Haque, K. Schoutens and E. H. Rezayi, *Bipartite entanglement entropy in fractional quantum hall states*, *Phys. Rev. B* **76** (Sep, 2007) 125310.

[132] C. M. Herdman, P.-N. Roy, R. G. Melko and A. Del Maestro, *Particle entanglement in continuum many-body systems via quantum monte carlo*, *Phys. Rev. B* **89** (Apr, 2014) 140501.

[133] R. Horodecki, P. Horodecki, M. Horodecki and K. Horodecki, *Quantum entanglement*, *Rev.Mod.Phys.* **81** (2009) 865–942, [quant-ph/0702225].

[134] B. Groisman, S. Popescu and A. Winter, *On the quantum, classical and total amount of correlations in a quantum state*, quant-ph/0410091.

[135] J. Lin, M. Marcolli, H. Ooguri and B. Stoica, *Tomography from Entanglement*, 1412.1879.

[136] N. Lashkari, C. Rabideau, P. Sabella-Garnier and M. Van Raamsdonk, *Inviolable energy conditions from entanglement inequalities*, 1412.3514.

[137] J. Bhattacharya, V. E. Hubeny, M. Rangamani and T. Takayanagi, *Entanglement density and gravitational thermodynamics*, 1412.5472.

[138] O. Gühne and G. Toth, *Entanglement detection*, *Physics Reports* **474** (2009) 1, [0811.2803].

[139] N. Gisin and H. Bechmann-Pasquinucci, *Bell inequality, bell states and maximally entangled states for n qubits*, *Phys.Lett.* **A246** (1998) 1–6, [quant-ph/9804045].

[140] V. Coffman, J. Kundu and W. K. Wootters, *Distributed entanglement*, *Phys.Rev.A* **61** (2000) 052306, [quant-ph/9907047].

[141] A. Wong and N. Christensen, *A potential multipartide entanglement measure*, quant-ph/0010052.

[142] G. Gour and N. R. Wallach, *All maximally entangled four qubits states*, 1006.0036.

[143] W. Dür, G. Vidal and J. I. Cirac, *Three qubits can be entangled in two inequivalent ways*, *Phys. Rev. A* **62** (2000) 062314, [quant-ph/0005115].

[144] G. Vidal, *Entanglement monotones*, *J.Mod.Opt.* **47** (2000) 355, [quant-ph/9807077].

[145] F. Verstraete, J. Dehaene, B. D. Moor and H. Verschelde, *Four qubits can be entangled in nine different ways*, *Phys. Rev. A, 65: 052112 (2002).* (2001) , [quant-ph/0109033].

[146] L. Lamata, J. Leon, D. Salgado and E. Solano, *Inductive entanglement classification of four qubits under slocc*, *Phys. Rev. A* **75** (2007) 022318, [quant-ph/0610233].

[147] B. Czech, P. Hayden, N. Lashkari and B. Swingle, *The Information Theoretic Interpretation of the Length of a Curve*, 1410.1540.

[148] L. Susskind, *ER=EPR, GHZ, and the Consistency of Quantum Measurements*, 1412.8483.

[149] M. Rota, *Tripartite information of highly entangled states*, 1512.03751.

[150] A. Kitaev and J. Preskill, *Topological entanglement entropy*, *Phys. Rev. Lett.* **96** (2006) 110404, [hep-th/0510092].

[151] H. Casini and M. Huerta, *Remarks on the entanglement entropy for disconnected regions*, *JHEP* **03** (2009) 048, [0812.1773].

[152] A. Higuchi and A. Sudbery, *How entangled can two couples get?*, quant-ph/0005013.

[153] P. Hosur, X.-L. Qi, D. A. Roberts and B. Yoshida, *Chaos in quantum channels*, 1511.04021.

[154] Y. Sekino and L. Susskind, *Fast Scramblers*, *JHEP* **10** (2008) 065, [0808.2096].

[155] N. Lashkari, D. Stanford, M. Hastings, T. Osborne and P. Hayden, *Towards the Fast Scrambling Conjecture*, *JHEP* **04** (2013) 022, [1111.6580].

[156] J. Maldacena, S. H. Shenker and D. Stanford, *A bound on chaos*, 1503.01409.

[157] P. Facchi, G. Florio, G. Parisi and S. Pascazio, *Maximally multipartite entangled states*, 0710.2868.

[158] A. J. Scott, *Multipartite entanglement, quantum-error-correcting codes, and entangling power of quantum evolutions*, *Phys. Rev. A* **69** (2003) 052330, [quant-ph/0310137].

[159] D. Gottesman, *Stabilizer codes and quantum error correction*, *PhD thesis, California Institute of Technology* (1997) .

[160] Z. Yang, P. Hayden and X.-L. Qi, *Bidirectional holographic codes and sub-AdS locality*, 1510.03784.

[161] A. Borras, A. Plastino, J. Batle, C. Zander, M. Casas and A. Plastino, *Multi-qubit systems: Highly entangled states and entanglement distribution*, 0803.3979.

[162] X. Zha, C. Yuan and Y. Zhang, *Generalized criterion of maximally multi-qubit entanglement*, 1204.6340.

[163] D. N. Page, *Average entropy of a subsystem*, *Phys. Rev. Lett.* **71** (1993) 1291–1294, [gr-qc/9305007].

[164] J. L. Lebowitz, *Statistical mechanics: A selective review of two central issues*, *Reviews of Modern Physics* **71** (1999) S346, [math-ph/0010018].

[165] A. Coser, E. Tonni and P. Calabrese, *Towards entanglement negativity of two disjoint intervals for a one dimensional free fermion*, 1508.00811.

[166] D. Poulin, A. Qarry, R. D. Somma and F. Verstraete, *Quantum simulation of time-dependent hamiltonians and the convenient illusion of hilbert space*, 1102.1360.

[167] N. Bao, S. Nezami, H. Ooguri, B. Stoica, J. Sully and M. Walter, *The Holographic Entropy Cone*, *JHEP* **09** (2015) 130, [1505.07839].

[168] R. Hübener, C. Kruszynska, L. Hartmann, W. Dür, F. Verstraete, J. Eisert et al., *Renormalization algorithm with graph enhancement*, 0802.1211.

[169] S. B. Giddings, *Universal quantum mechanics*, 0711.0757.

[170] S. Weinberg, *Quantum mechanics without state vectors*, 1405.3483.

[171] K. Papadodimas and S. Raju, *State-dependent bulk-boundary maps and black hole complementarity*, 1310.6335.

[172] D. Marolf and J. Polchinski, *Violations of the born rule in cool state-dependent horizons*, 1506.01337.